Supporting Information for "Estimating radiative forcing with a nonconstant feedback parameter and linear response"

Hege-Beate Fredriksen[1], Maria Rugenstein[2]and Rune Graversen[1,3]

[1]Department of Physics and Technology, UiT the Arctic University of Norway, Tromsø, Norway

[2]Colorado State University, Fort Collins, USA

[3]The Norwegian Meteorological Institute, Norway

Contents of this file

Introduction This document repeats Figures 1, 3 and 4 for all models and available RCP scenarios. For a description of the figures, see the NorESM1-M figures in the main manuscript.

Text S1 and S2 elaborates some of the mathematics needed to 1) derive the temperature response, and 2) understand the relationship between our linear model and the non-parametric linear models considered in other papers.

Table S1 in the end lists the piControl trend values used when subtracting linear trends from the variables of the abrupt4xCO$_2$ experiment.

————

November 5, 2021, 9:27am

:

Text S1: Deriving temperature response

To show that Eq. (7) is the solution of Eq. (6), we start by rewriting to:

$$\frac{d\mathbf{T}(t)}{dt} = \mathbf{C}^{-1}\mathbf{K}\mathbf{T}(t) + \mathbf{C}^{-1}\mathbf{F}(t)$$

We consider first the homogeneous problem

$$\frac{d\mathbf{T}(t)}{dt} = \mathbf{A}\mathbf{T}(t)$$

where $\mathbf{A} = \mathbf{C}^{-1}\mathbf{K}$. The matrix of possible solutions $\mathbf{x}_i(t)$ to this problem is the fundamental matrix

$$\mathbf{\Phi}(t) = [\mathbf{x}_1(t) \,|\, \mathbf{x}_2(t) \,|\, \ldots \,|\, \mathbf{x}_n(t)].$$

$e^{\mathbf{A}t}$ is a fundamental matrix when $\mathbf{A}$ consists of constant coefficients, since

$$\frac{d\mathbf{\Phi}(t)}{dt} = \frac{de^{\mathbf{A}t}}{dt} = \mathbf{A}e^{\mathbf{A}t} = \mathbf{A}\mathbf{\Phi}(t).$$

According to the variation of parameters formula for first-order linear systems $\frac{d\mathbf{x}}{dt} = \mathbf{P}(t)\mathbf{x} + \mathbf{f}(t)$, a particular solution is given by

$$\mathbf{x}_p(t) = \mathbf{\Phi}(t) \int \mathbf{\Phi}(t)^{-1}\mathbf{f}(t)dt$$

(see e.g. Edwards and Penney (2007)). For our problem, this means that the particular solution is

$$\mathbf{x}_p(t) = e^{\mathbf{A}t} \int e^{-\mathbf{A}t}\mathbf{C}^{-1}\mathbf{F}(t)dt.$$

Given an initial value $\mathbf{T}(0) = \mathbf{T}_0$, the full solution can be written as

$$\mathbf{T}(t) = e^{\mathbf{C}^{-1}\mathbf{K}t}\mathbf{T}_0 + \int_0^t e^{(t-s)\mathbf{C}^{-1}\mathbf{K}}\mathbf{C}^{-1}\mathbf{F}(s) \, ds,$$

or alternatively, if we know the full history of the system,

$$\mathbf{T}(t) = \int_{-\infty}^t e^{(t-s)\mathbf{C}^{-1}\mathbf{K}}\mathbf{C}^{-1}\mathbf{F}(s) \, ds.$$

November 5, 2021, 9:27am

Text S2: Relation to non-parametric impulse-response models

To find the relation between linear model considered here and linear models considered in e.g. Larson and Portmann (2016); Good, Gregory, and Lowe (2011); Good, Gregory, Lowe, and Andrews (2013), we start with the general equation from the end of Section 2.1: $T(t) = \int_{-\infty}^{t} G(t-s)F(s)ds$. As noted by Hasselmann, Sausen, Maier-Reimer, and Voss (1993), such a convolution integral can also describe a general climate state variable $\Phi(t)$ that responds linearly to a forcing:

$$\Phi(t) = \int_{0}^{t} G(t-s)F(s)ds \tag{1}$$

assuming $F(t) = 0$ for $t \leq 0$. If the forcing takes the form of a unit step-function, which is 0 for $t \leq 0$ and 1 for $t > 0$, the climate response is:

$$R(t) = \int_{0}^{t} G(t-s)ds$$

and $\frac{dR}{dt} = G(t)$. By performing an integration by parts, we note that Eq. (1) can be rewritten to

$$\Phi(t) = \int_{0}^{t} \frac{dF}{ds} R(t-s)ds \tag{2}$$

where the additional term $R(0)F(t) - R(t)F(0) = 0$ because $R(0) = 0$ and $F(0) = 0$. Discretizing this integral using time steps of years results in the same type of sum used by Larson and Portmann (2016); Good et al. (2011, 2013):

$$\Phi_i = \sum_{j=0}^{i} \Delta F_j R_{i-j} \tag{3}$$

If using a response to a step-forcing ΔF_s instead of the unit response, the response needs to be normalized by ΔF_s.

November 5, 2021, 9:27am

References

Edwards, C., & Penney, D. (2007). *Differential equations and boundary value problems: Computing and modelling (Fourth edition)*. Pearson.

Good, P., Gregory, J. M., & Lowe, J. A. (2011). A step-response simple climate model to reconstruct and interpret AOGCM projections. *Geophysical Research Letters*, *38*, L01703. https://doi.org/10.1029/2010GL045208

Good, P., Gregory, J. M., Lowe, J. A., & Andrews, T. (2013). Abrupt CO2 experiments as tools for predicting and understanding CMIP5 representative concentration pathway projections. *Climate Dynamics*, *40*(3), 1041–1053. https://doi.org/10.1007/s00382-012-1410-4

Hasselmann, K., Sausen, R., Maier-Reimer, E., & Voss, R. (1993). On the cold start problem in transient simulations with coupled atmosphere-ocean models. *Climate Dynamics*, *9*(6), 53–61. https://doi.org/10.1007/BF00210008

Larson, E. J. L., & Portmann, R. W. (2016). A Temporal Kernel Method to Compute Effective Radiative Forcing in CMIP5 Transient Simulations. *Journal of Climate*, *29*(4), 1497-1509. https://doi.org/10.1175/JCLI-D-15-0577.1
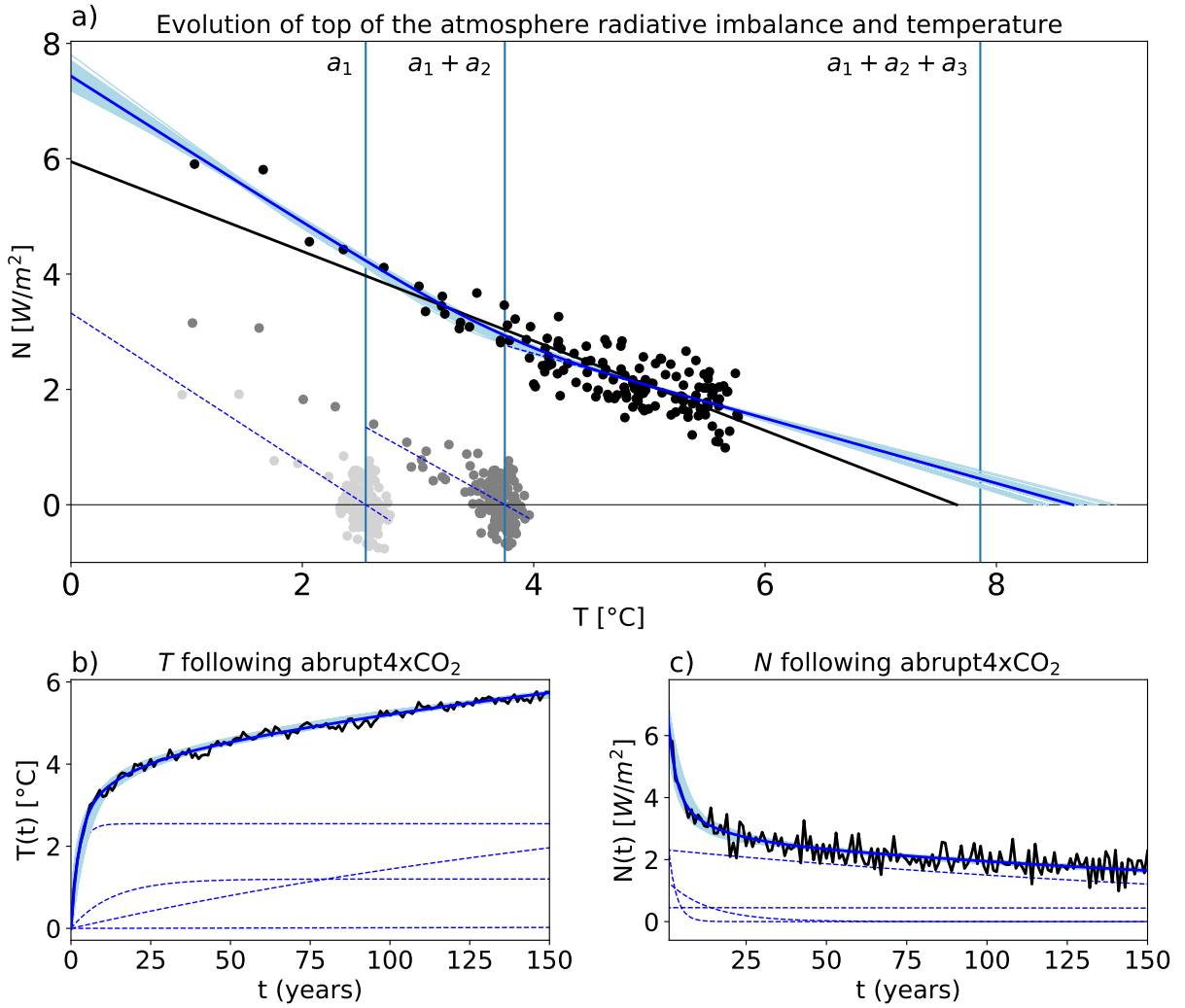
Figure S1. As Figure 1, but for the model ACCESS1-0.
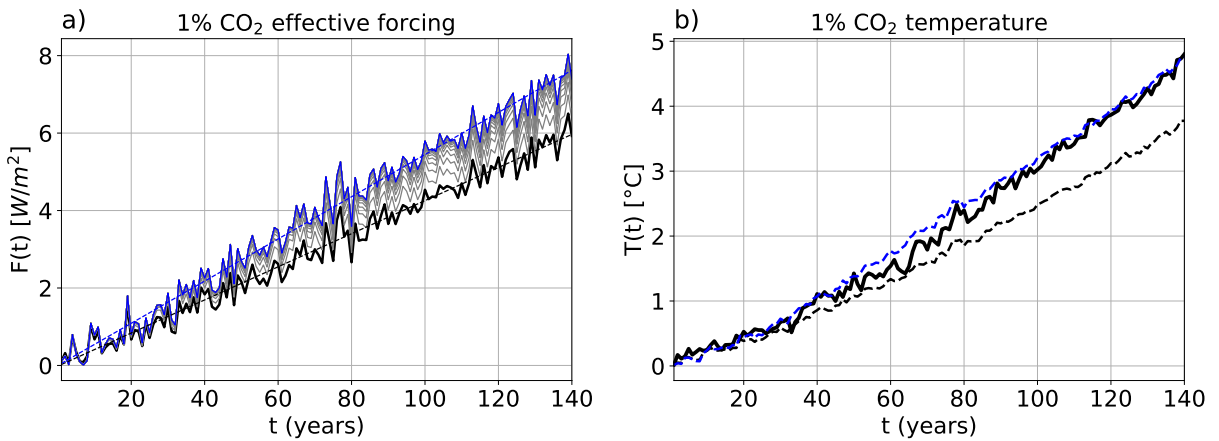
Figure S2. As Figure 3, but for the model ACCESS1-0.

:
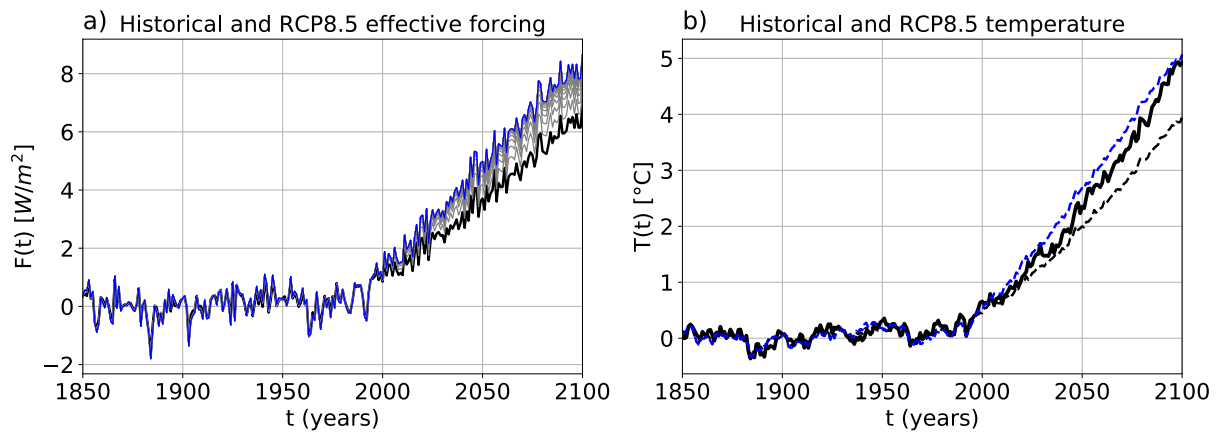
Figure S3. As Figure 4, but for the model ACCESS1-0.
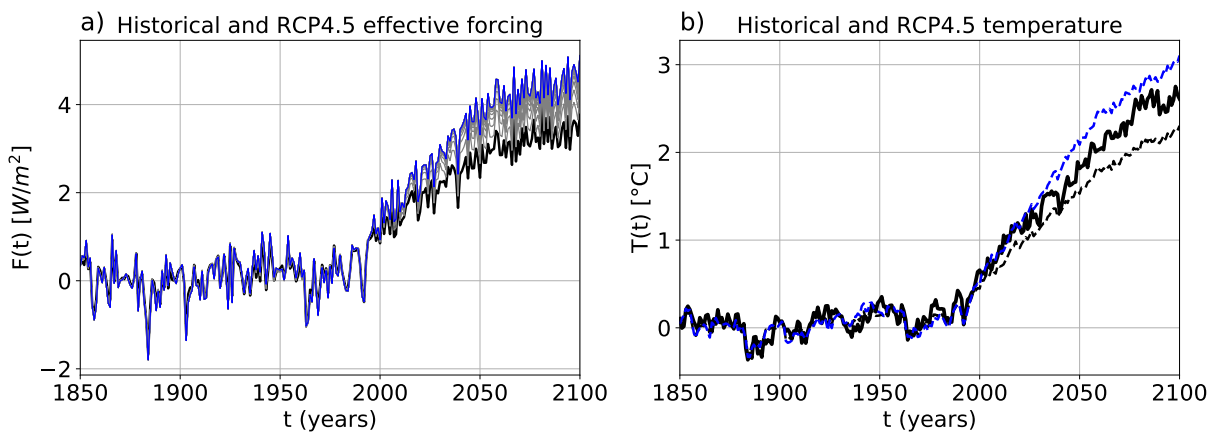
Figure S4. As Figure 4, but for the model ACCESS1-0 and experiment RCP4.5.

November 5, 2021, 9:27am

a) Evolution of top of the atmosphere radiative imbalance and temperature
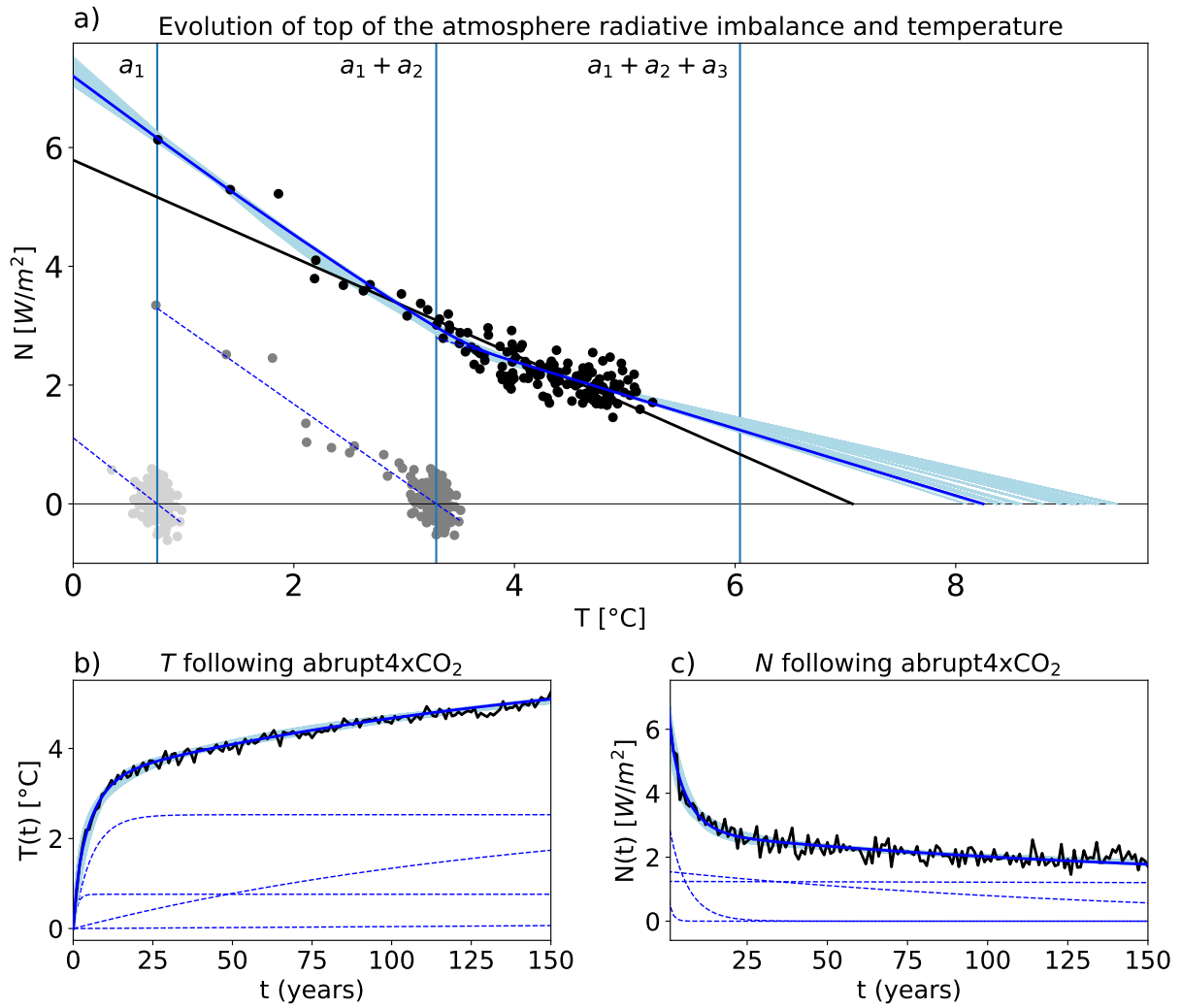
Figure S5. As Figure 1, but for the model ACCESS1-3.
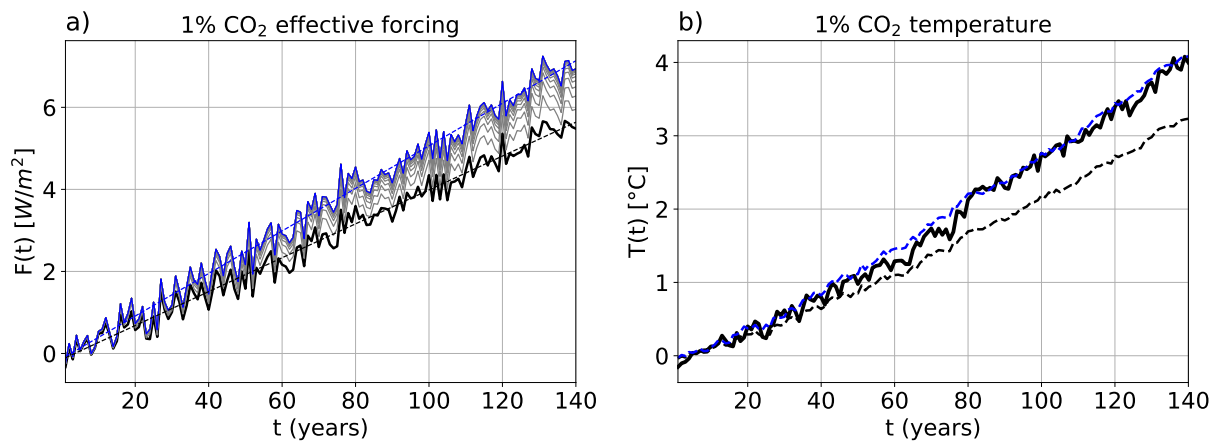
Figure S6. As Figure 3, but for the model ACCESS1-3.
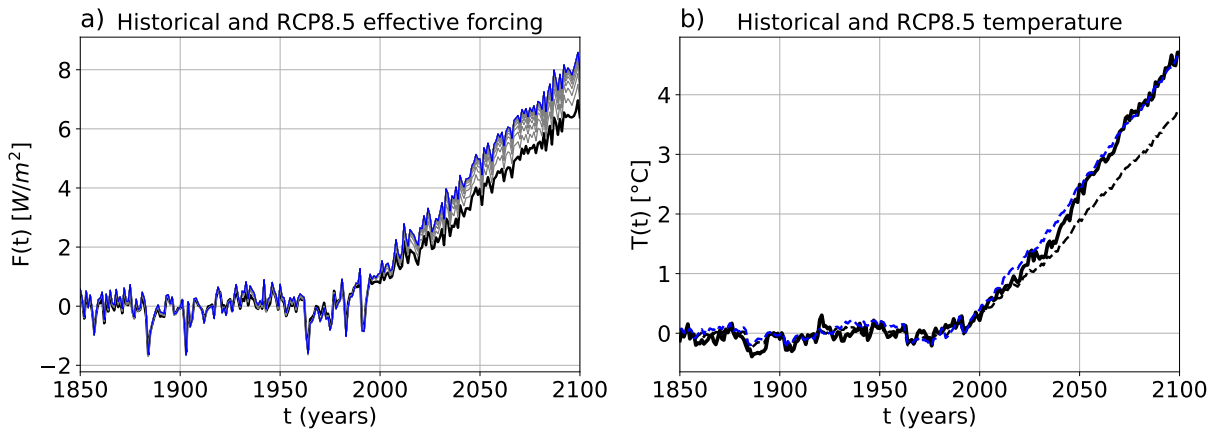
Figure S7. As Figure 4, but for the model ACCESS1-3.
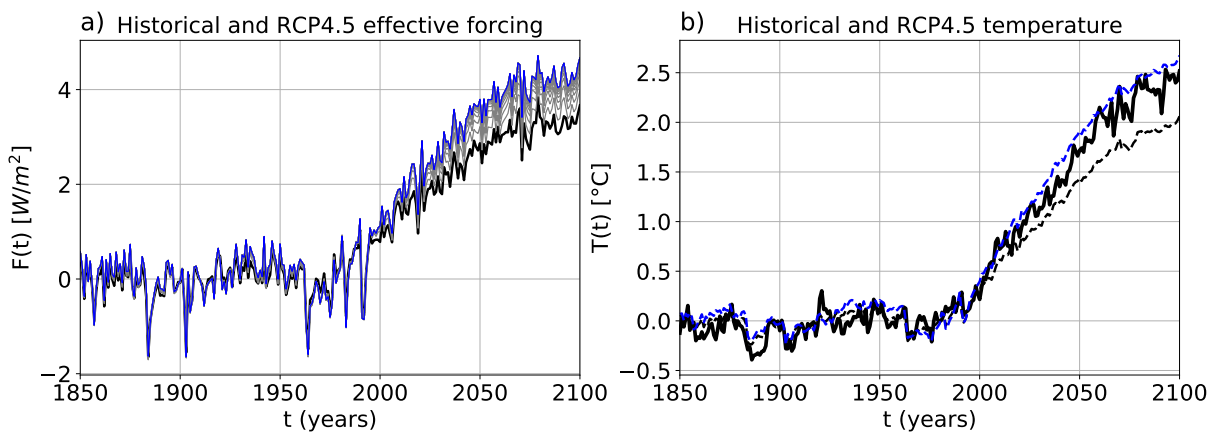
**Figure S8.** As Figure 4, but for the model ACCESS1-3 and experiment RCP4.5.

a) Evolution of top of the atmosphere radiative imbalance and temperature

b) T following abrupt4xCO$_2$

c) N following abrupt4xCO$_2$
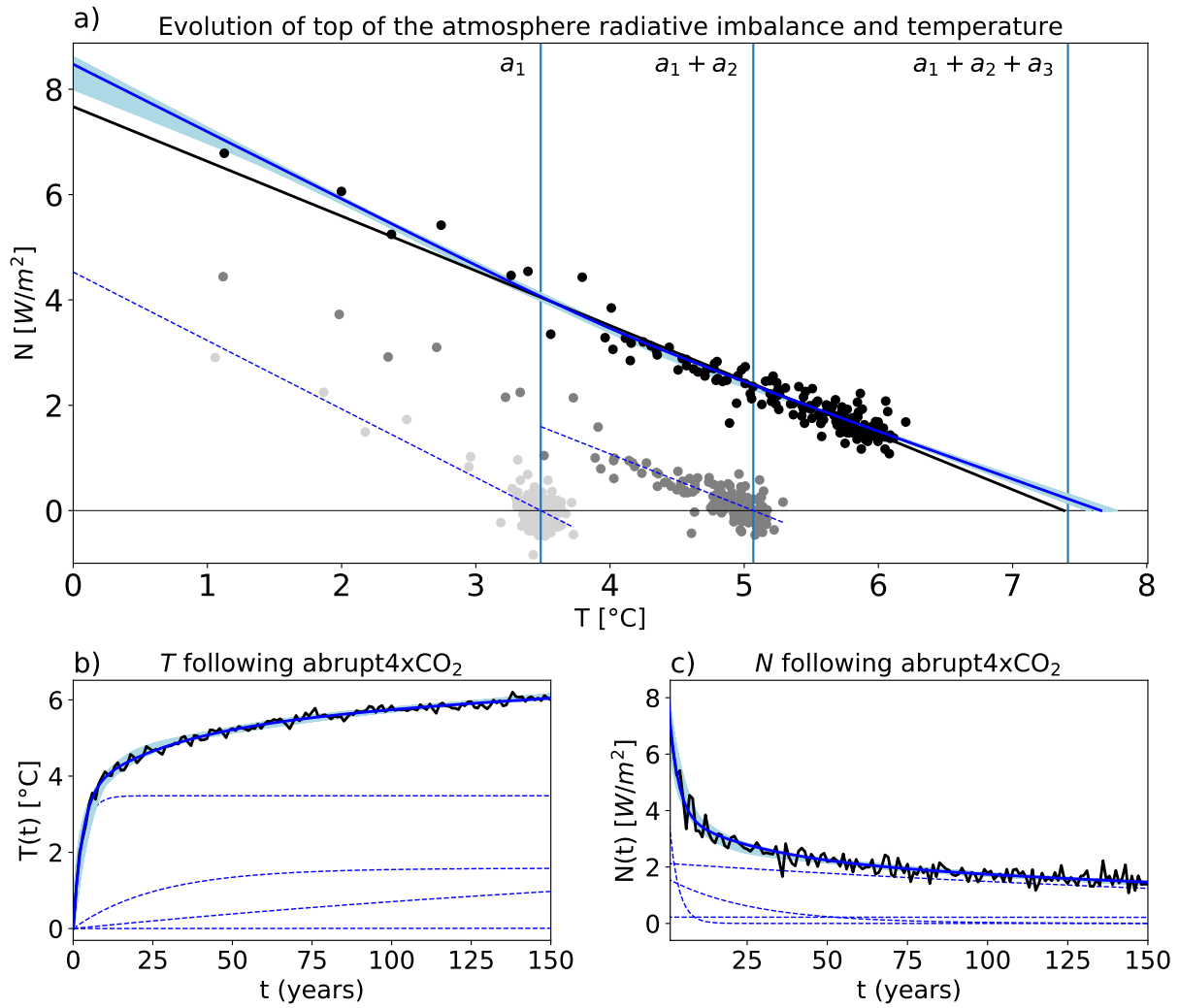
Figure S9. As Figure 1, but for the model CanESM2.

a) 1% CO$_2$ effective forcing

b) 1% CO$_2$ temperature
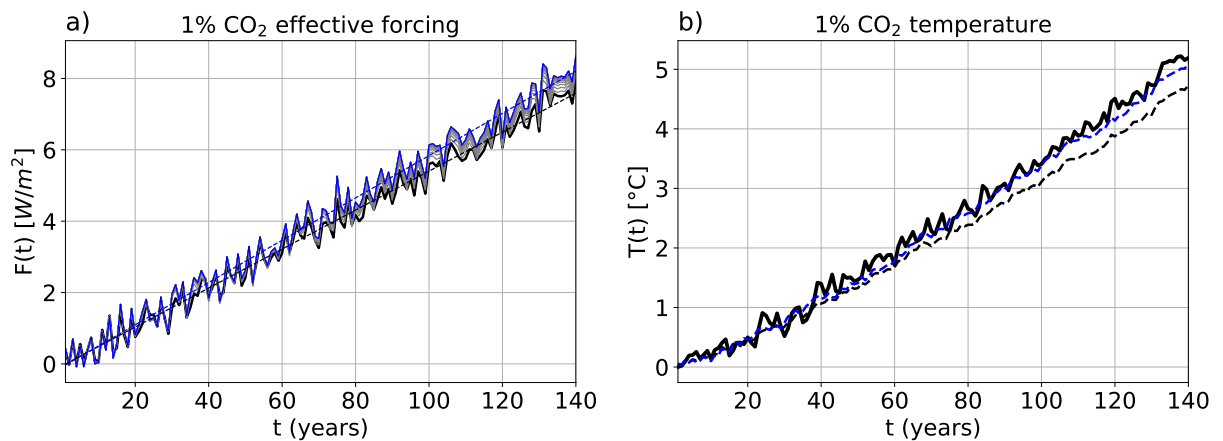
Figure S10. As Figure 3, but for the model CanESM2.

November 5, 2021, 9:27am
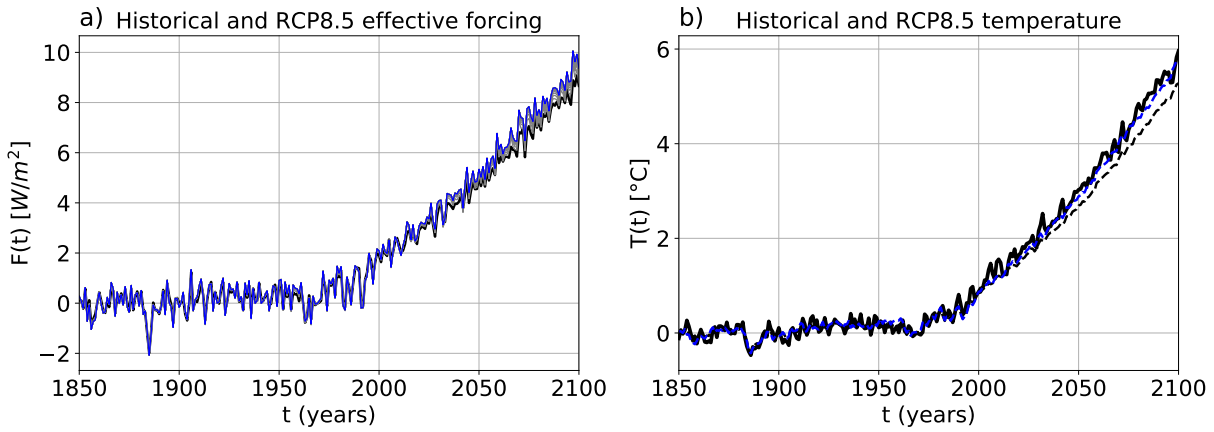
Figure S11. As Figure 4, but for the model CanESM2.
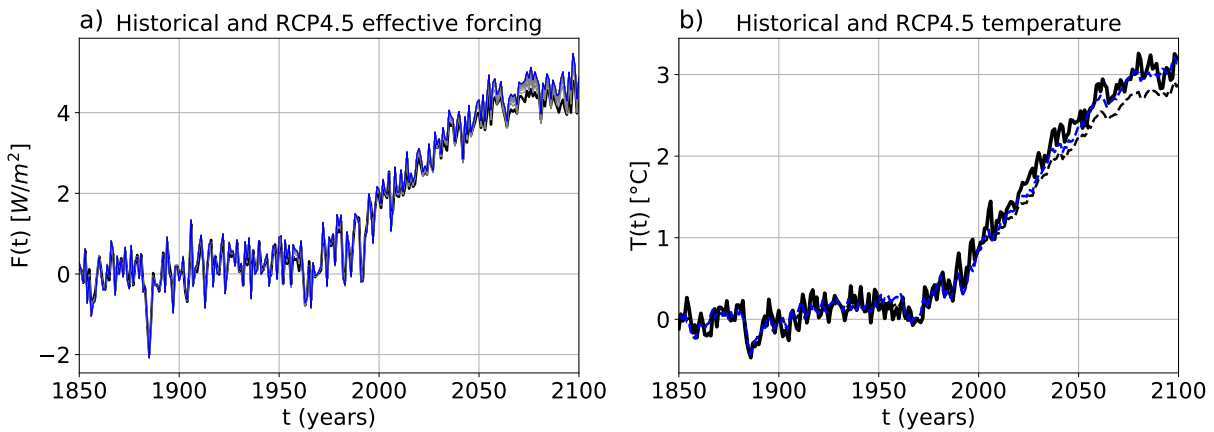
Figure S12. As Figure 4, but for the model CanESM2 and experiment RCP4.5.
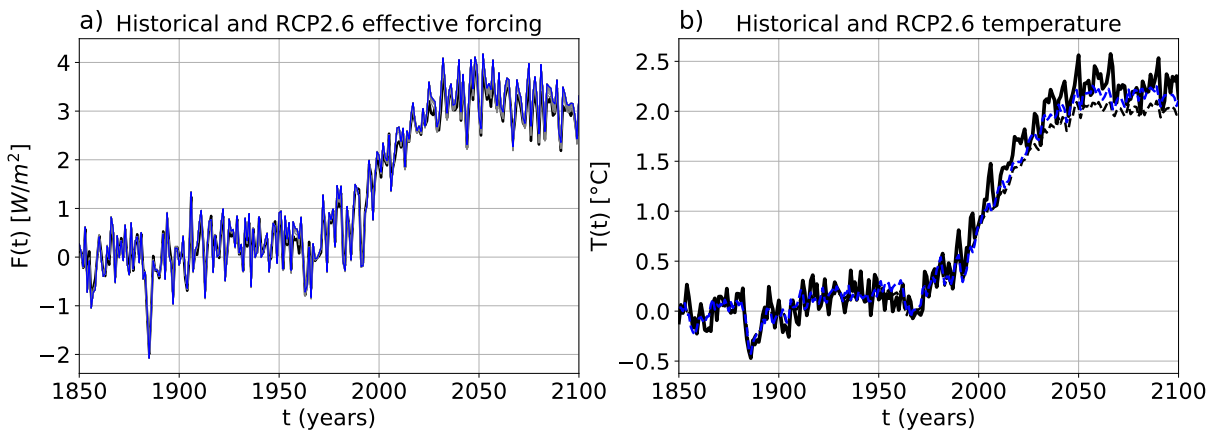
**Figure S13.** As Figure 4, but for the model CanESM2 and experiment RCP2.6.

a) Evolution of top of the atmosphere radiative imbalance and temperature

b) *T* following abrupt4xCO$_2$

c) *N* following abrupt4xCO$_2$
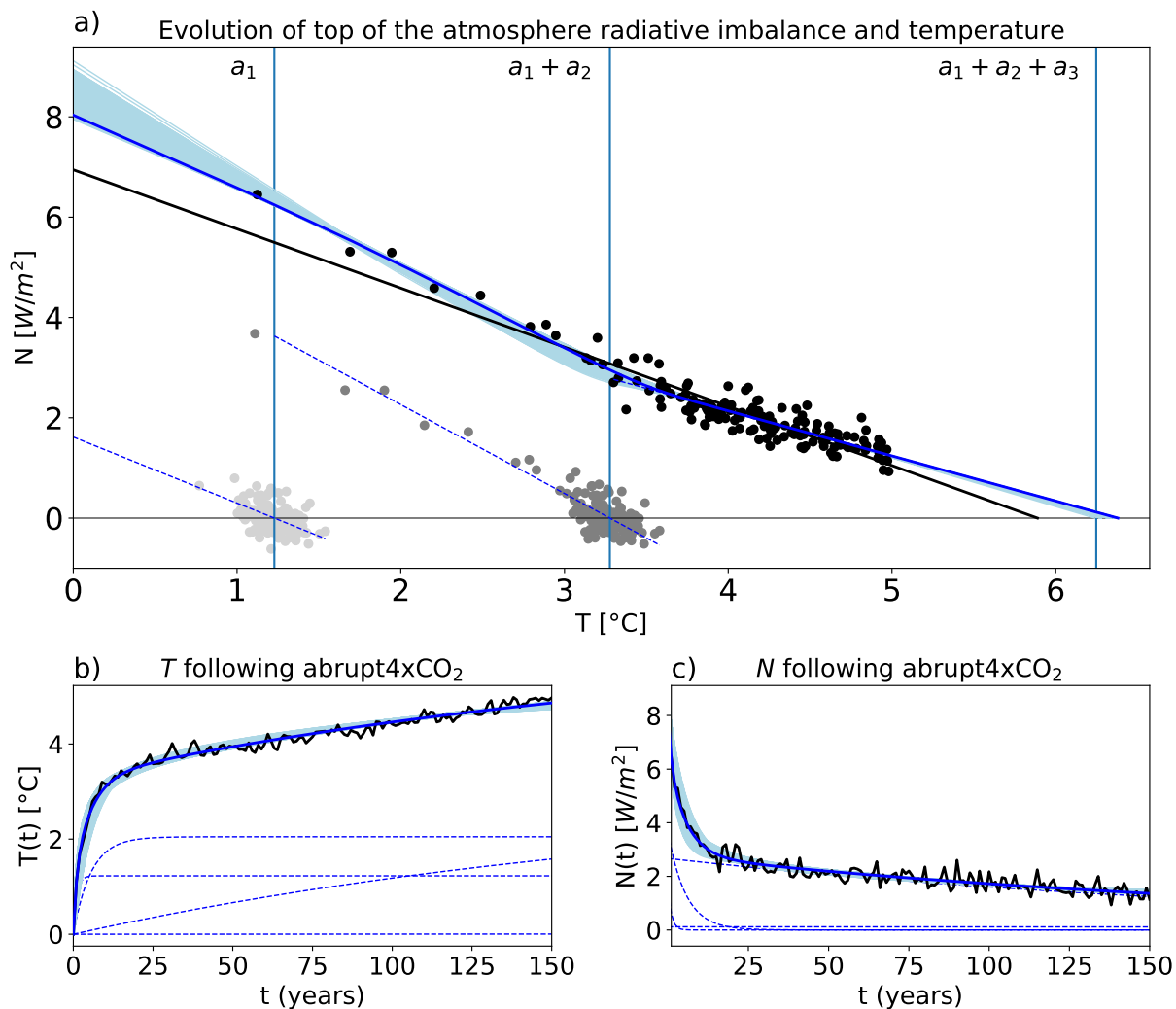
Figure S14. As Figure 1, but for the model CCSM4.

a) 1% CO$_2$ effective forcing

b) 1% CO$_2$ temperature
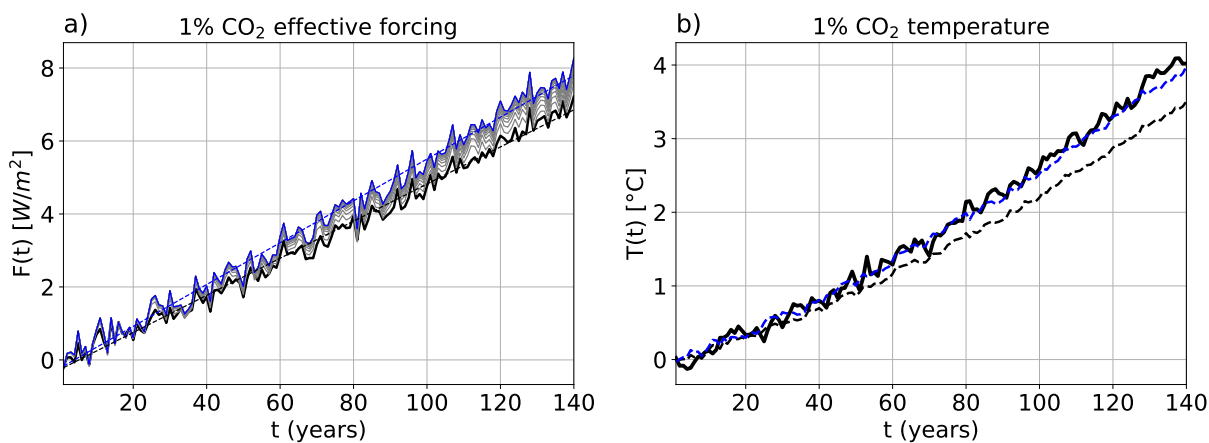
Figure S15. As Figure 3, but for the model CCSM4.
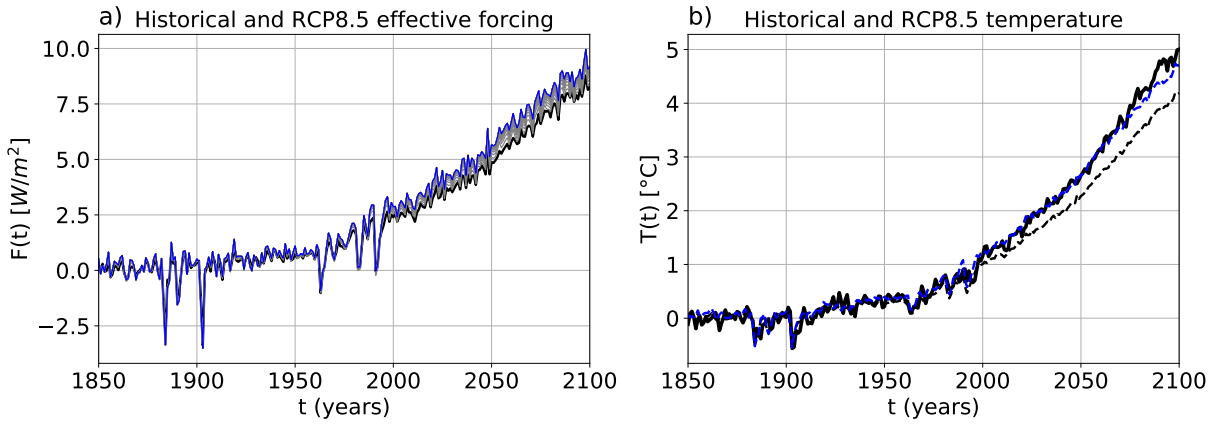
Figure S16. As Figure 4, but for the model CCSM4.
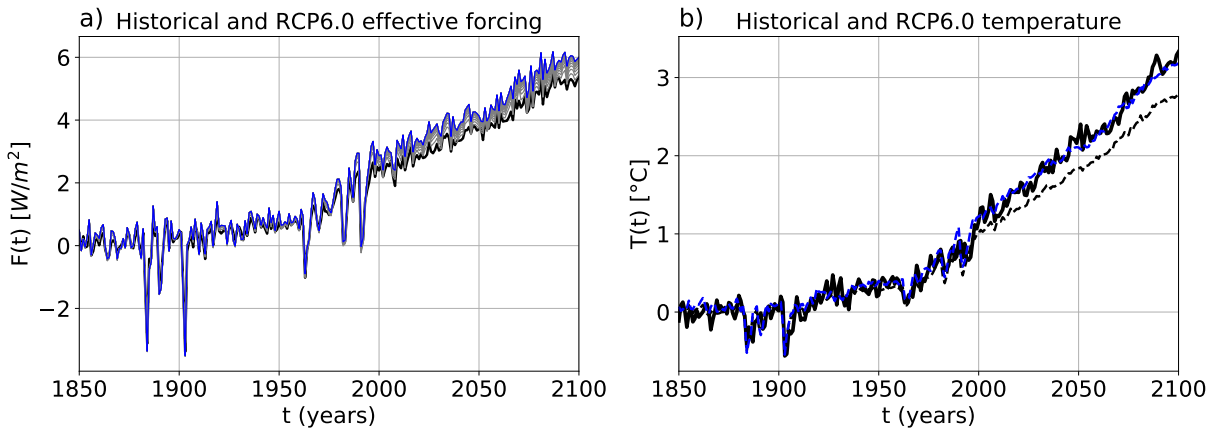
Figure S17. As Figure 4, but for the model CCSM4 and experiment RCP6.0.
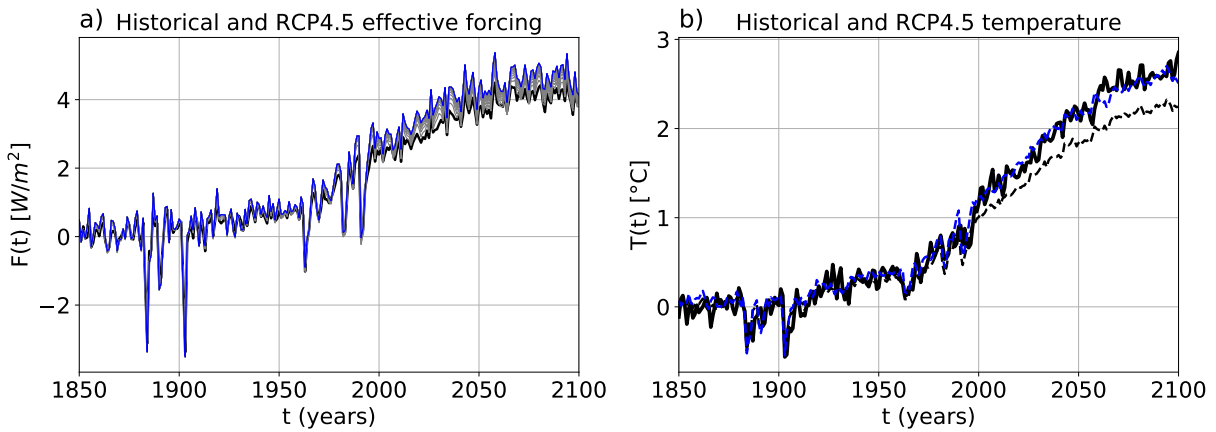
Figure S18. As Figure 4, but for the model CCSM4 and experiment RCP4.5.
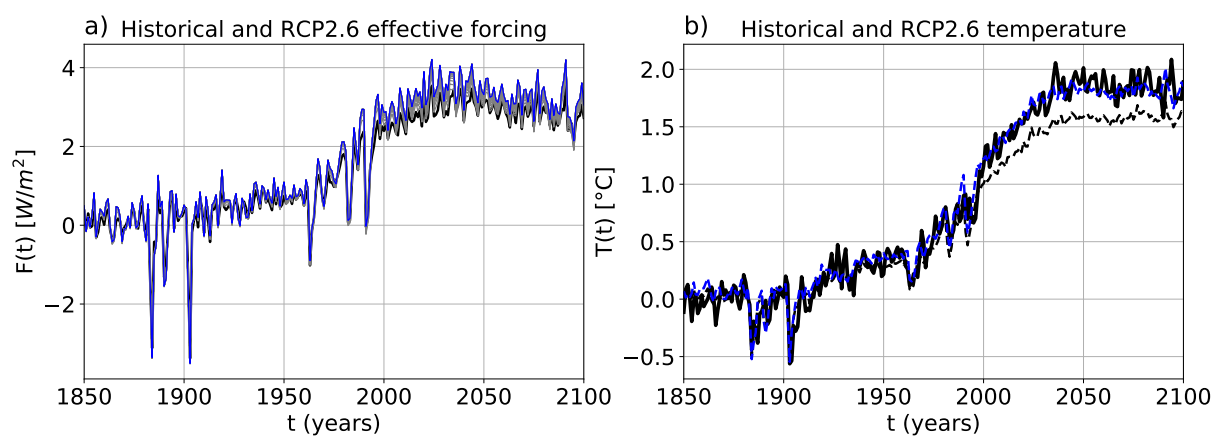
Figure S19. As Figure 4, but for the model CCSM4 and experiment RCP2.6.
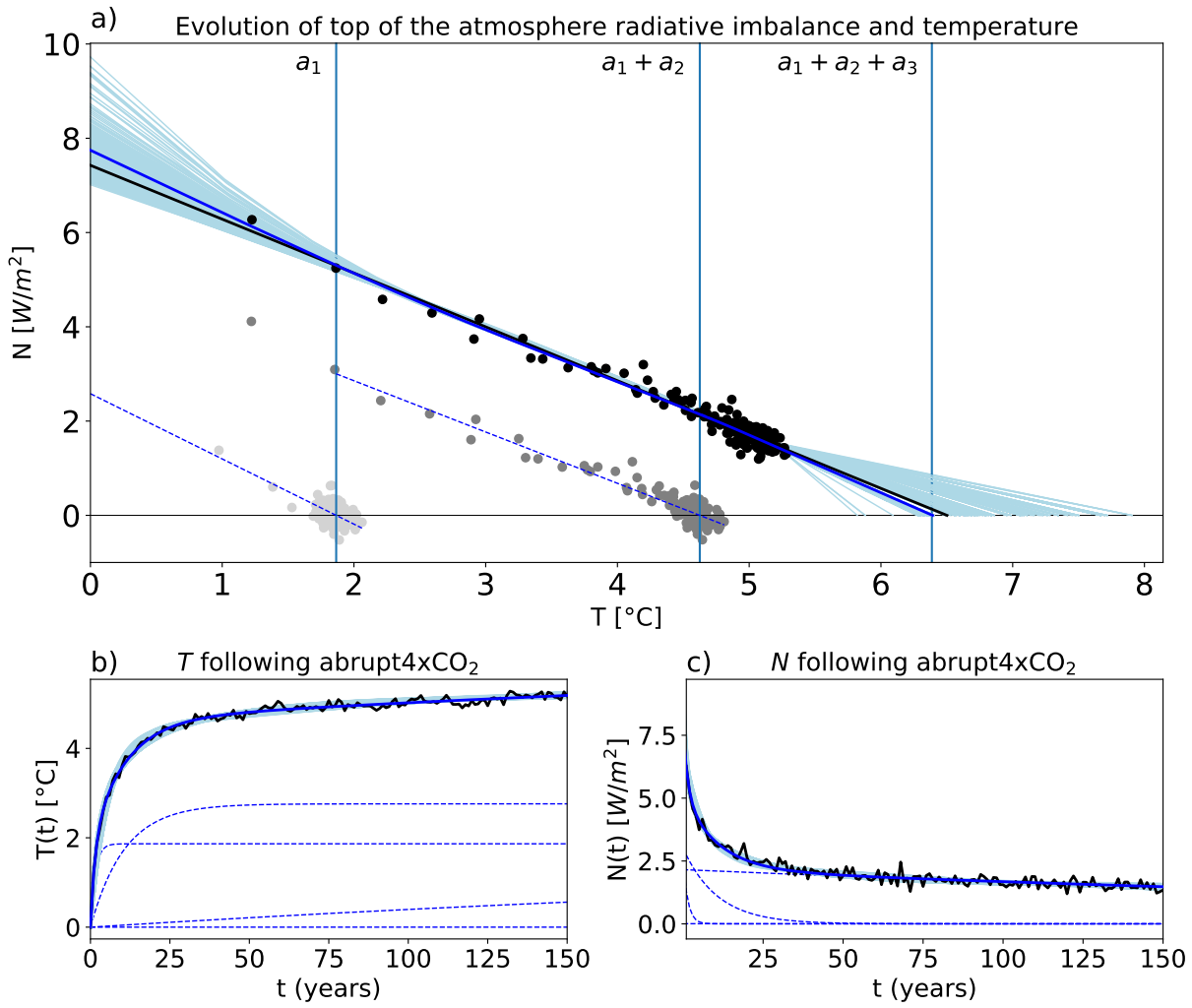
Figure S20. As Figure 1, but for the model CNRM-CM5.
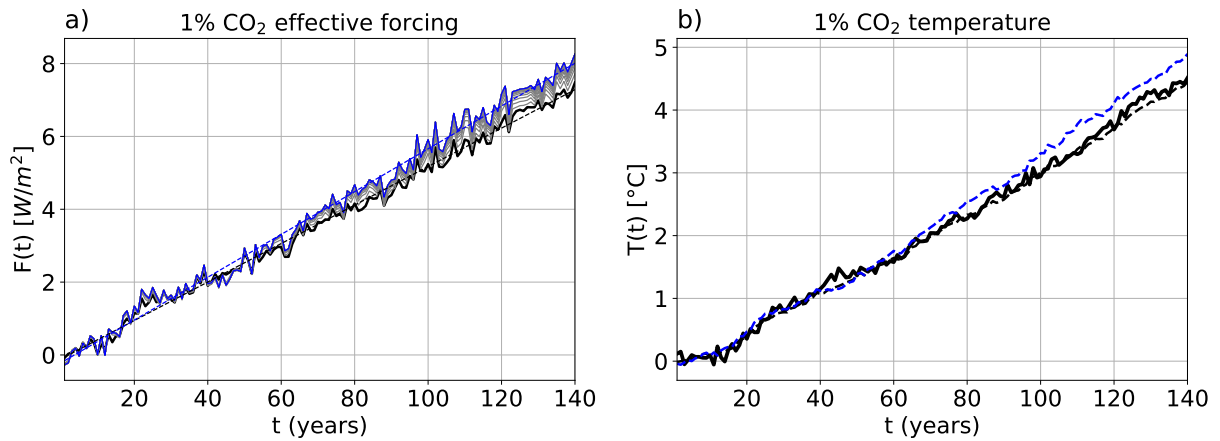
Figure S21. As Figure 3, but for the model CNRM-CM5.

November 5, 2021, 9:27am
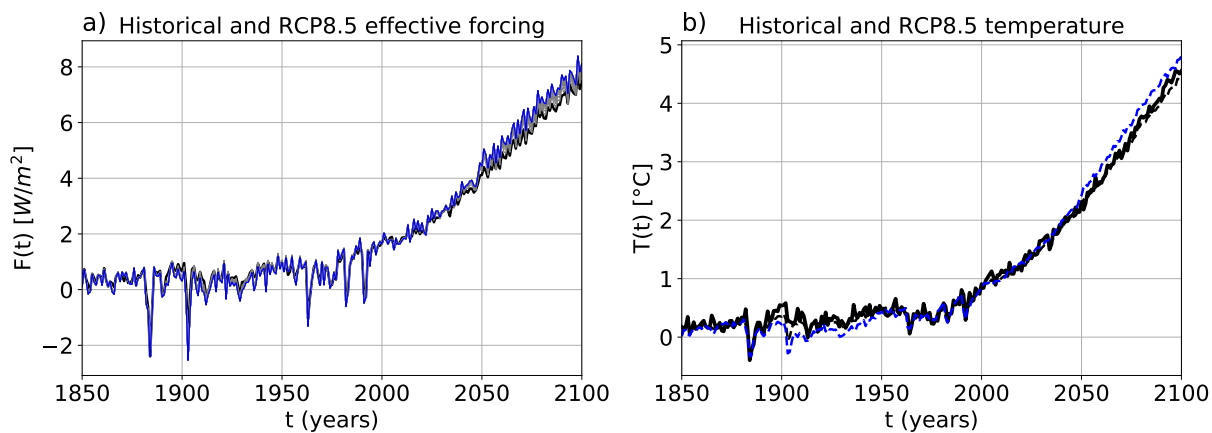
Figure S22. As Figure 4, but for the model CNRM-CM5.
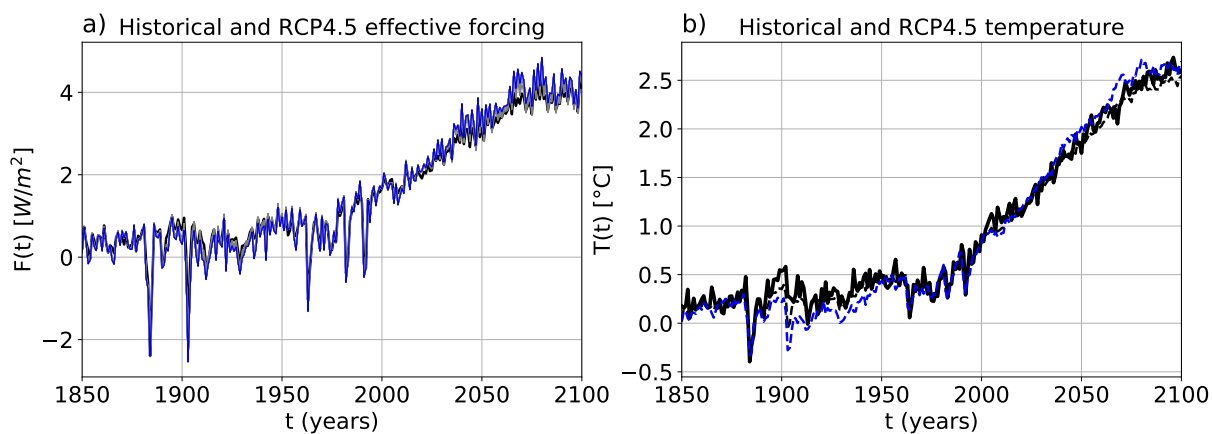
Figure S23. As Figure 4, but for the model CNRM-CM5 and experiment RCP4.5.
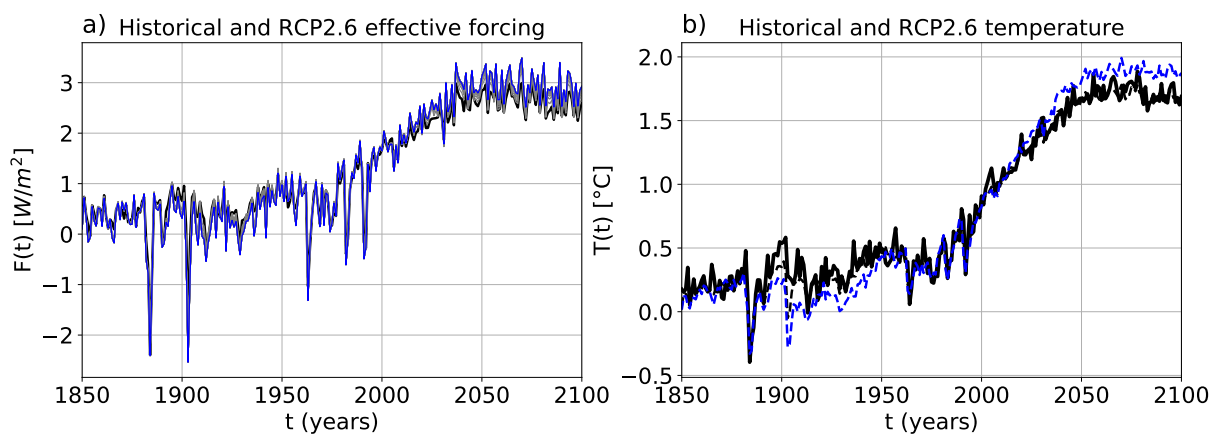
**Figure S24.** As Figure 4, but for the model CNRM-CM5 and experiment RCP2.6.

November 5, 2021, 9:27am

a)
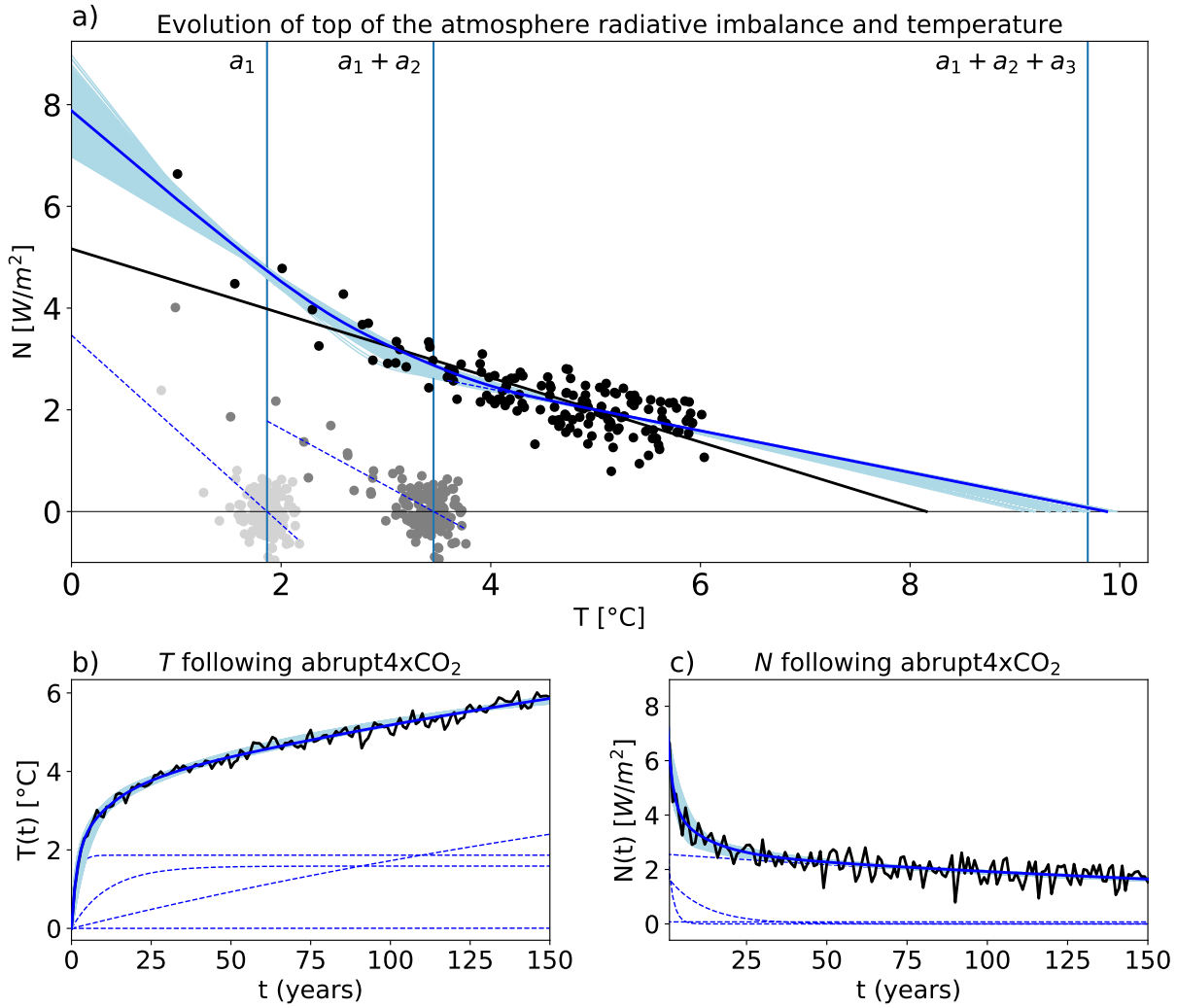
Figure S25. As Figure 1, but for the model CSIRO-Mk3-6-0.
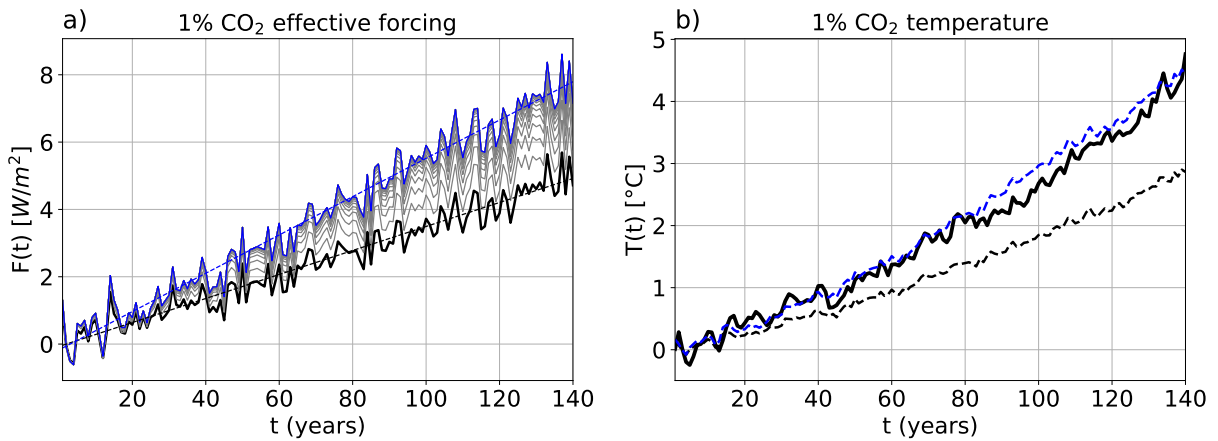
Figure S26. As Figure 3, but for the model CSIRO-Mk3-6-0.

November 5, 2021, 9:27am
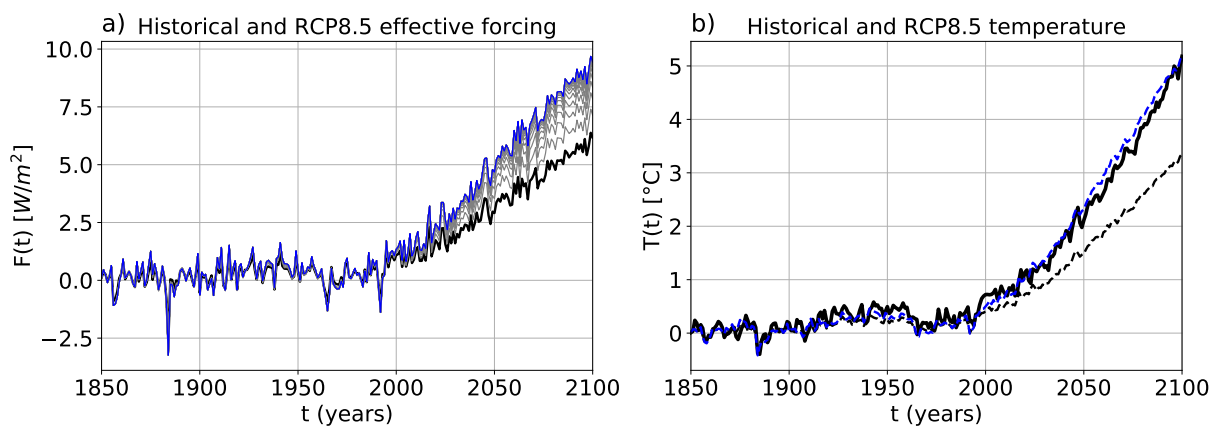
Figure S27. As Figure 4, but for the model CSIRO-Mk3-6-0.
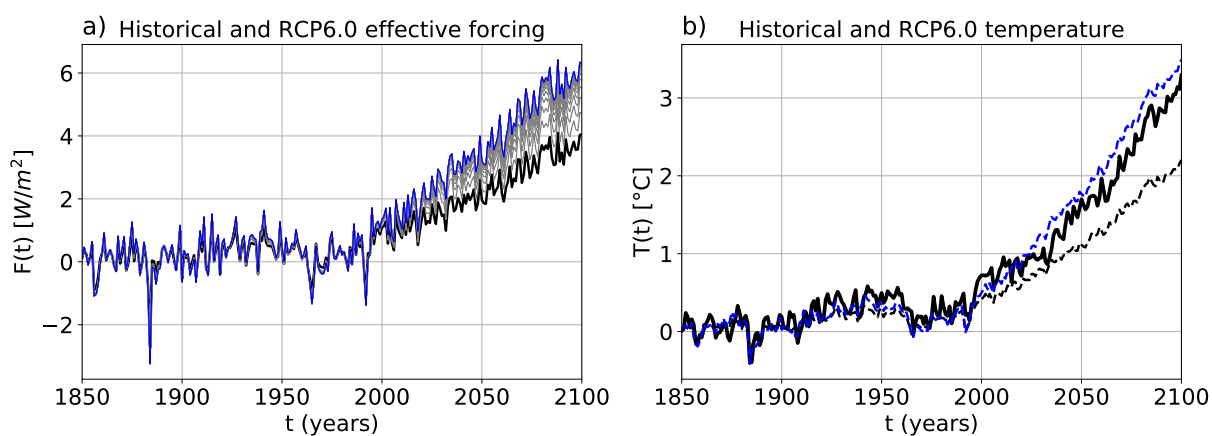
Figure S28. As Figure 4, but for the model CSIRO-Mk3-6-0 and experiment RCP6.0.
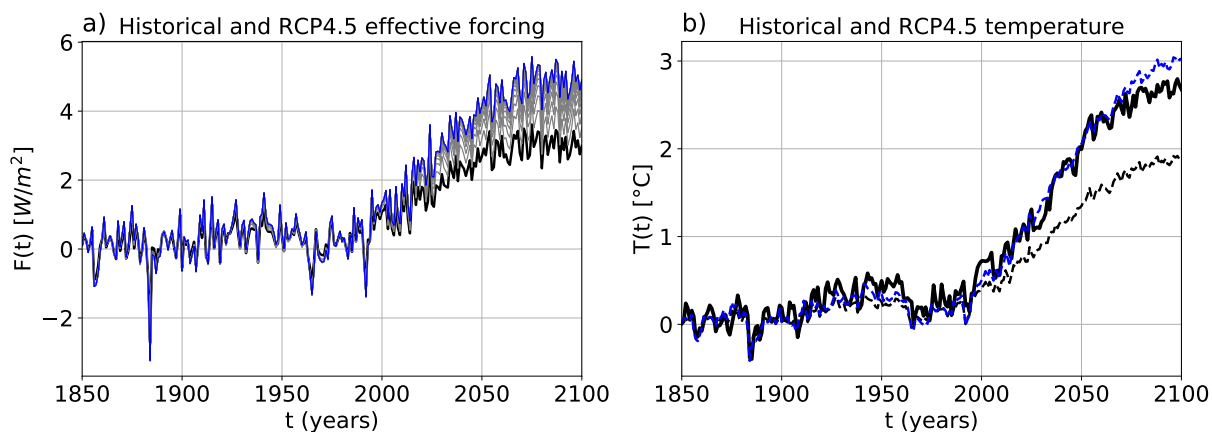
Figure S29. As Figure 4, but for the model CSIRO-Mk3-6-0 and experiment RCP4.5.

a) Historical and RCP2.6 effective forcing

b) Historical and RCP2.6 temperature
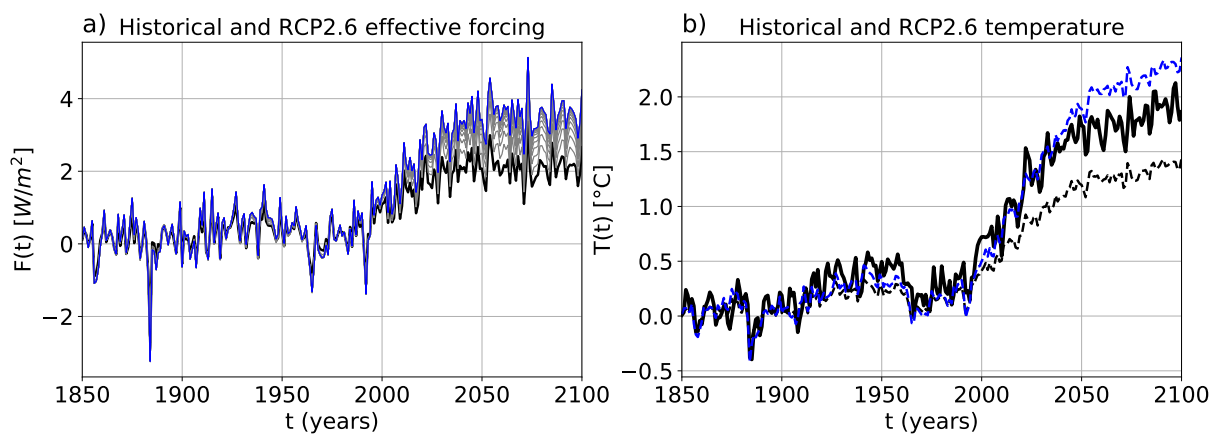
Figure S30. As Figure 4, but for the model CSIRO-Mk3-6-0 and experiment RCP2.6.

a) Evolution of top of the atmosphere radiative imbalance and temperature

b) T following abrupt4xCO$_2$

c) N following abrupt4xCO$_2$
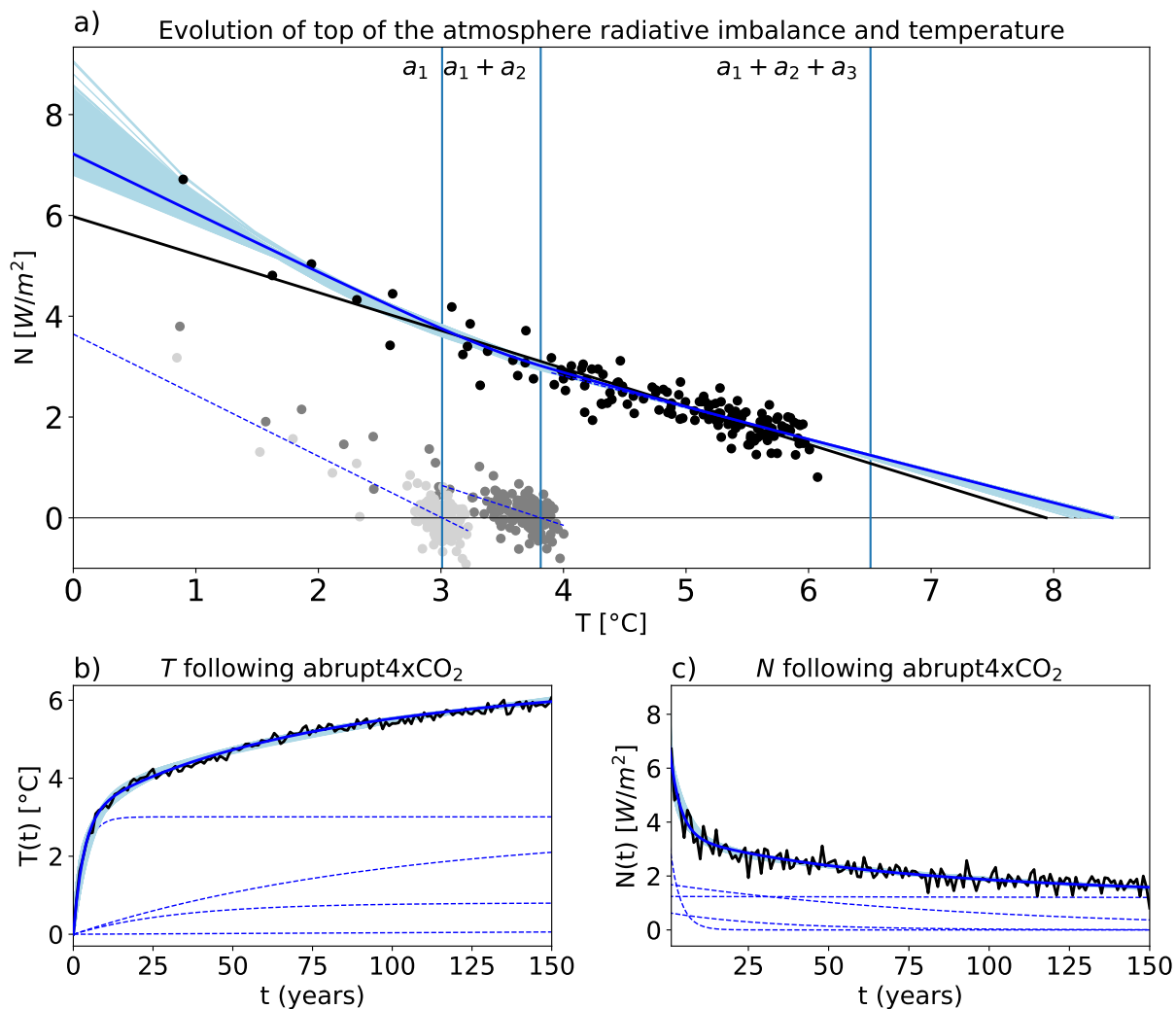
Figure S31. As Figure 1, but for the model GFDL-CM3.

a) 1% CO$_2$ effective forcing

b) 1% CO$_2$ temperature
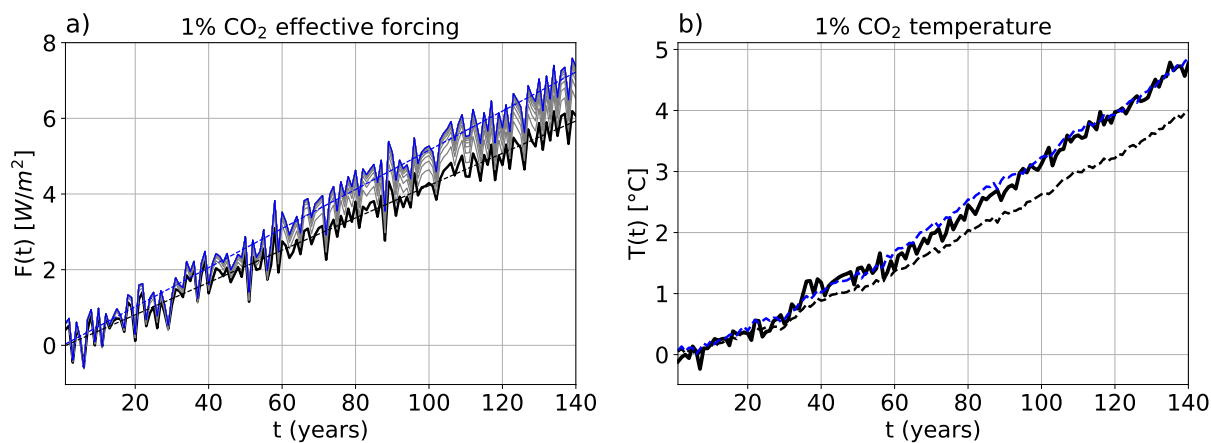
Figure S32. As Figure 3, but for the model GFDL-CM3.

:
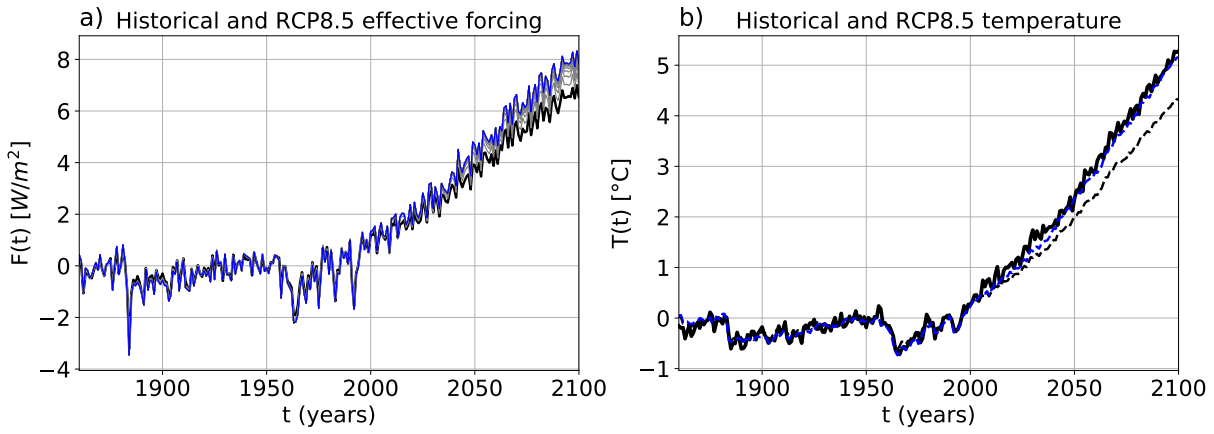
Figure S33. As Figure 4, but for the model GFDL-CM3.
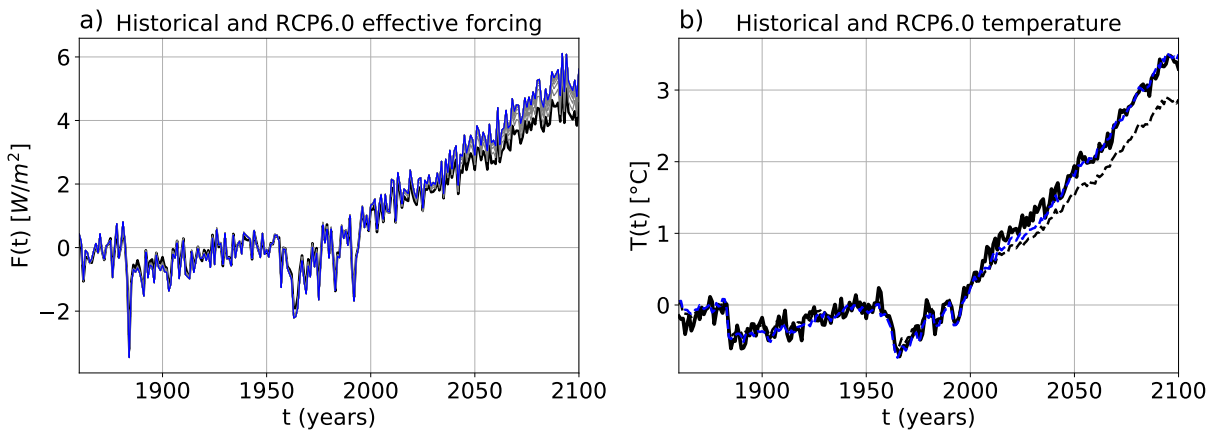
Figure S34. As Figure 4, but for the model GFDL-CM3 and experiment RCP6.0.
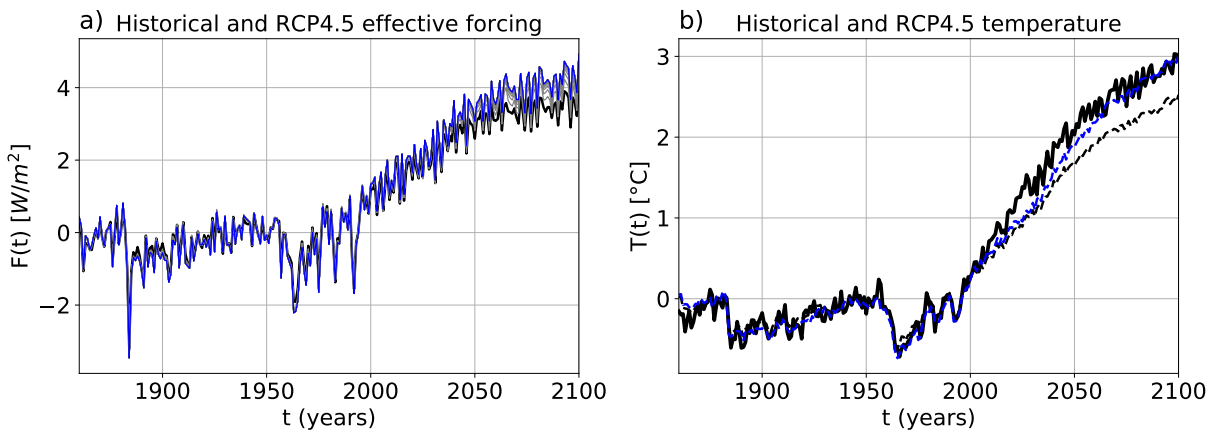
Figure S35. As Figure 4, but for the model GFDL-CM3 and experiment RCP4.5.
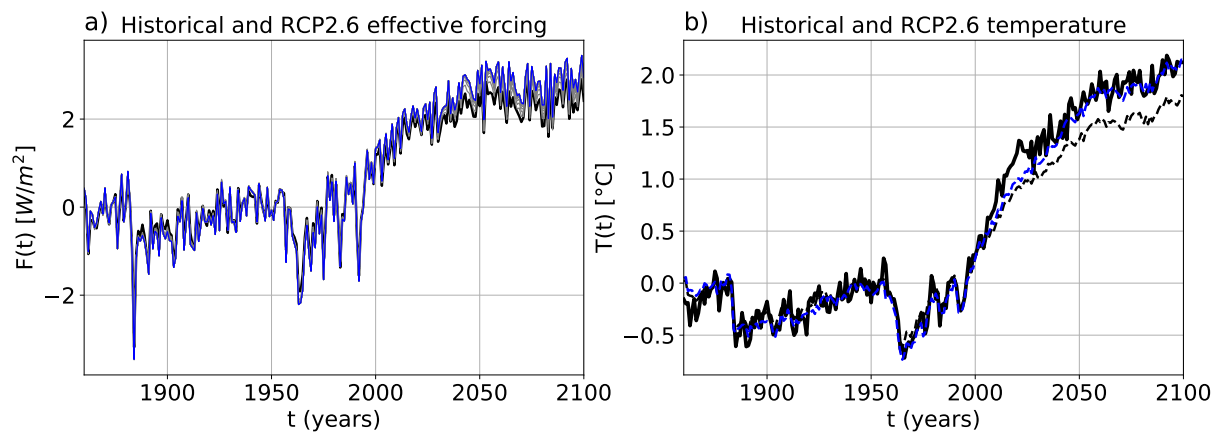
Figure S36. As Figure 4, but for the model GFDL-CM3 and experiment RCP2.6.

:
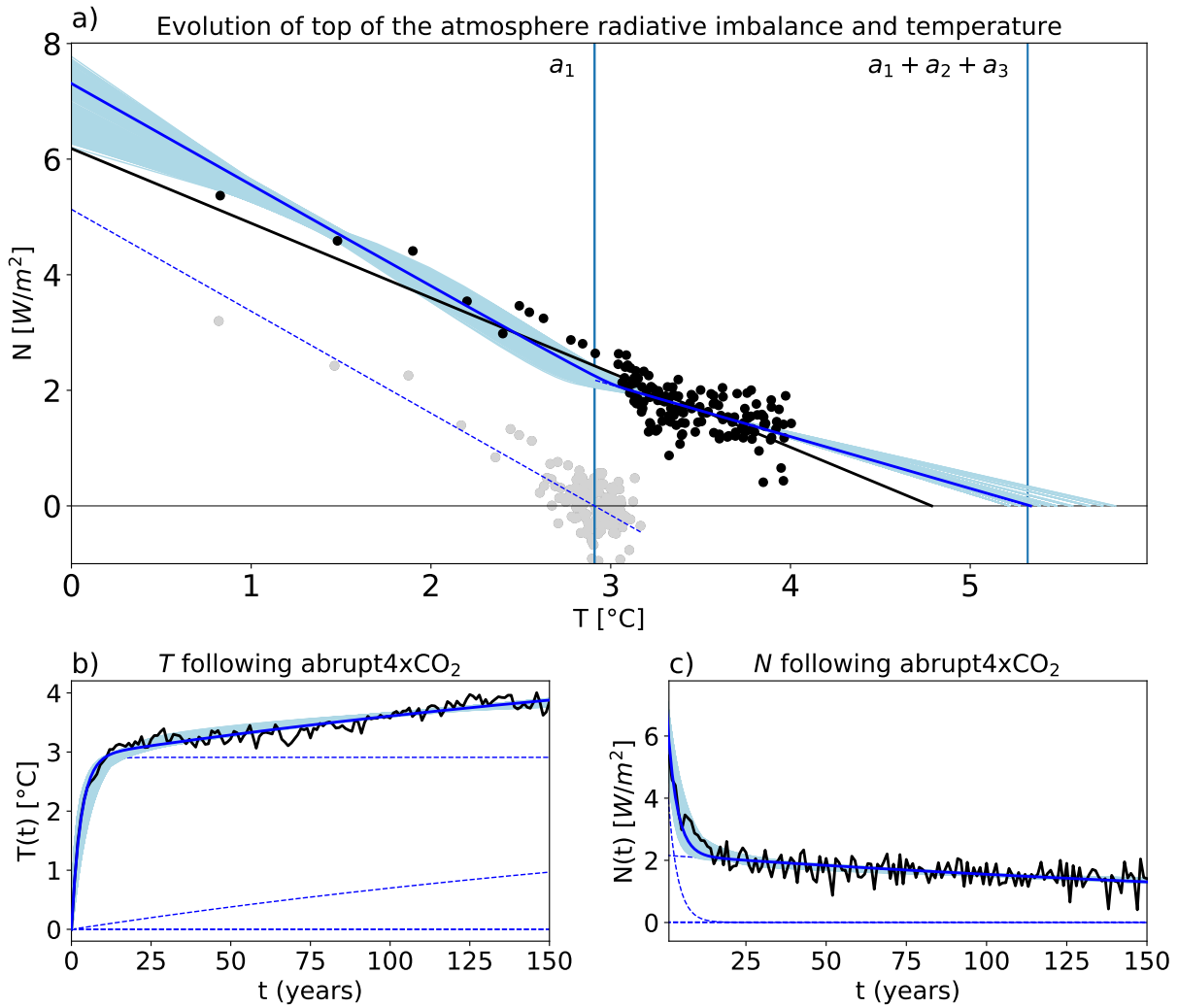
Figure S37. As Figure 1, but for the model GFDL-ESM2G.
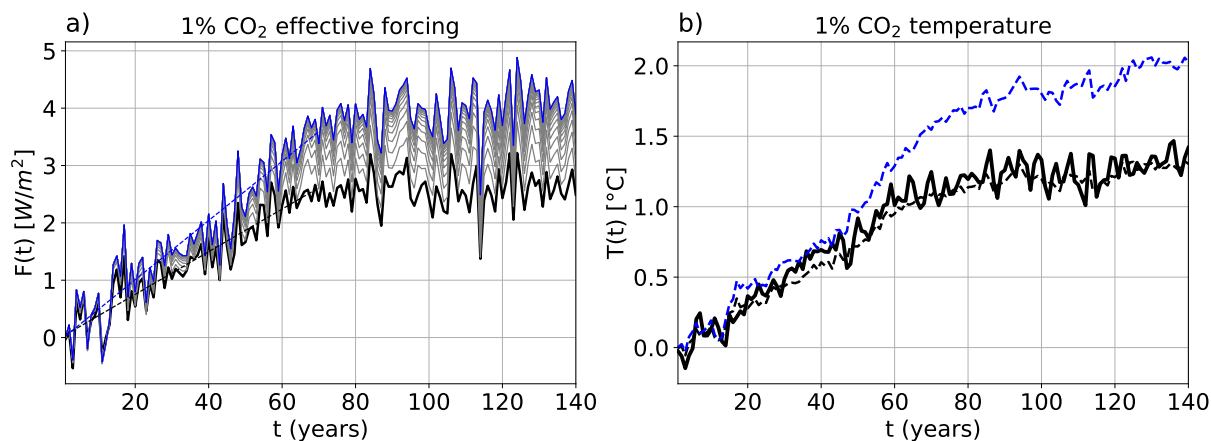
Figure S38. As Figure 3, but for the model GFDL-ESM2G. Note that in this model CO_2 increases only until we reach a doubling after 70 years.
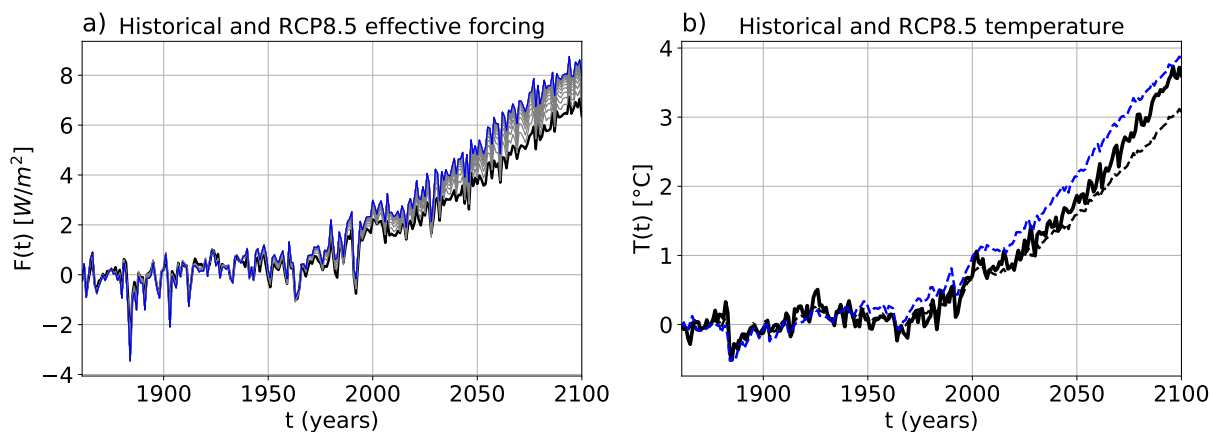
Figure S39. As Figure 4, but for the model GFDL-ESM2G.
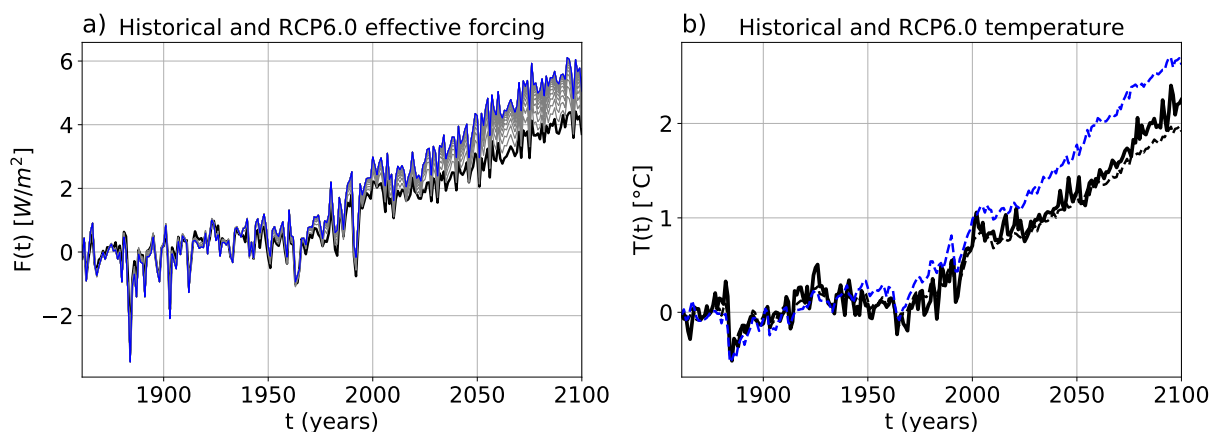
**Figure S40.** As Figure 4, but for the model GFDL-ESM2G and experiment RCP6.0.

November 5, 2021, 9:27am
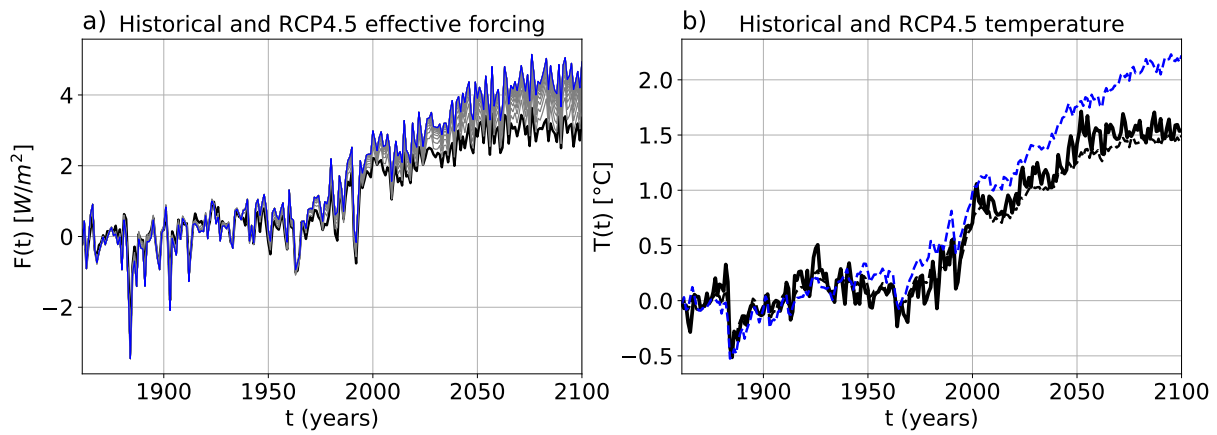
Figure S41. As Figure 4, but for the model GFDL-ESM2G and experiment RCP4.5.
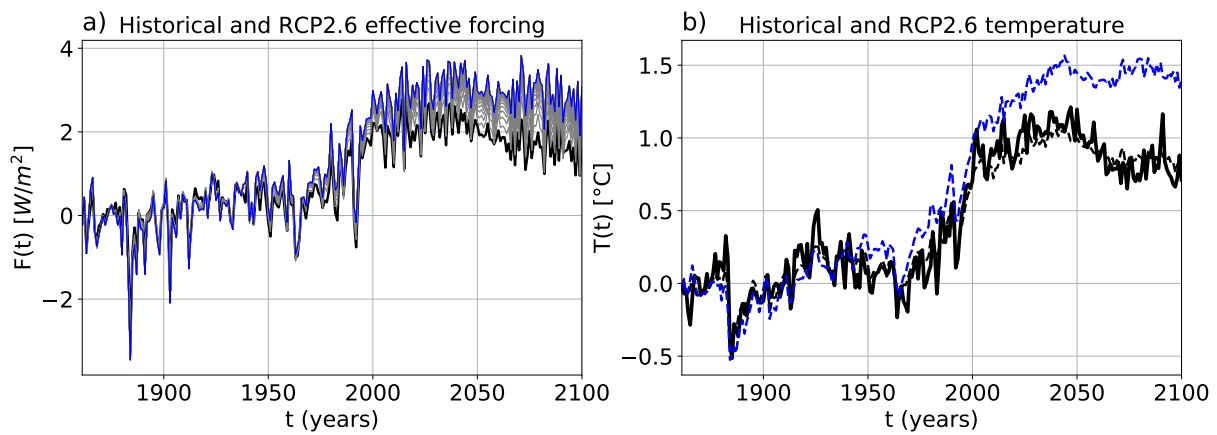
Figure S42. As Figure 4, but for the model GFDL-ESM2G and experiment RCP2.6.

a) Evolution of top of the atmosphere radiative imbalance and temperature

b) *T* following abrupt4xCO$_2$

c) *N* following abrupt4xCO$_2$
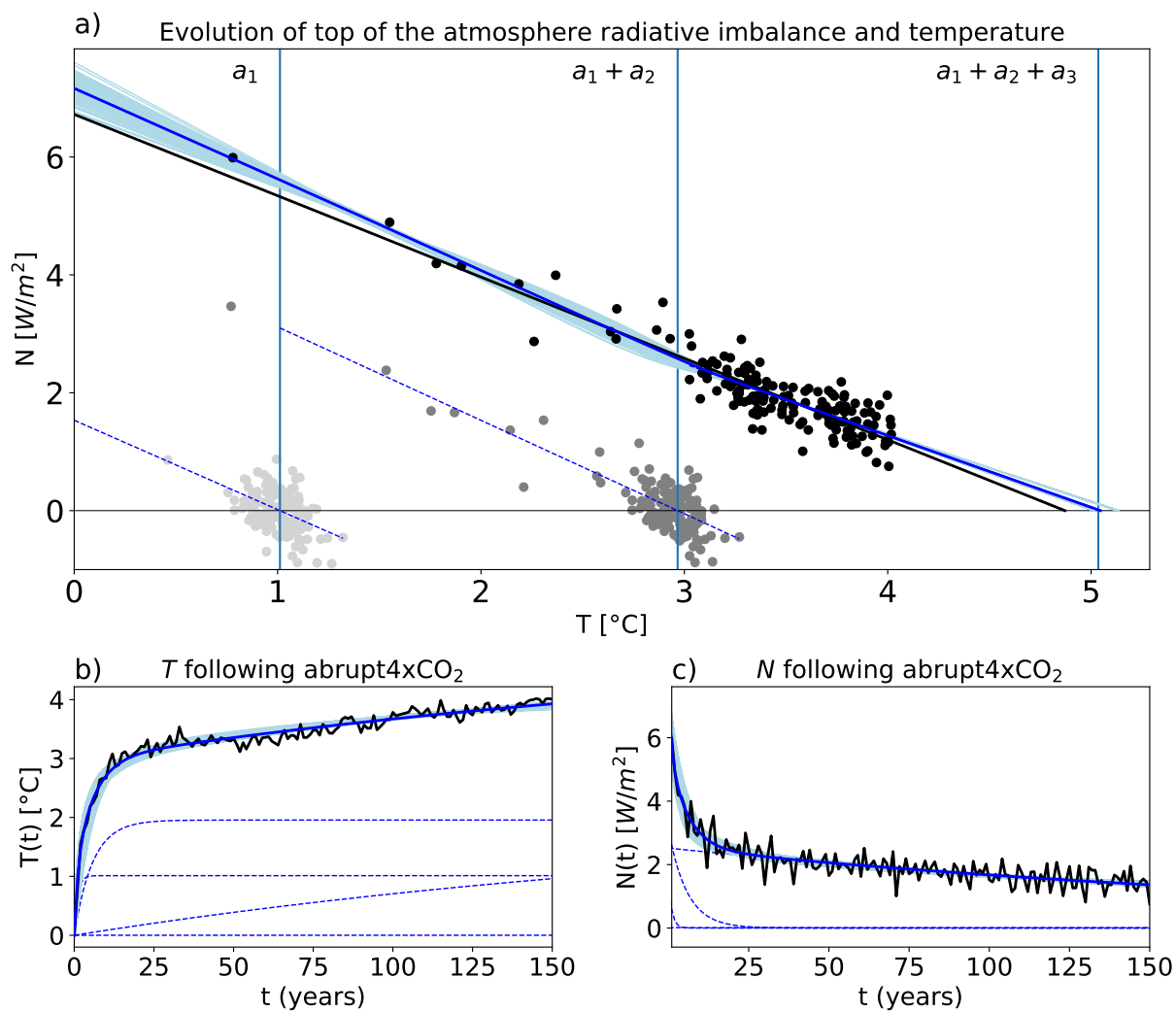
Figure S43. As Figure 1, but for the model GFDL-ESM2M.
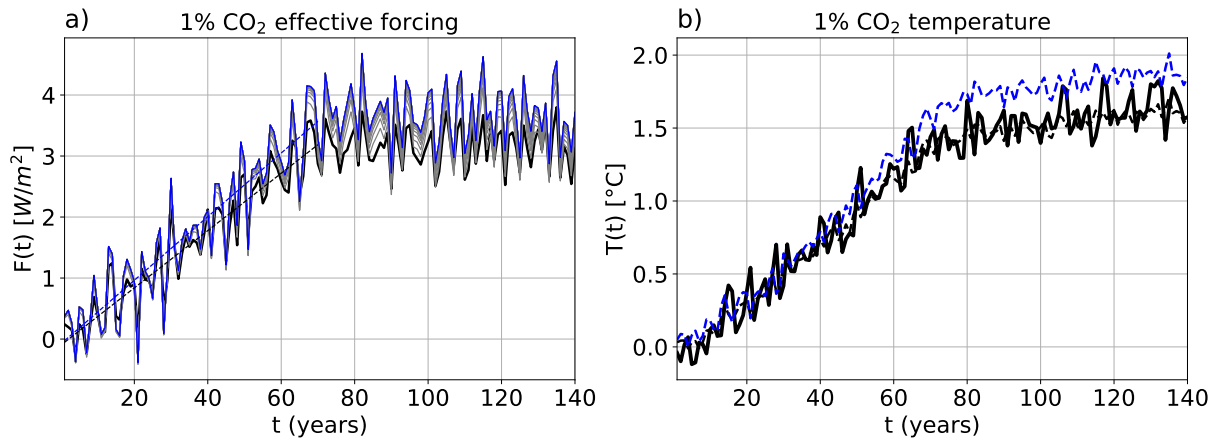
Figure S44. As Figure 3, but for the model GFDL-ESM2M. Note that in this model CO_2 increases only until we reach a doubling after 70 years.
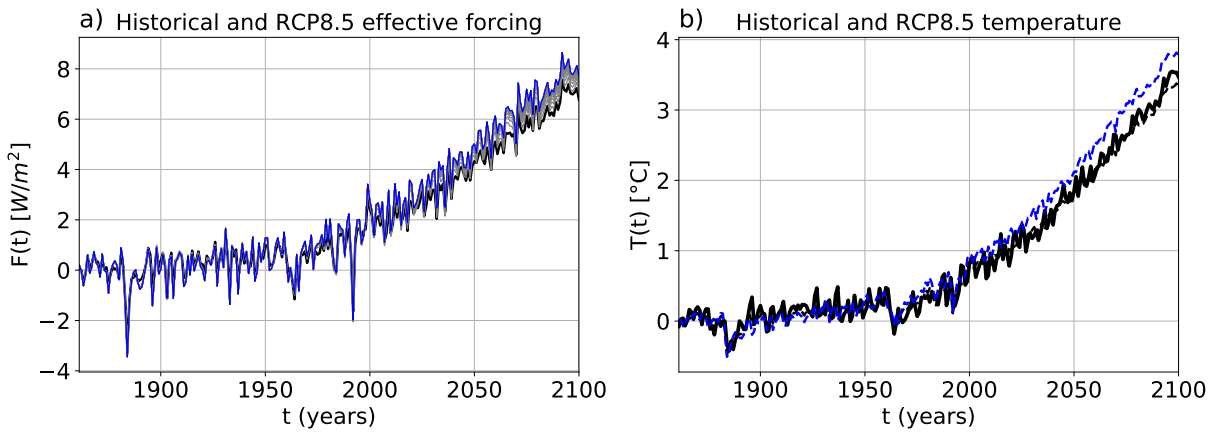
Figure S45. As Figure 4, but for the model GFDL-ESM2M.
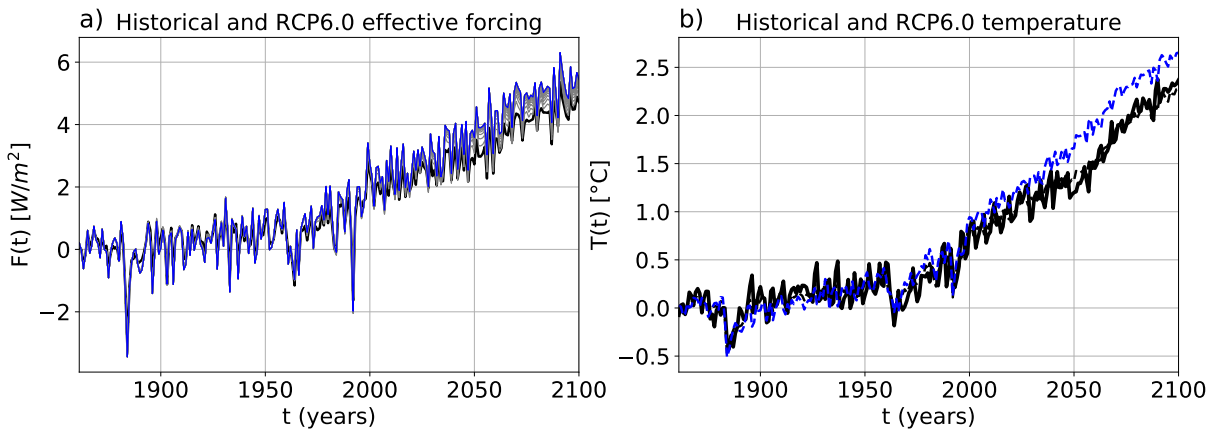
Figure S46. As Figure 4, but for the model GFDL-ESM2M and experiment RCP6.0.
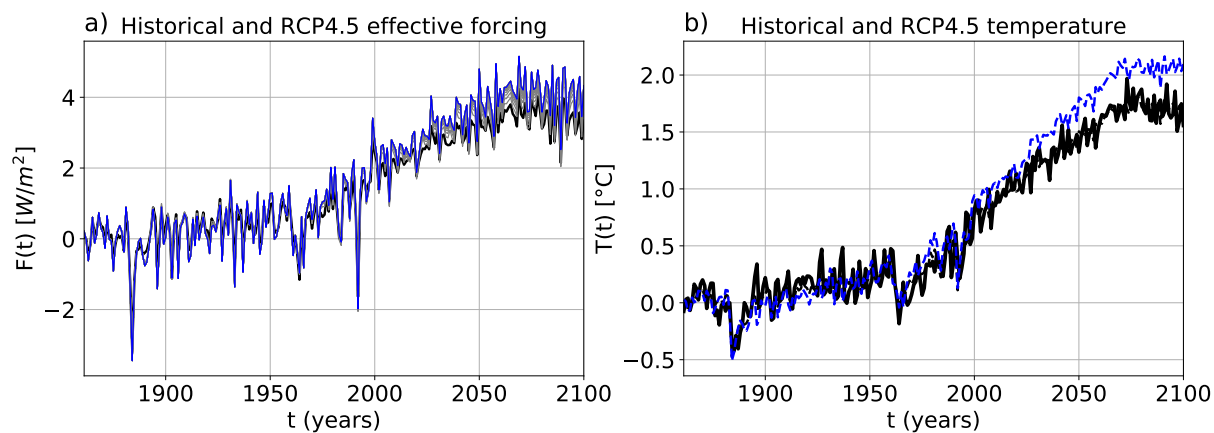
**Figure S47.** As Figure 4, but for the model GFDL-ESM2M and experiment RCP4.5.
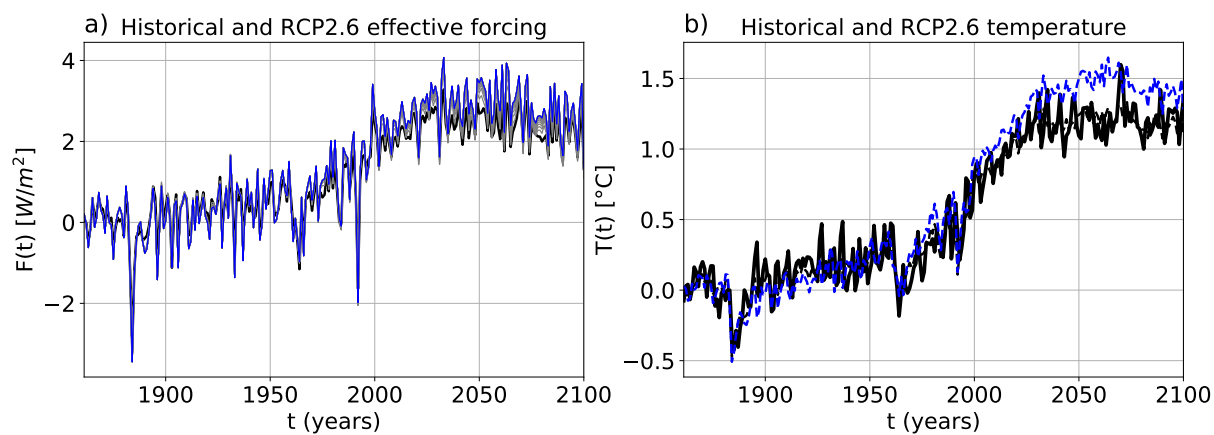
**Figure S48.** As Figure 4, but for the model GFDL-ESM2M and experiment RCP2.6.
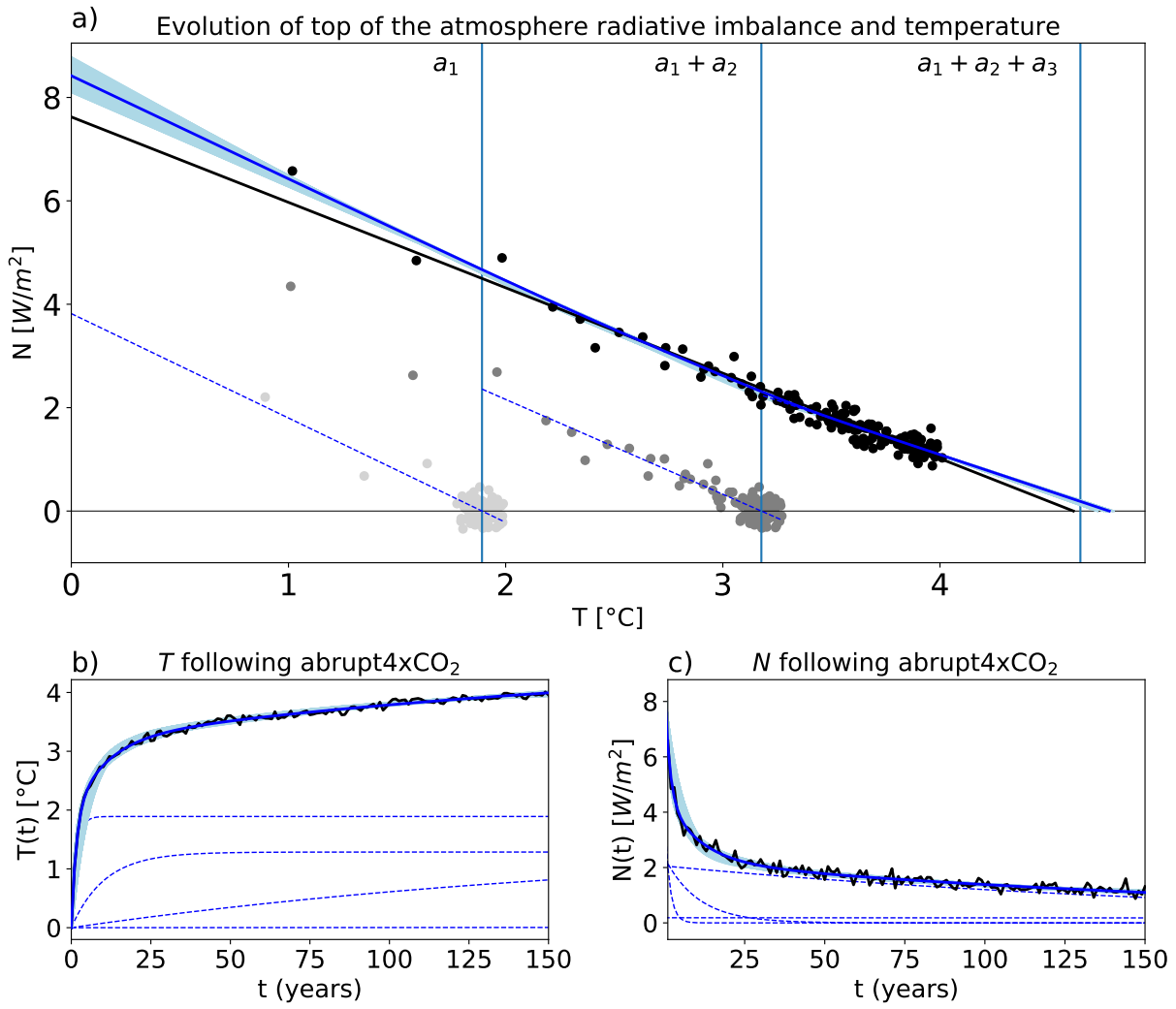
**Figure S49.** As Figure 1, but for the model GISS-E2-H.
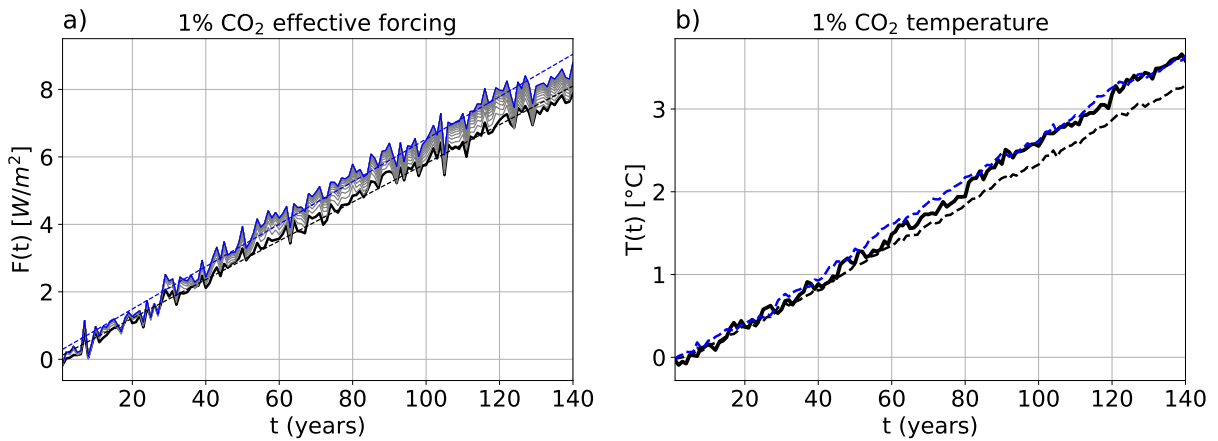


Figure S50. As Figure 3, but for the model GISS-E2-H.

November 5, 2021, 9:27am
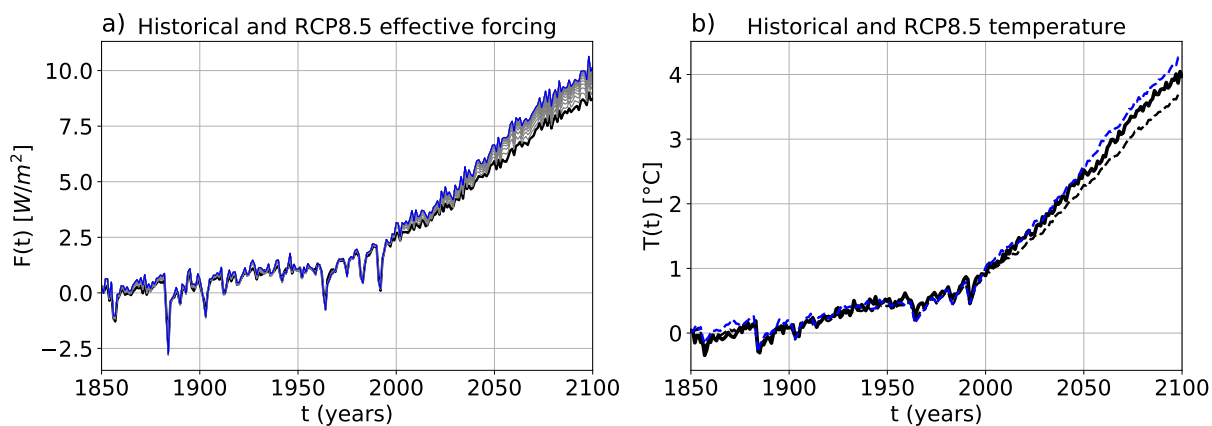
**Figure S51.** As Figure 4, but for the model GISS-E2-H.
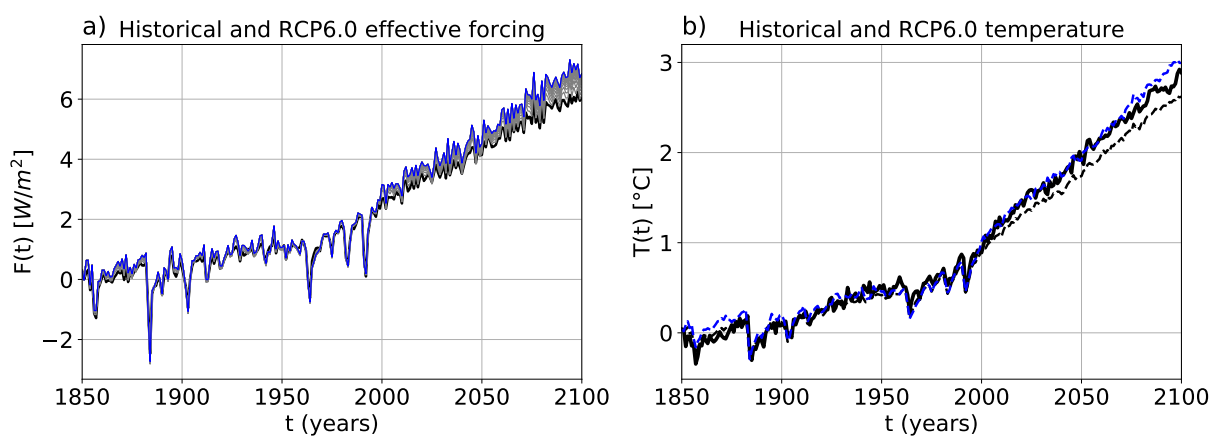
Figure S52. As Figure 4, but for the model GISS-E2-H and experiment RCP6.0.
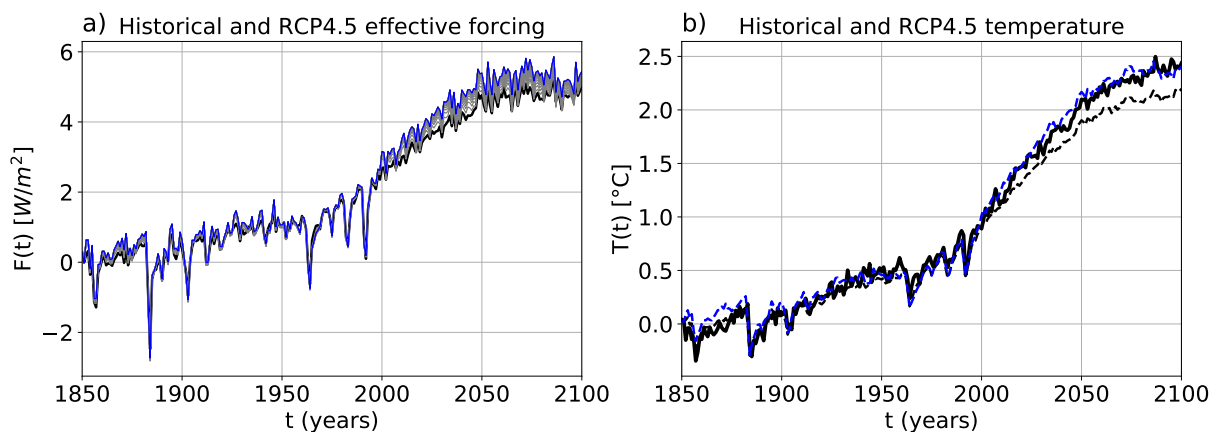

**Figure S53.** As Figure 4, but for the model GISS-E2-H and experiment RCP4.5.
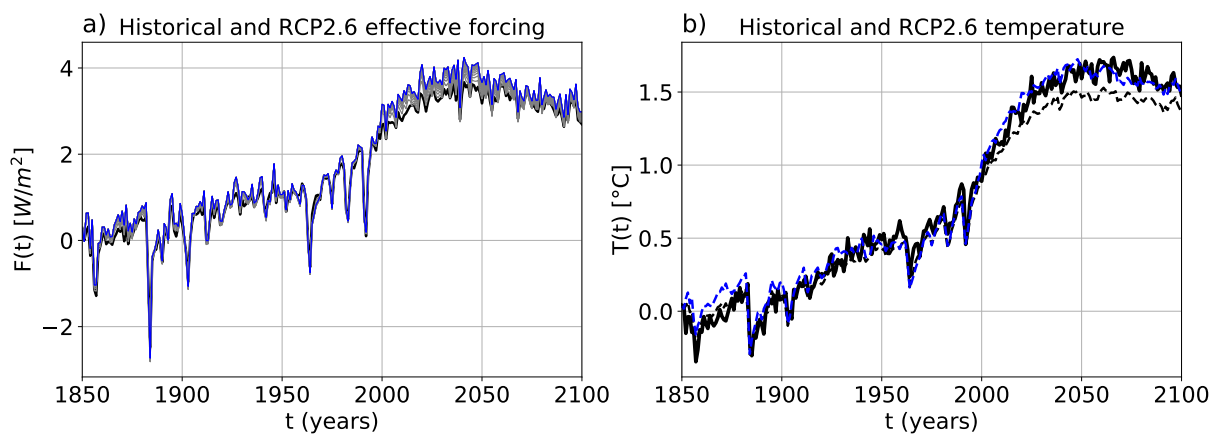
**Figure S54.**   As Figure 4, but for the model GISS-E2-H and experiment RCP2.6.

a)
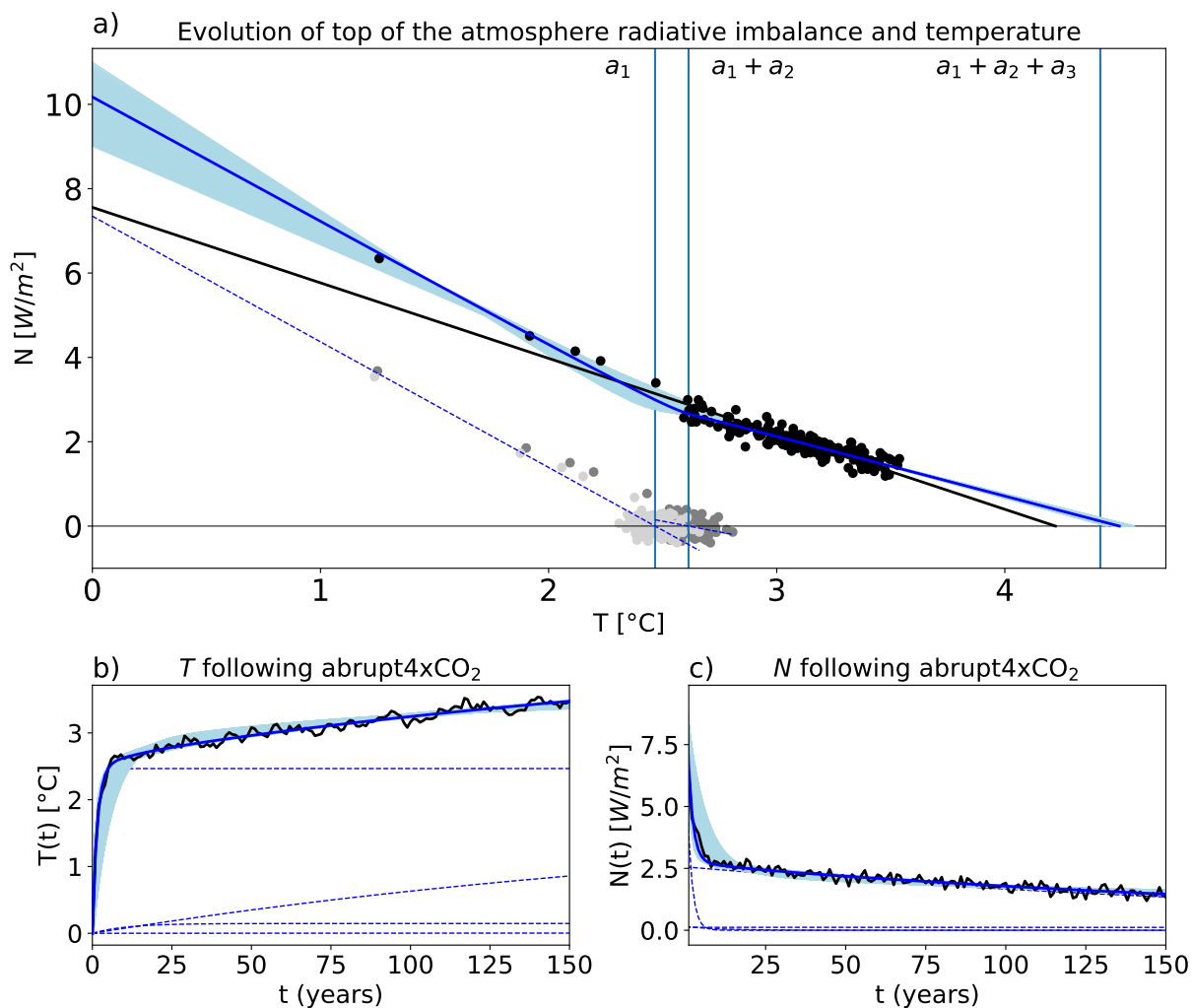
Figure S55. As Figure 1, but for the model GISS-E2-R.
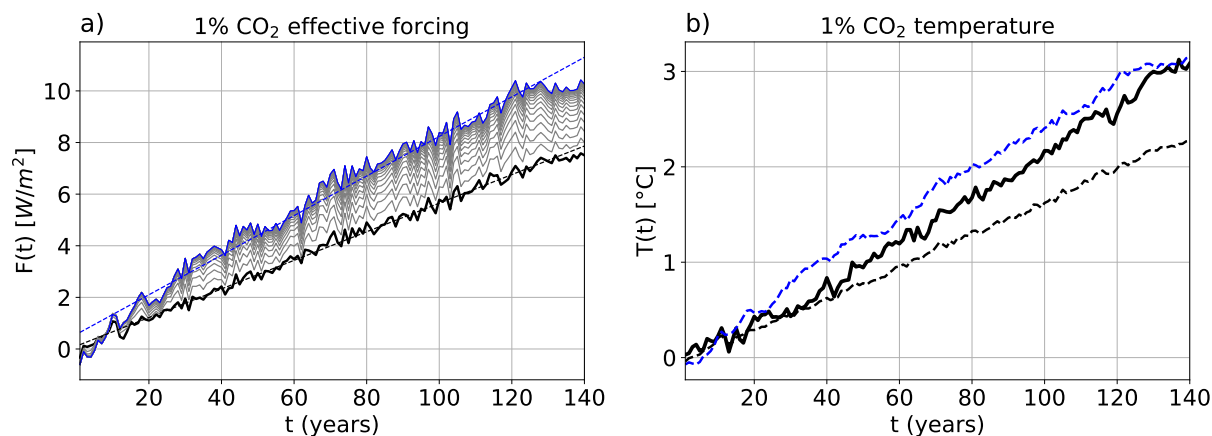

Figure S56. As Figure 3, but for the model GISS-E2-R.
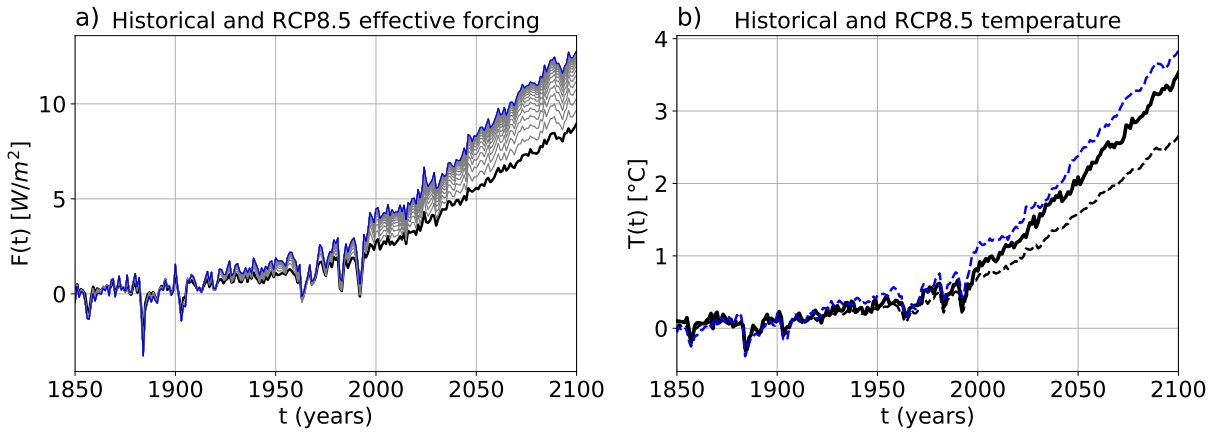
**Figure S57.** As Figure 4, but for the model GISS-E2-R.
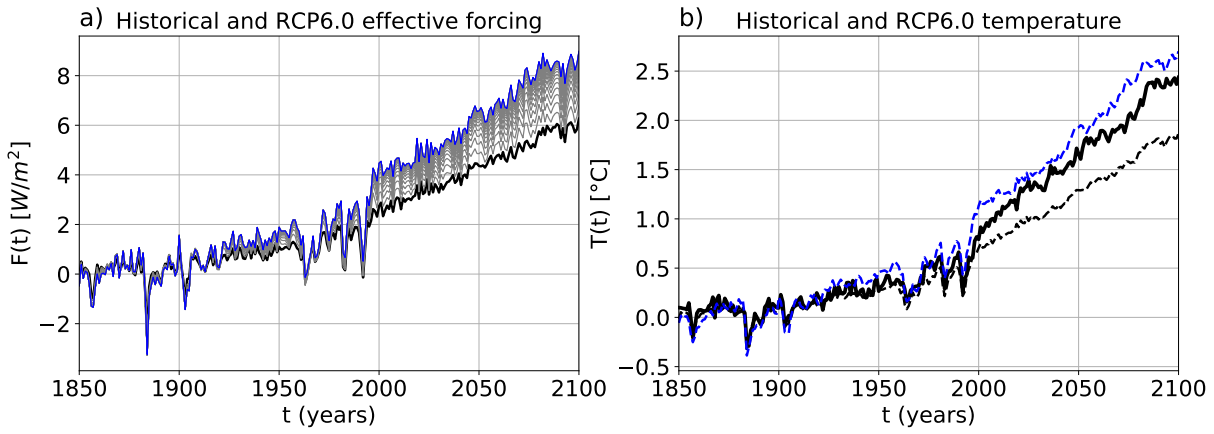
Figure S58. As Figure 4, but for the model GISS-E2-R and experiment RCP6.0.
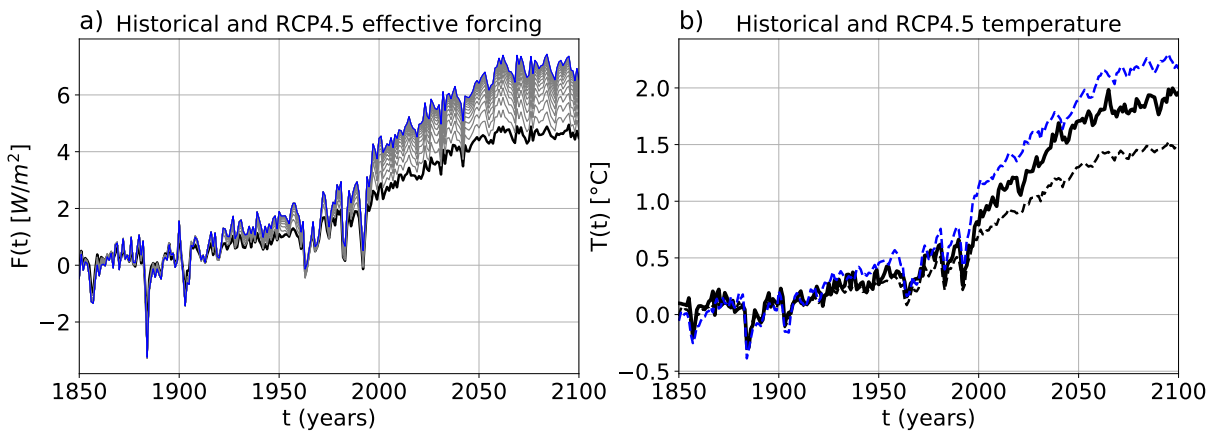
Figure S59. As Figure 4, but for the model GISS-E2-R and experiment RCP4.5.
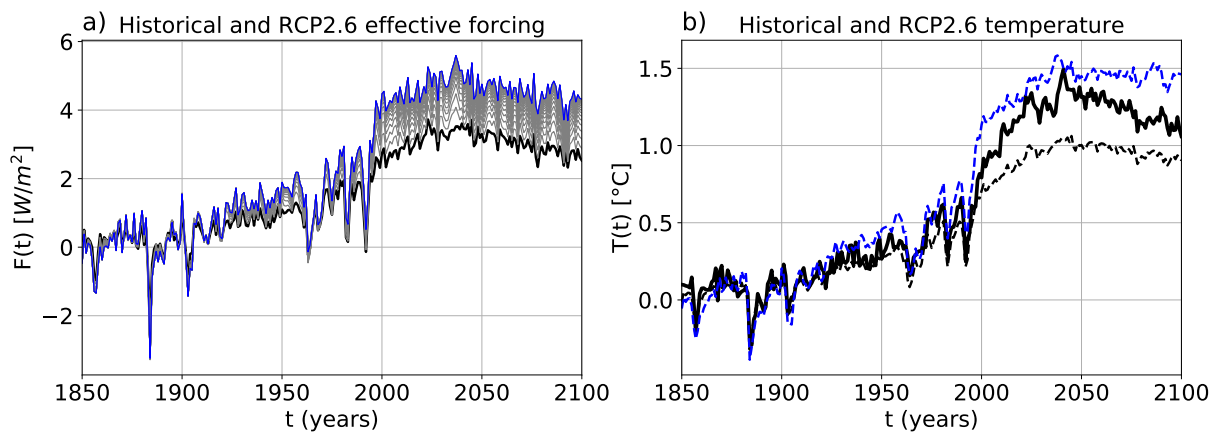
Figure S60. As Figure 4, but for the model GISS-E2-R and experiment RCP2.6.

a)

Evolution of top of the atmosphere radiative imbalance and temperature

b) *T* following abrupt4xCO$_2$

c) *N* following abrupt4xCO$_2$
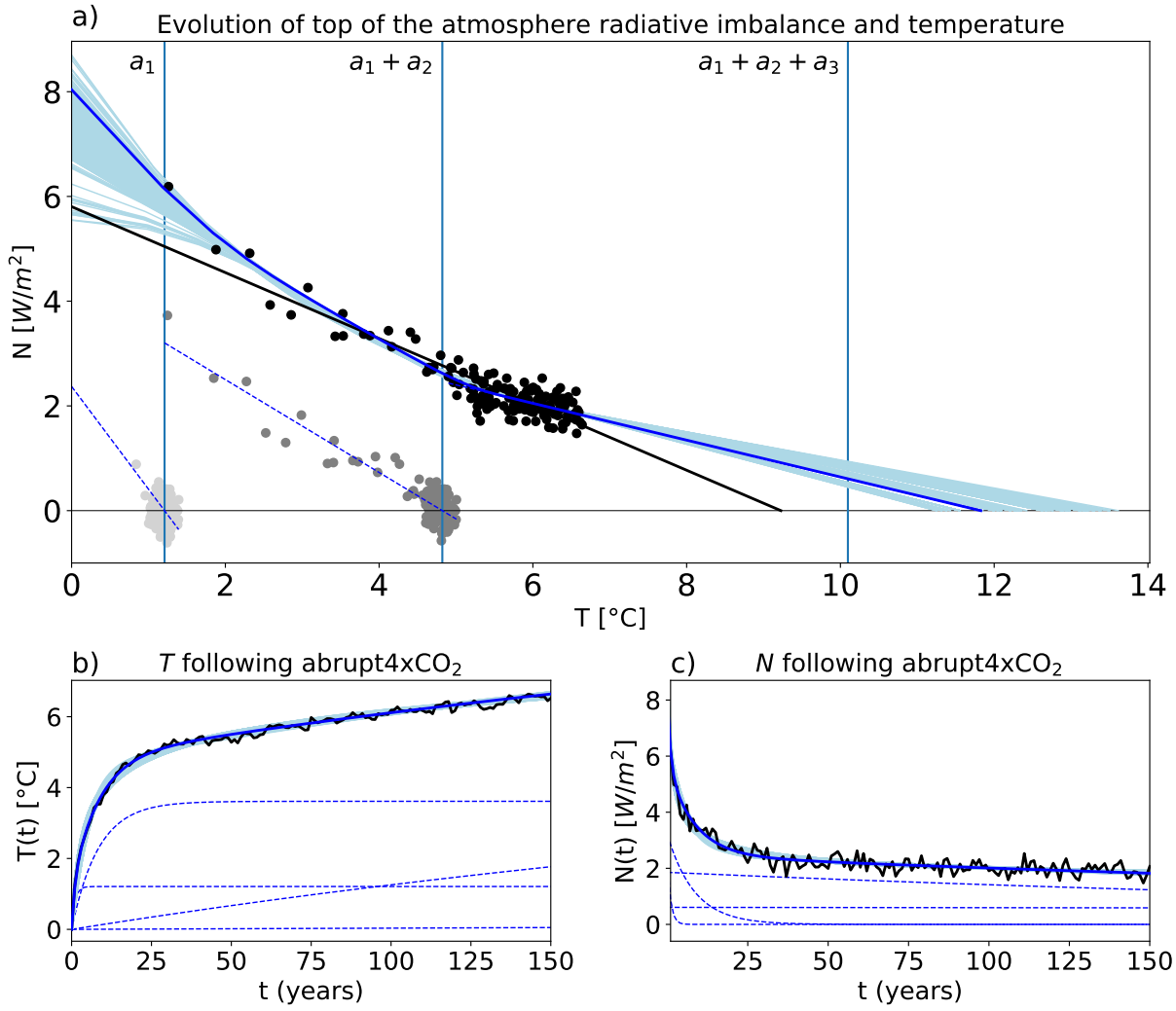
Figure S61.   As Figure 1, but for the model HadGEM2-ES.

a) 1% CO$_2$ effective forcing

b) 1% CO$_2$ temperature
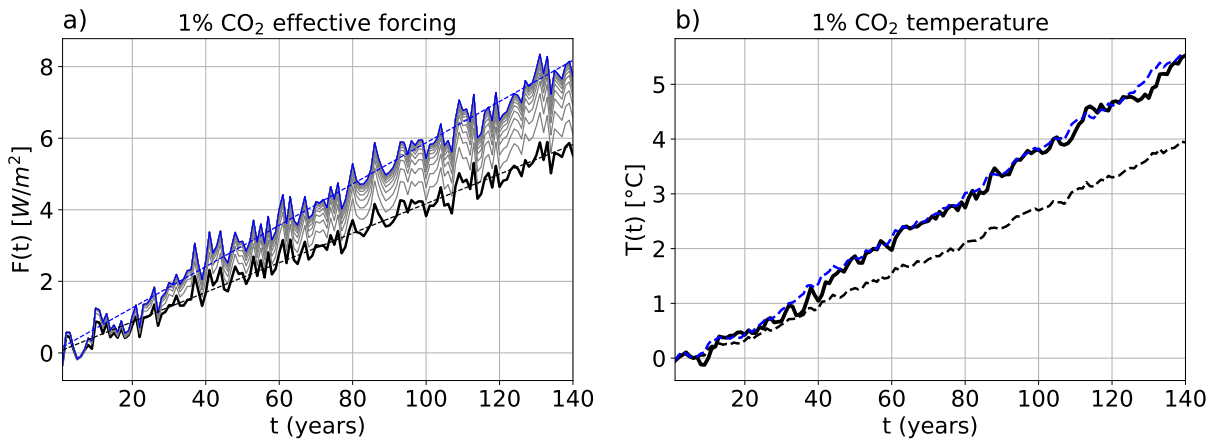
Figure S62.   As Figure 3, but for the model HadGEM2-ES.
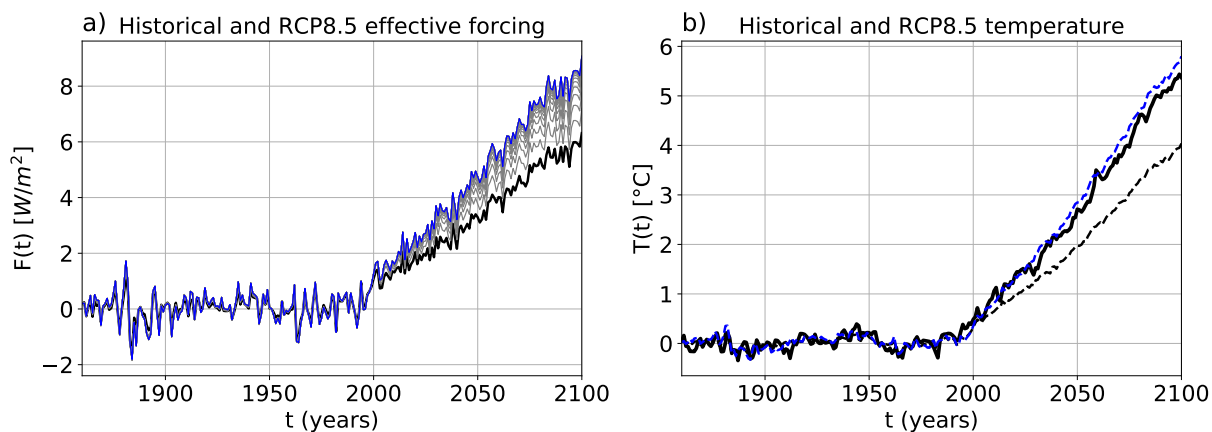
Figure S63. As Figure 4, but for the model HadGEM2-ES.
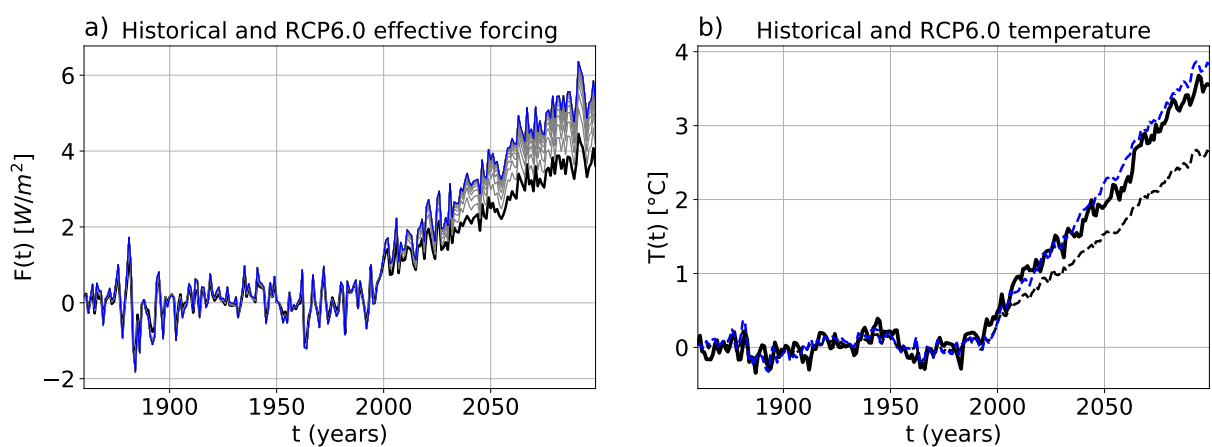
**Figure S64.** As Figure 4, but for the model HadGEM2-ES and experiment RCP6.0.
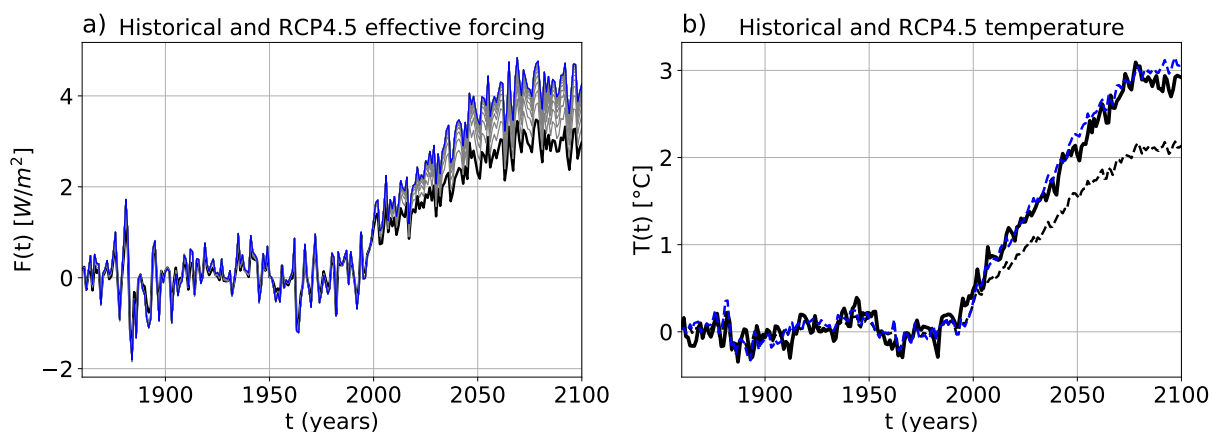
Figure S65. As Figure 4, but for the model HadGEM2-ES and experiment RCP4.5.

November 5, 2021, 9:27am
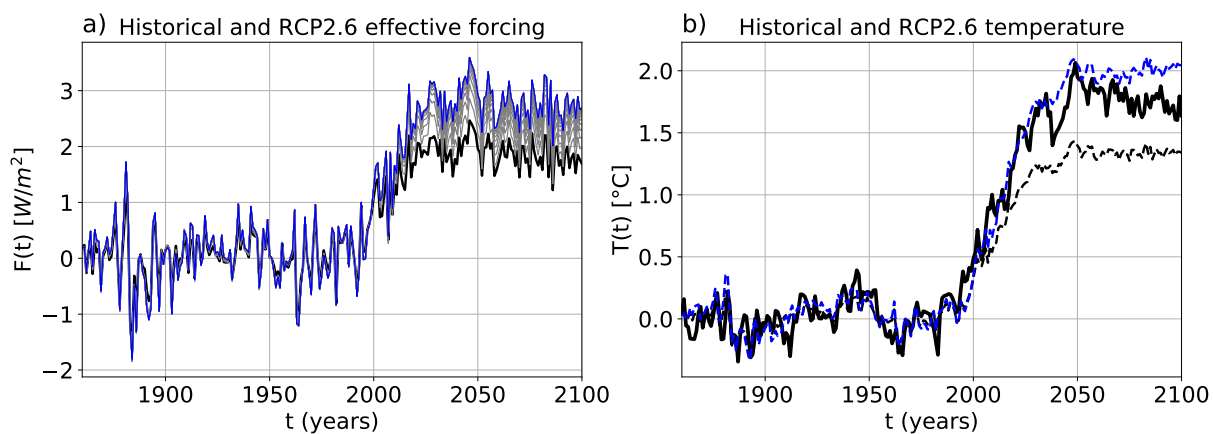
Figure S66.   As Figure 4, but for the model HadGEM2-ES and experiment RCP2.6.

a)
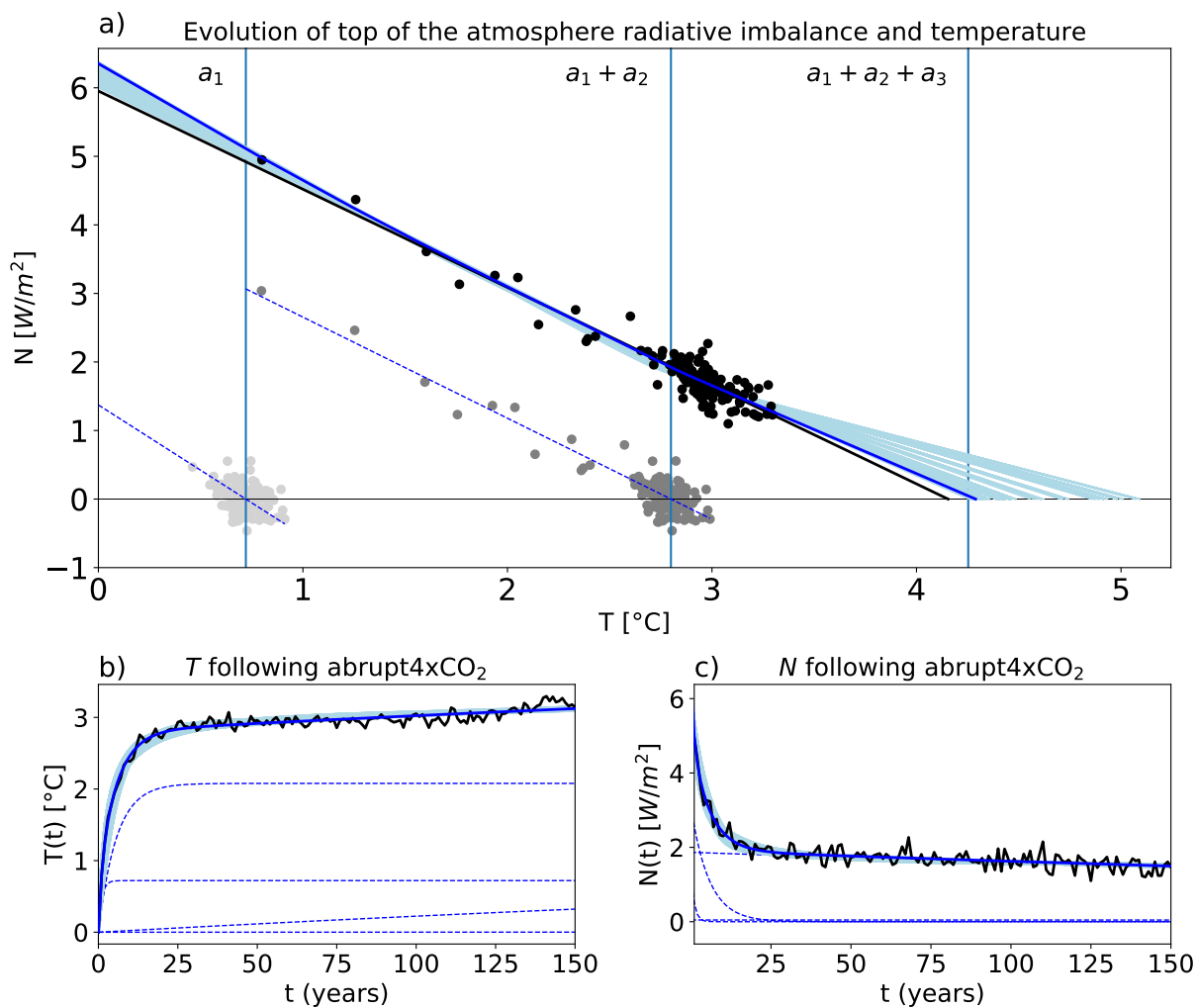
Figure S67. As Figure 1, but for the model inmcm4.
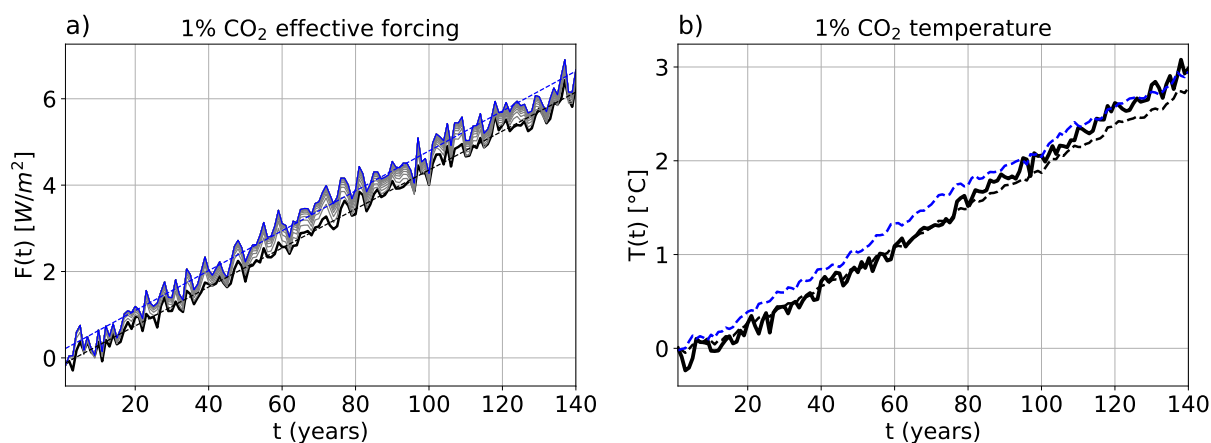
Figure S68. As Figure 3, but for the model inmcm4.

:
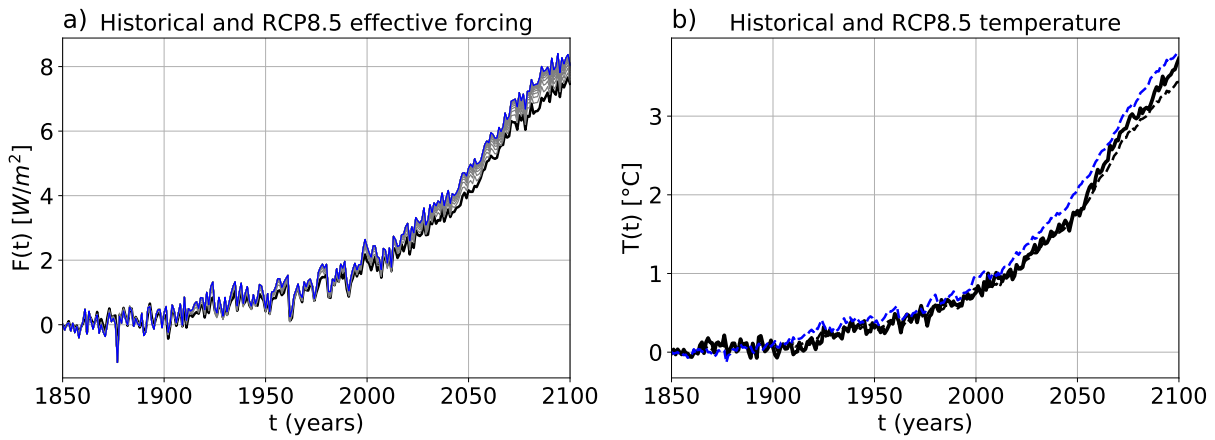
**Figure S69.**   As Figure 4, but for the model inmcm4.
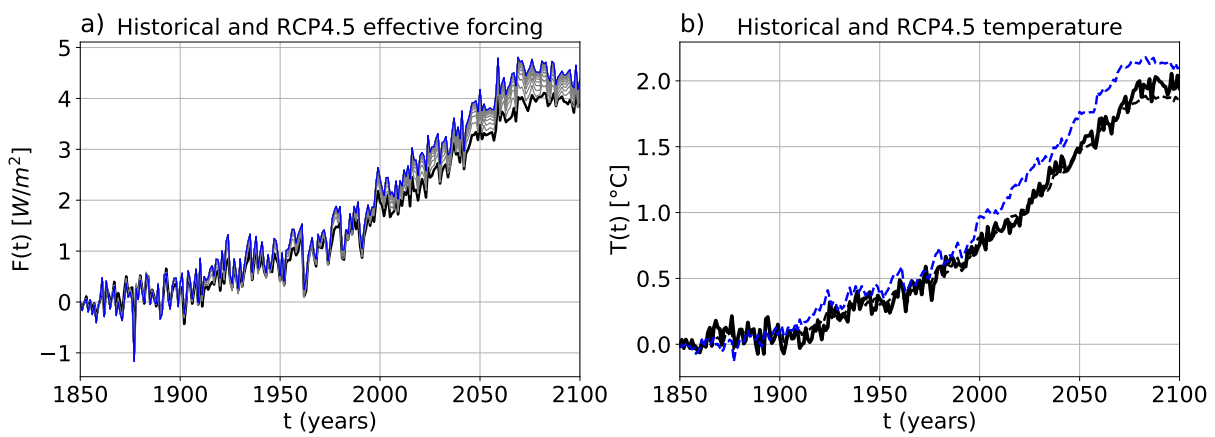
**Figure S70.**   As Figure 4, but for the model inmcm4 and experiment RCP4.5.

a) Evolution of top of the atmosphere radiative imbalance and temperature

b) *T* following abrupt4xCO$_2$

c) *N* following abrupt4xCO$_2$
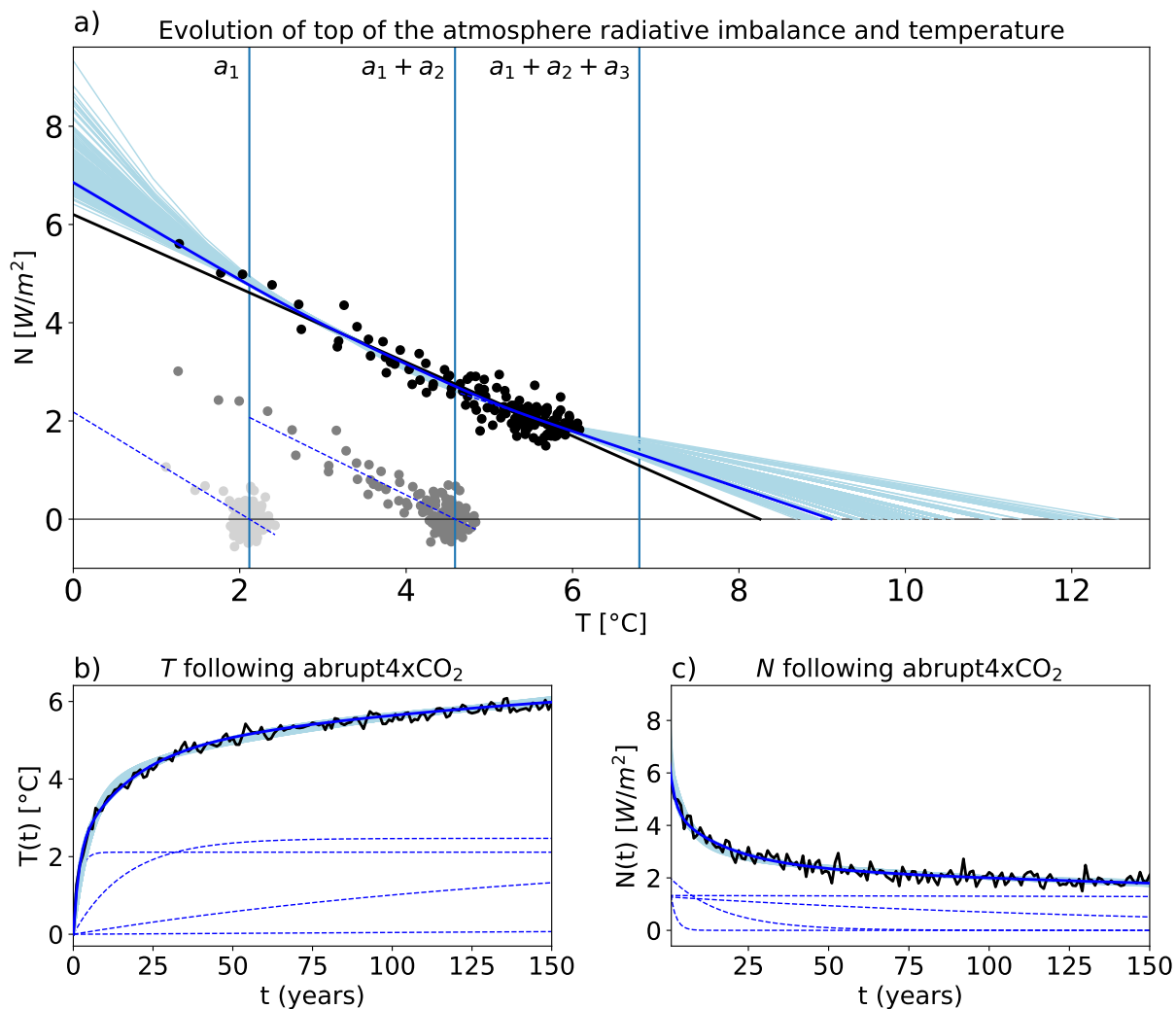
Figure S71. As Figure 1, but for the model IPSL-CM5A-LR.

a) 1% CO$_2$ effective forcing

b) 1% CO$_2$ temperature
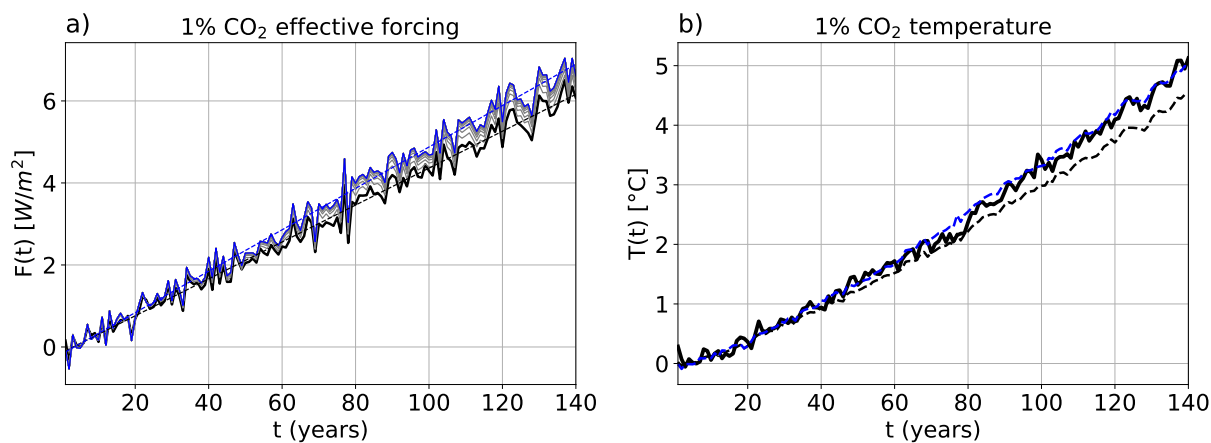
Figure S72. As Figure 3, but for the model IPSL-CM5A-LR.

November 5, 2021, 9:27am
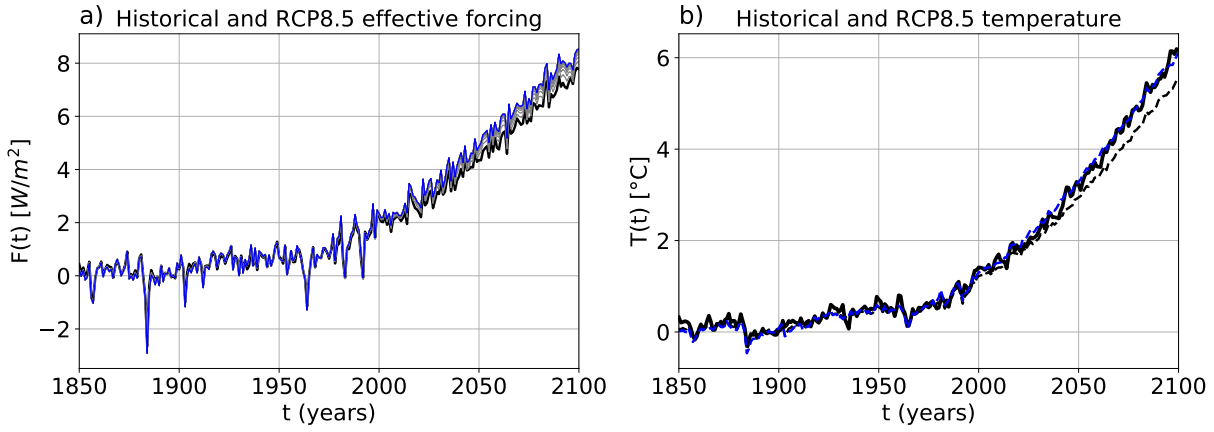
**Figure S73.** As Figure 4, but for the model IPSL-CM5A-LR.
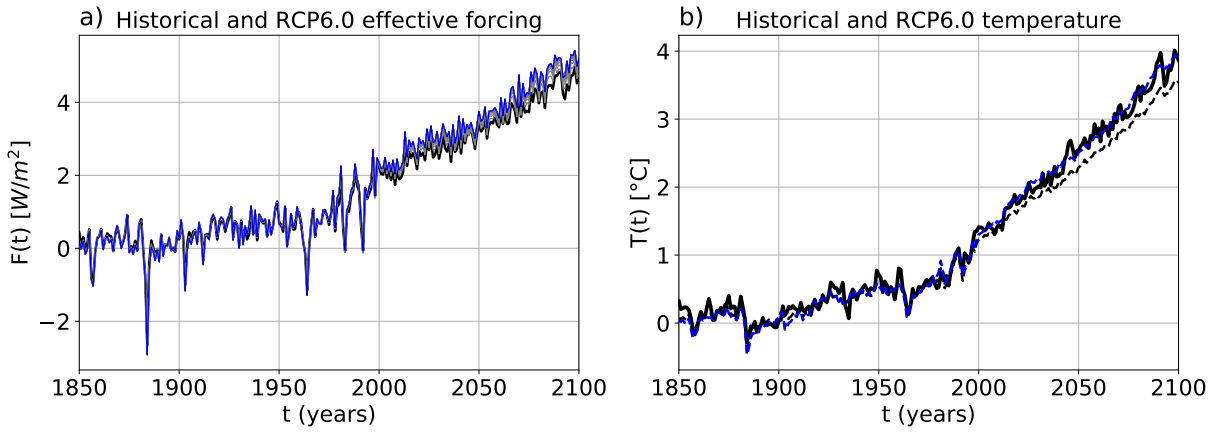
Figure S74. As Figure 4, but for the model IPSL-CM5A-LR and experiment RCP6.0.
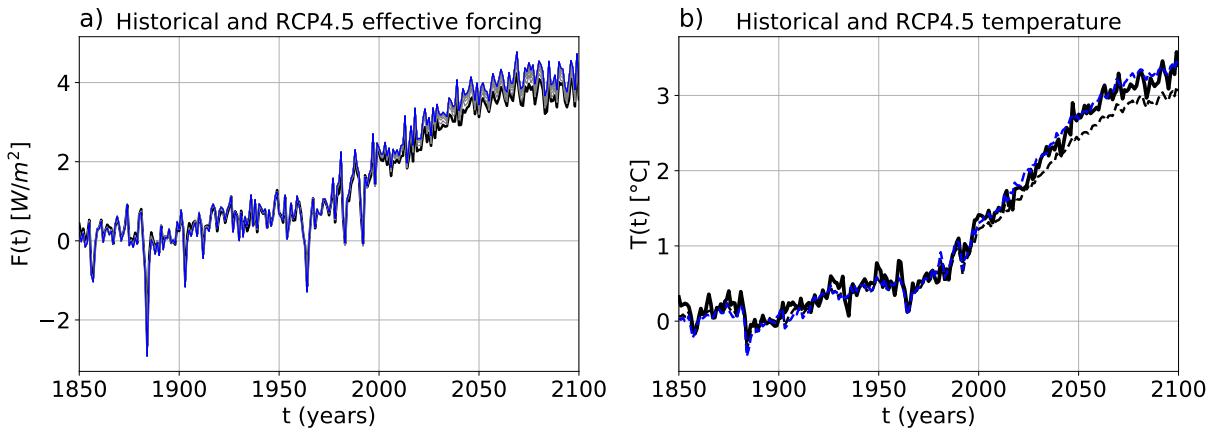

**Figure S75.** As Figure 4, but for the model IPSL-CM5A-LR and experiment RCP4.5.
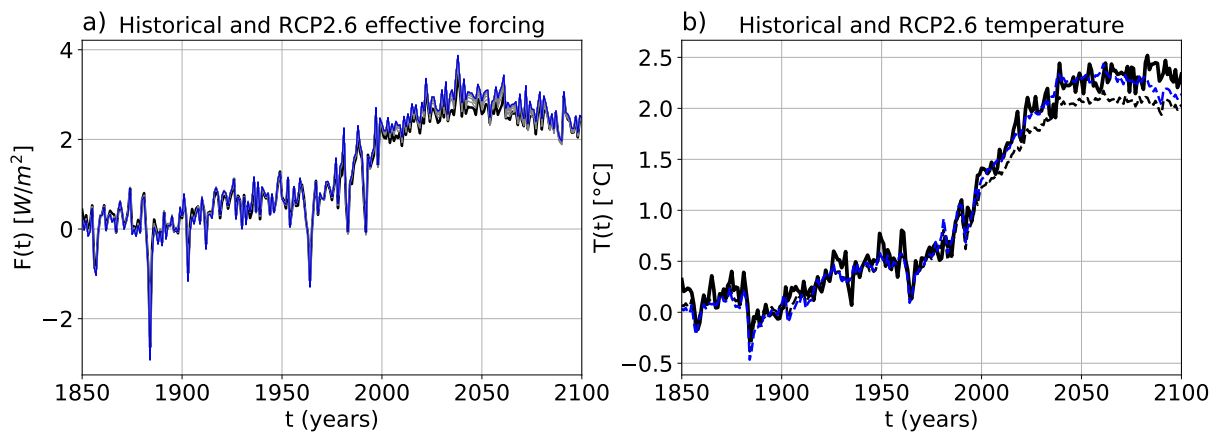
**Figure S76.** As Figure 4, but for the model IPSL-CM5A-LR and experiment RCP2.6.
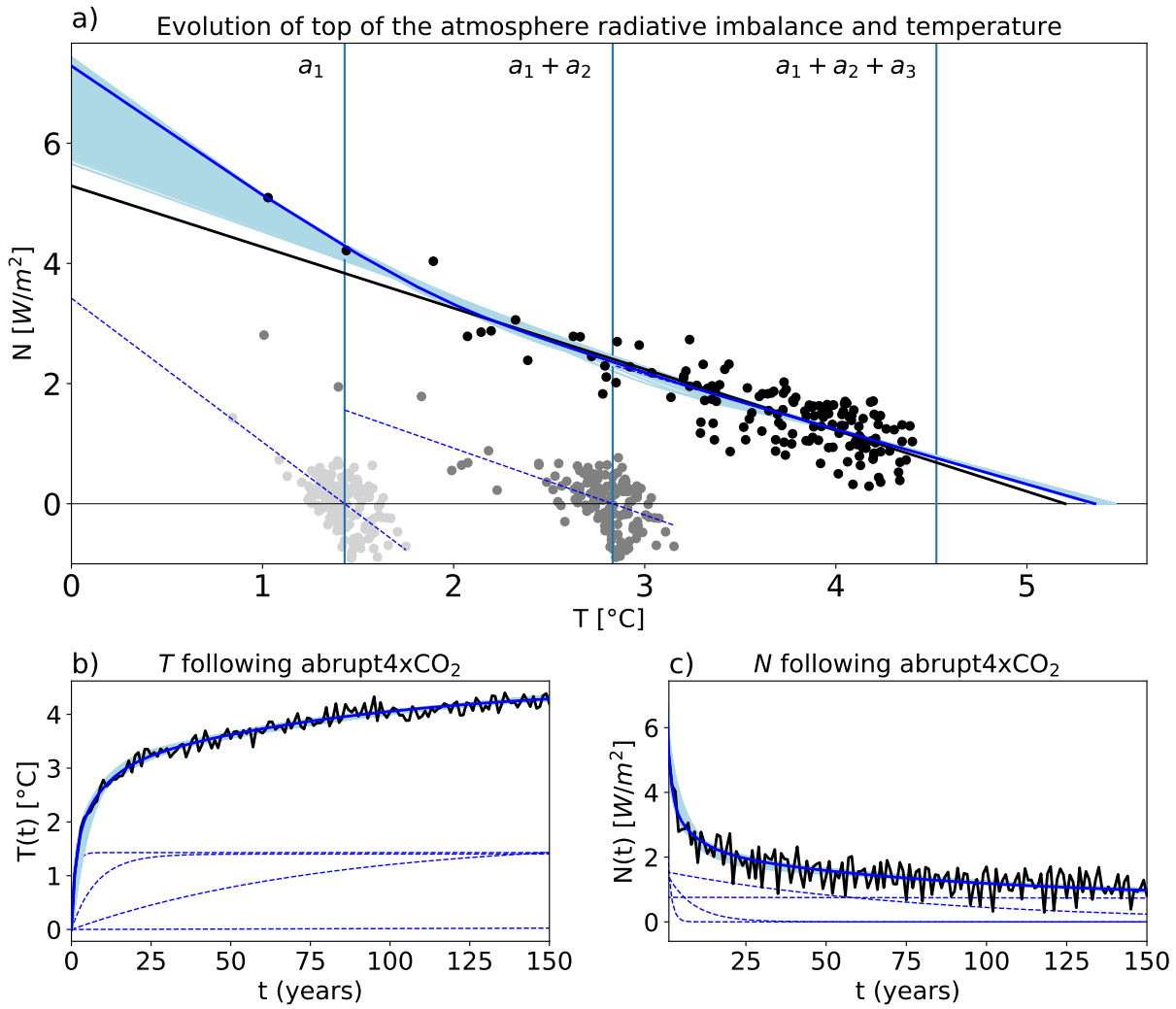
Figure S77.   As Figure 1, but for the model IPSL-CM5B-LR.
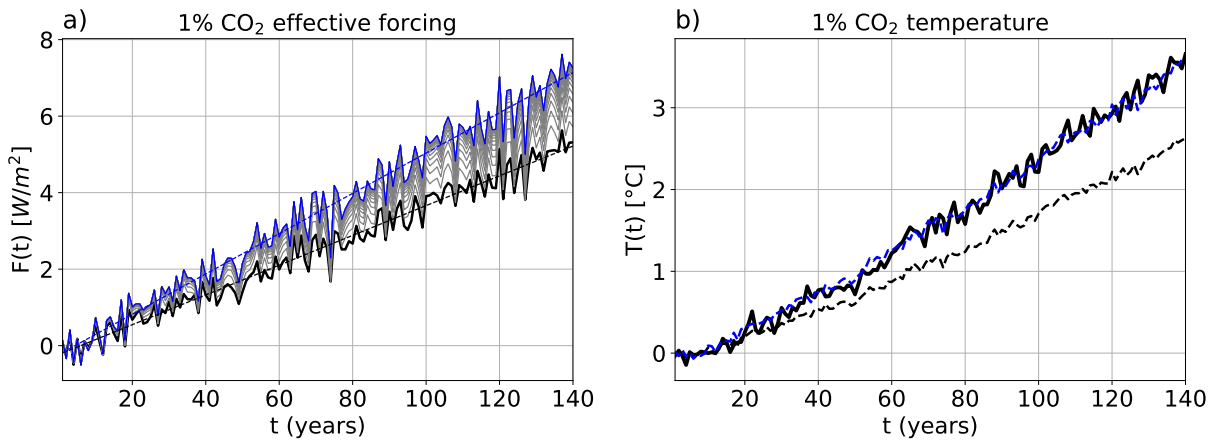
**Figure S78.**   As Figure 3, but for the model IPSL-CM5B-LR.
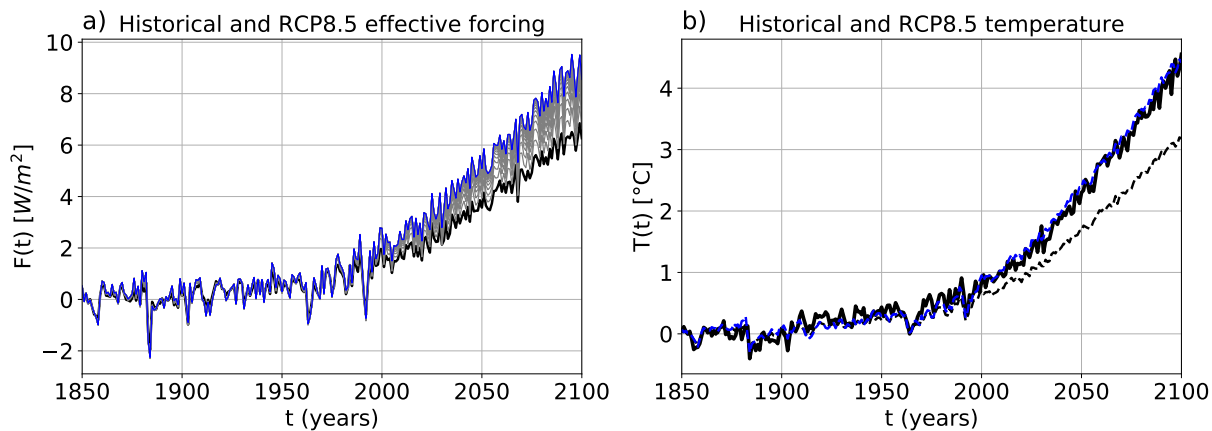
**Figure S79.** As Figure 4, but for the model IPSL-CM5B-LR.
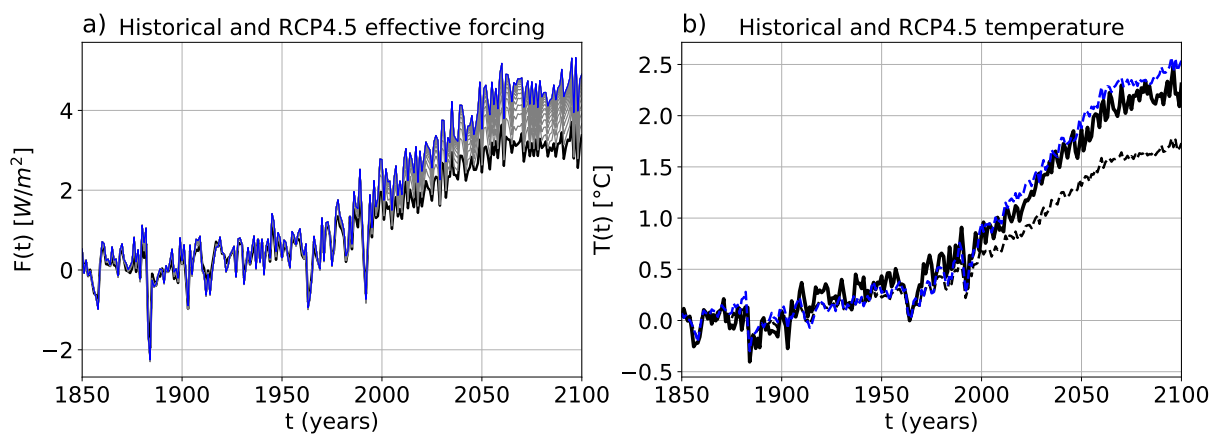
Figure S80. As Figure 4, but for the model IPSL-CM5B-LR and experiment RCP4.5.

November 5, 2021, 9:27am

a)
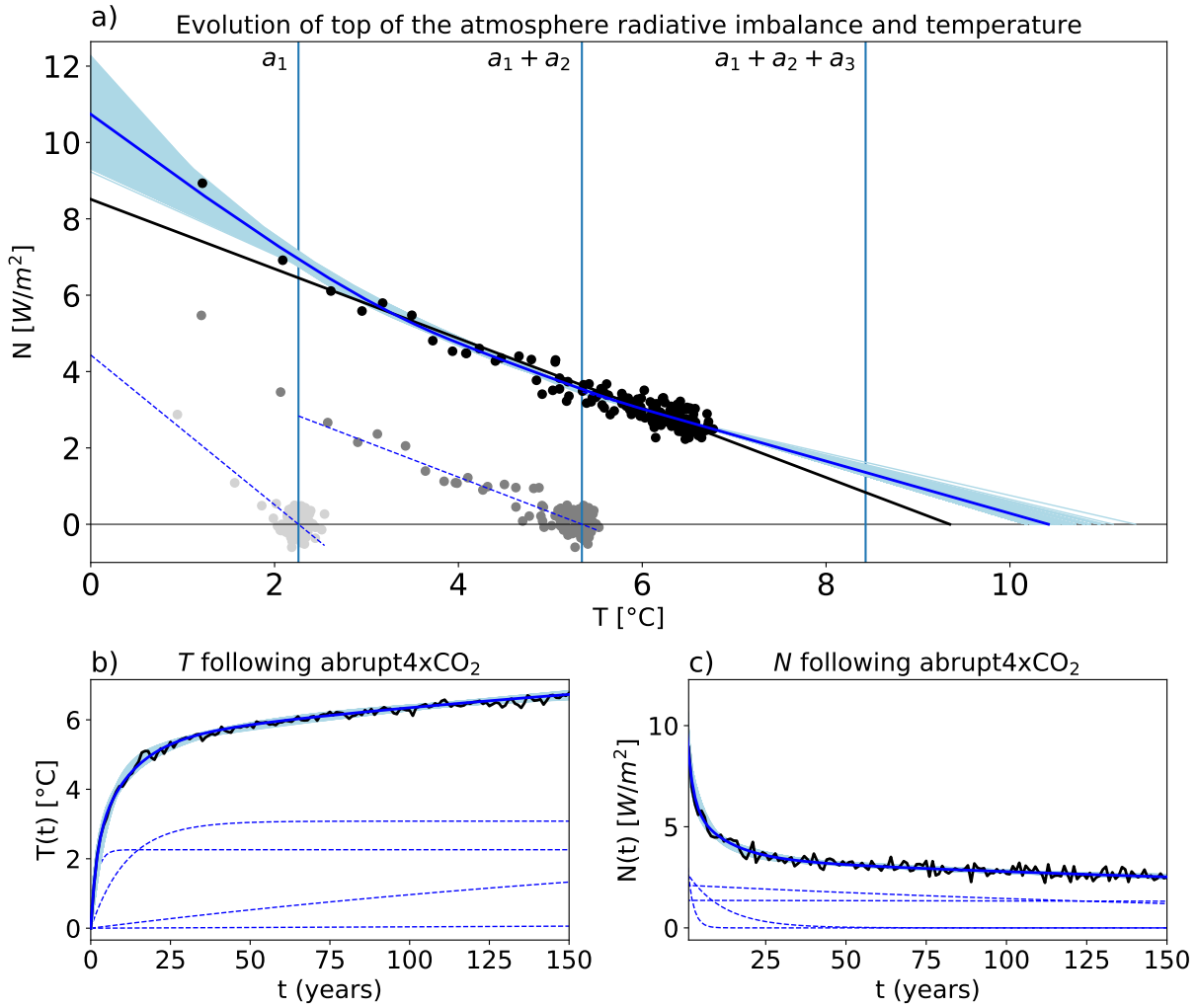
Figure S81.   As Figure 1, but for the model MIROC-ESM.
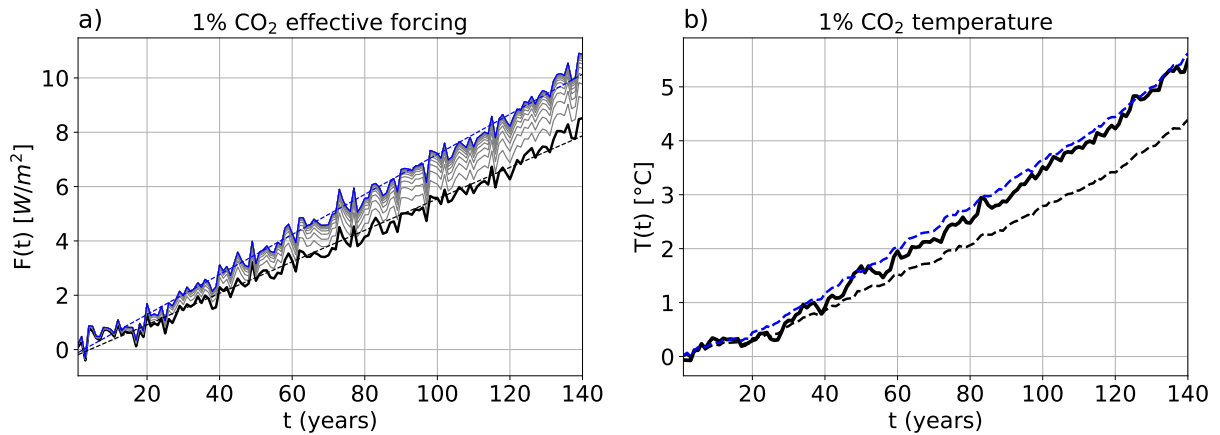
Figure S82.   As Figure 3, but for the model MIROC-ESM.
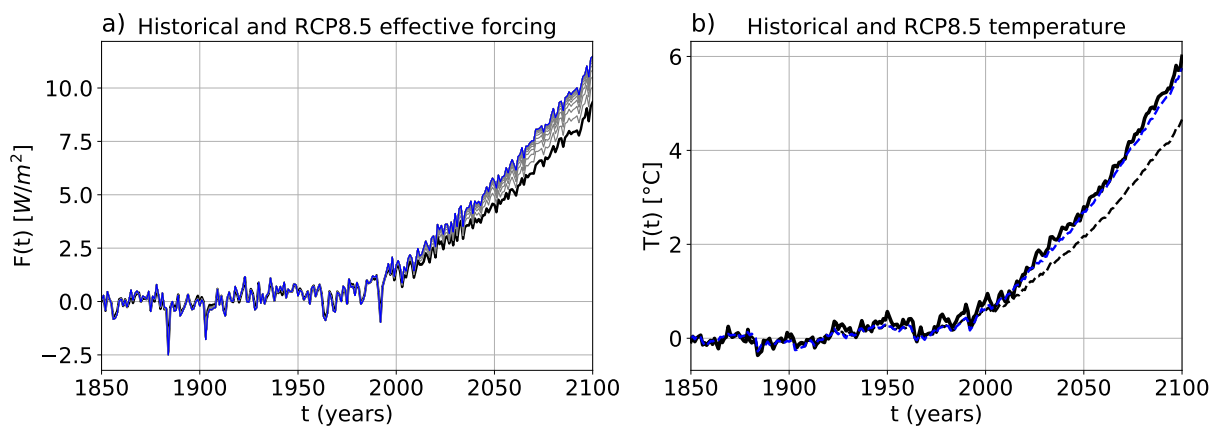
**Figure S83.** As Figure 4, but for the model MIROC-ESM.
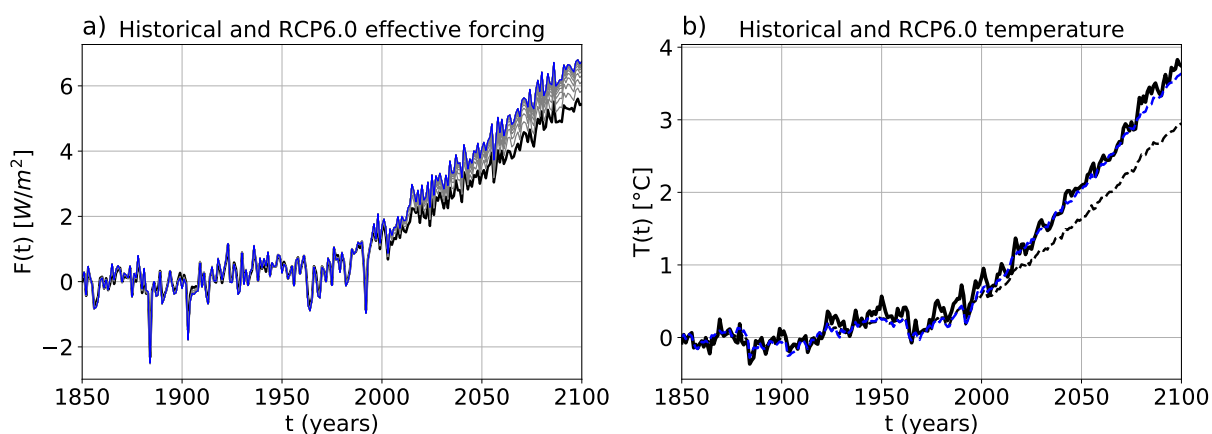
**Figure S84.** As Figure 4, but for the model MIROC-ESM and experiment RCP6.0.
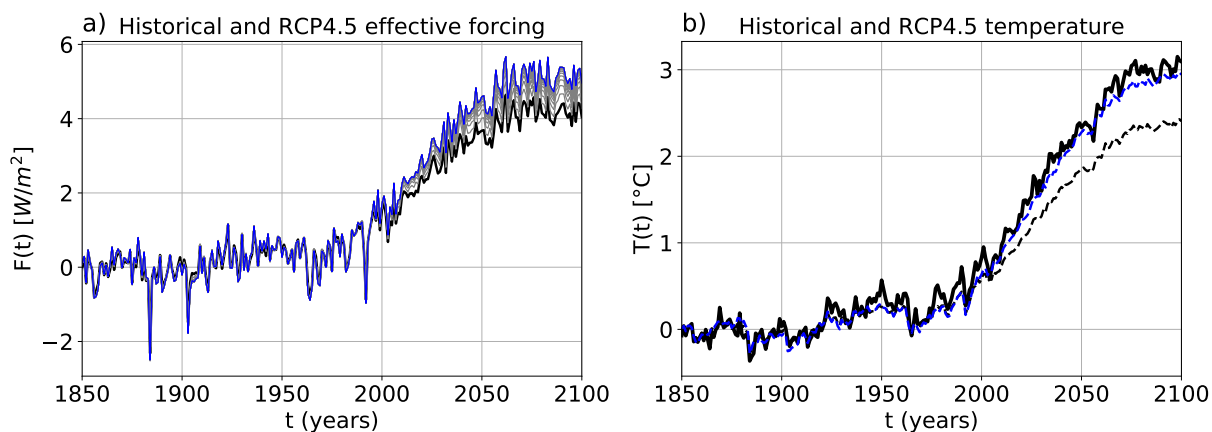
Figure S85. As Figure 4, but for the model MIROC-ESM and experiment RCP4.5.

November 5, 2021, 9:27am
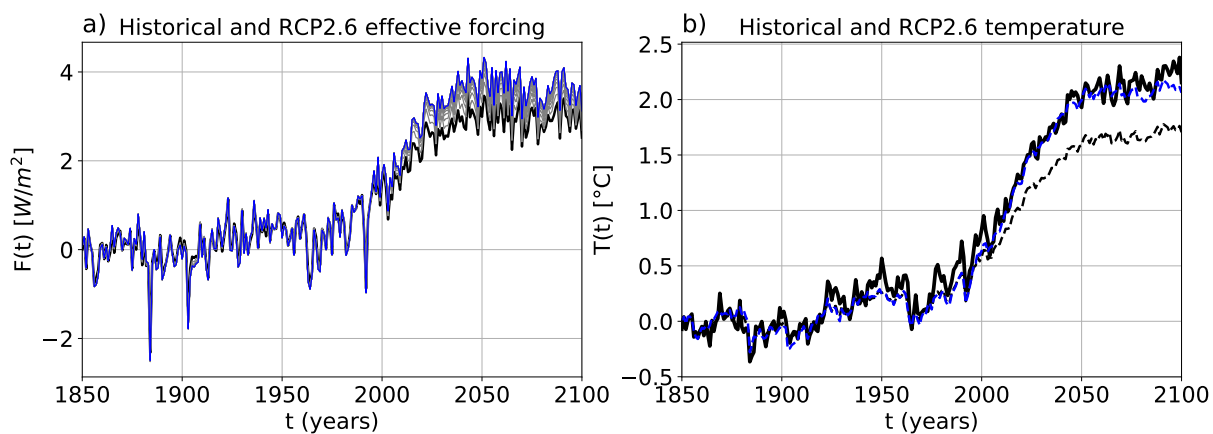
Figure S86. As Figure 4, but for the model MIROC-ESM and experiment RCP2.6.

a) Evolution of top of the atmosphere radiative imbalance and temperature

a_1 $a_1 + a_2$ $a_1 + a_2 + a_3$

b) *T* following abrupt4xCO$_2$

c) *N* following abrupt4xCO$_2$
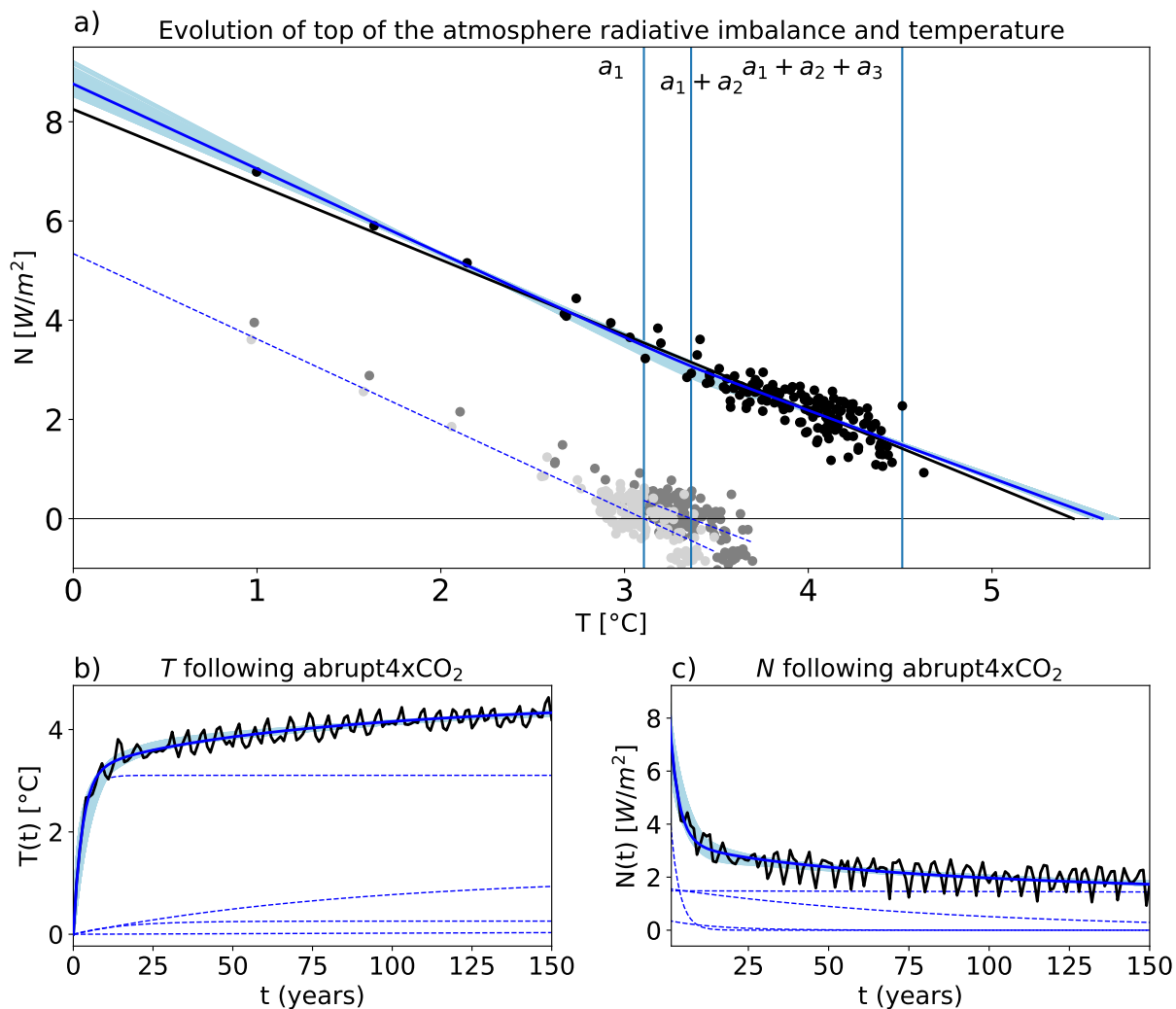
Figure S87. As Figure 1, but for the model MIROC5.

a) 1% CO$_2$ effective forcing

b) 1% CO$_2$ temperature
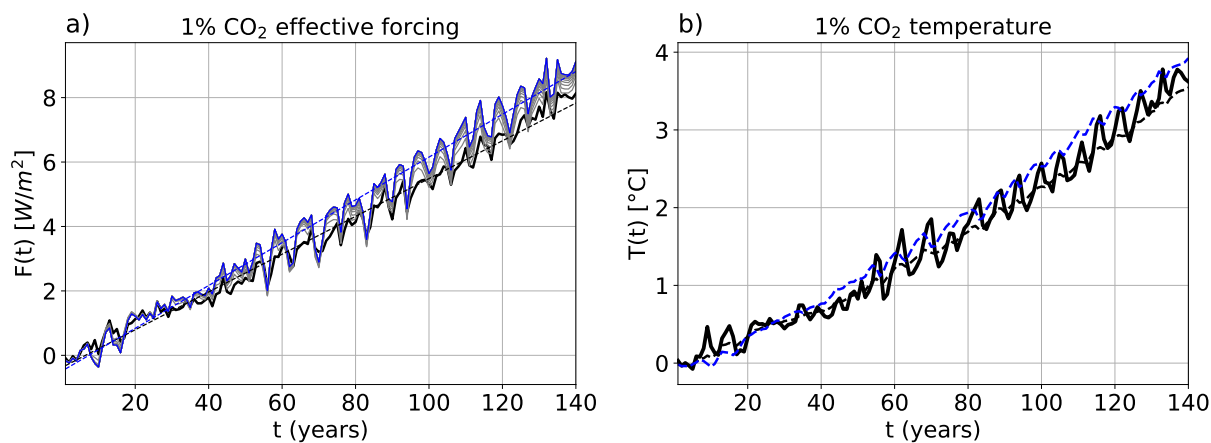
Figure S88. As Figure 3, but for the model MIROC5.

November 5, 2021, 9:27am
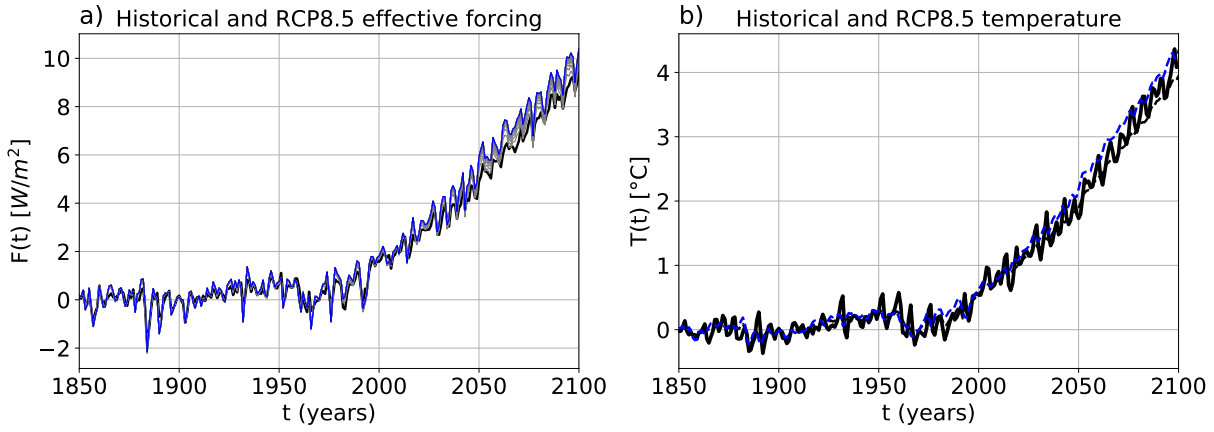
Figure S89.   As Figure 4, but for the model MIROC5.
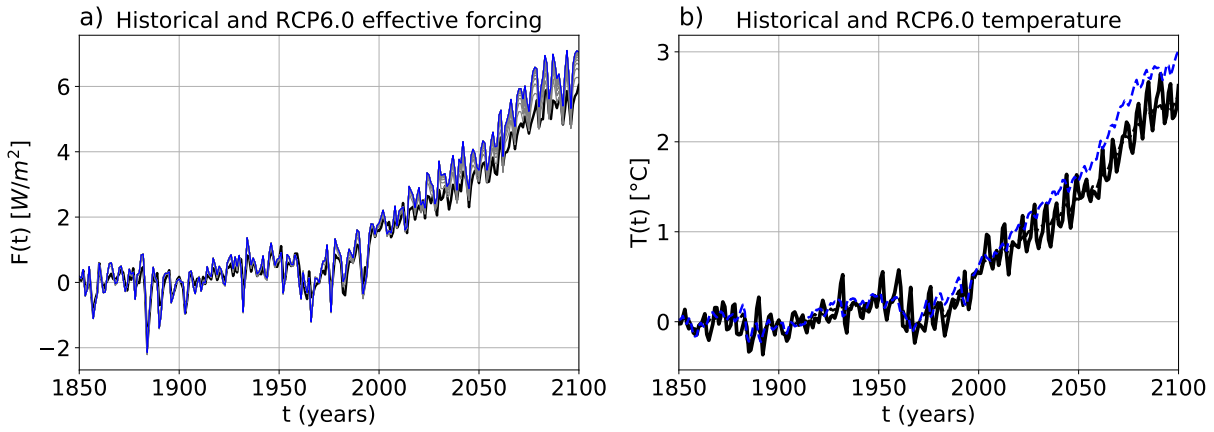
Figure S90.   As Figure 4, but for the model MIROC5 and experiment RCP6.0.
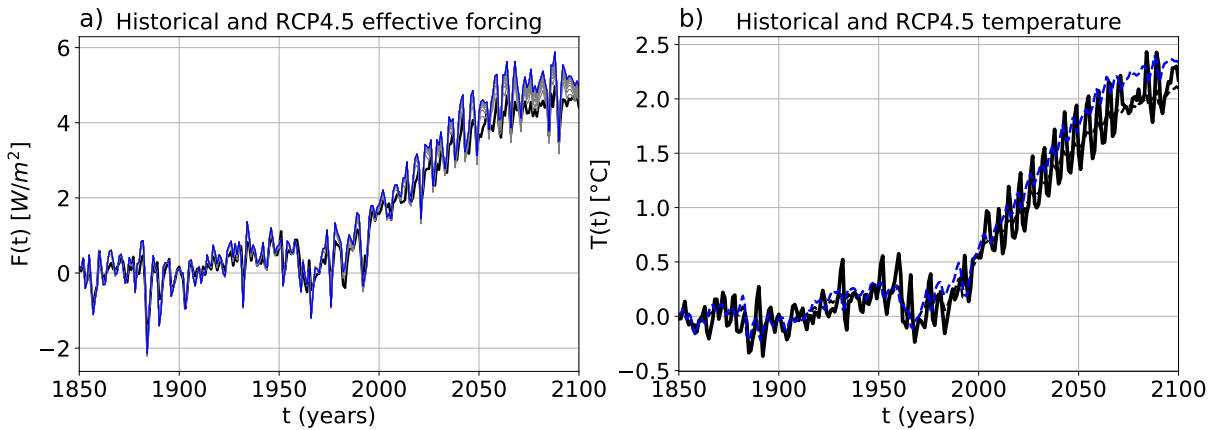
**Figure S91.**   As Figure 4, but for the model MIROC5 and experiment RCP4.5.
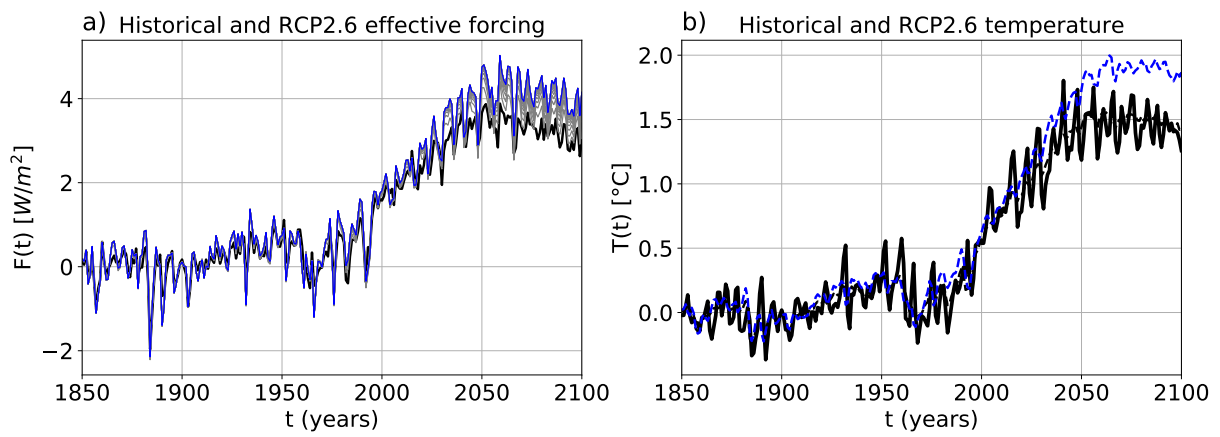
Figure S92. As Figure 4, but for the model MIROC5 and experiment RCP2.6.
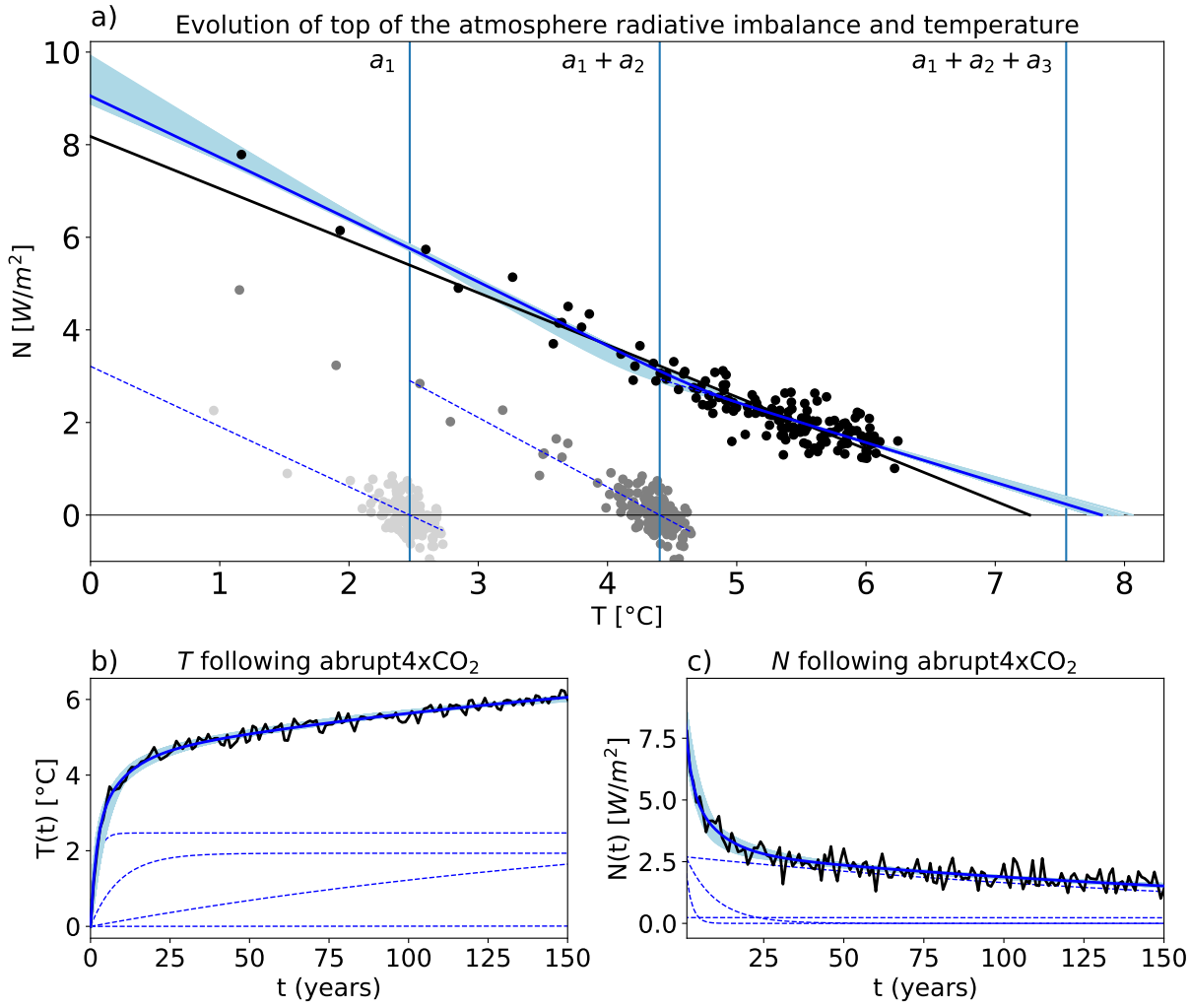
Figure S93. As Figure 1, but for the model MPI-ESM-LR.
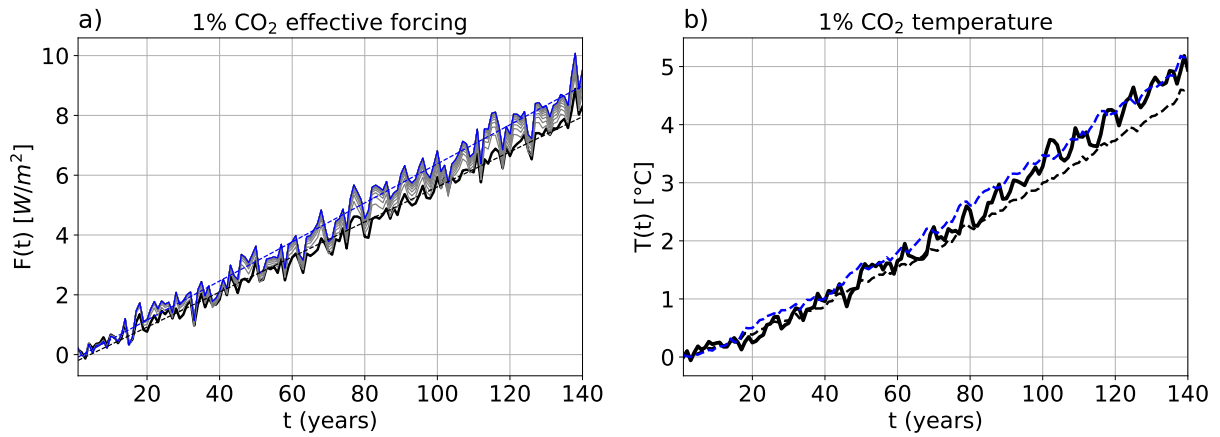
Figure S94. As Figure 3, but for the model MPI-ESM-LR.

November 5, 2021, 9:27am
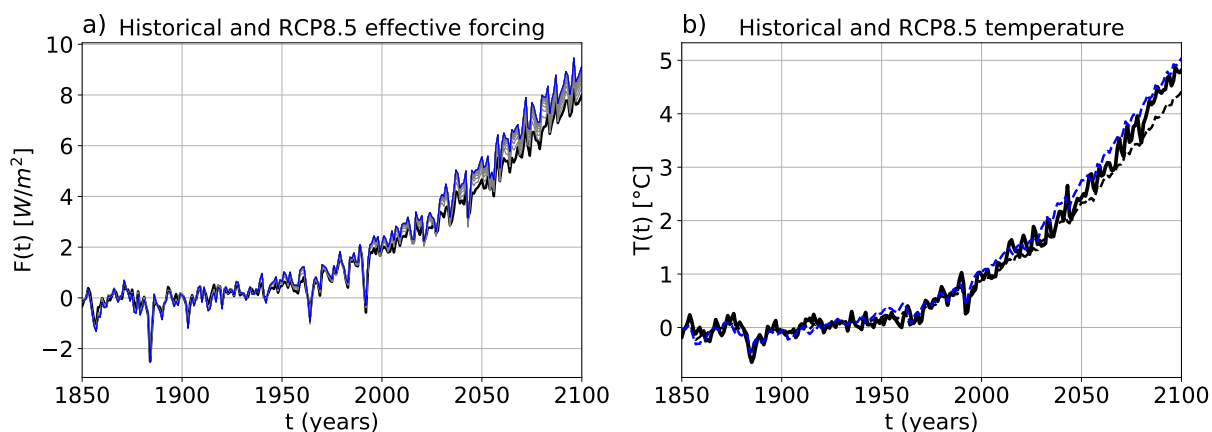
Figure S95. As Figure 4, but for the model MPI-ESM-LR.
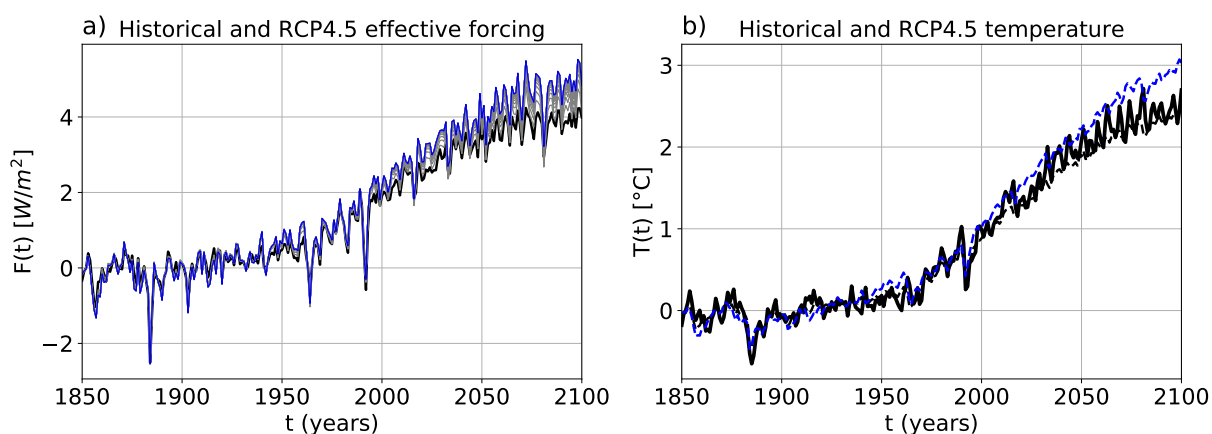
Figure S96. As Figure 4, but for the model MPI-ESM-LR and experiment RCP4.5.
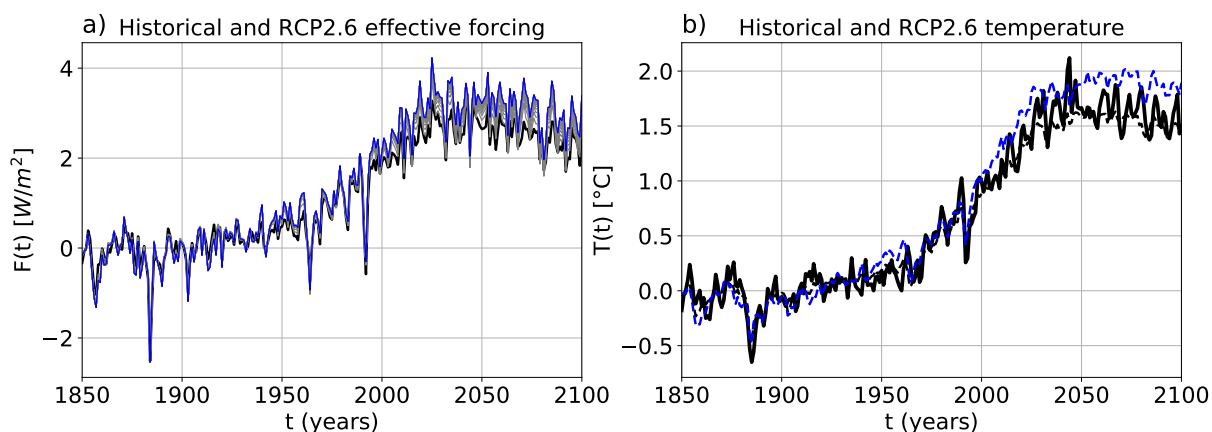
Figure S97. As Figure 4, but for the model MPI-ESM-LR and experiment RCP2.6.

November 5, 2021, 9:27am

a) Evolution of top of the atmosphere radiative imbalance and temperature

b) *T* following abrupt4xCO$_2$

c) *N* following abrupt4xCO$_2$
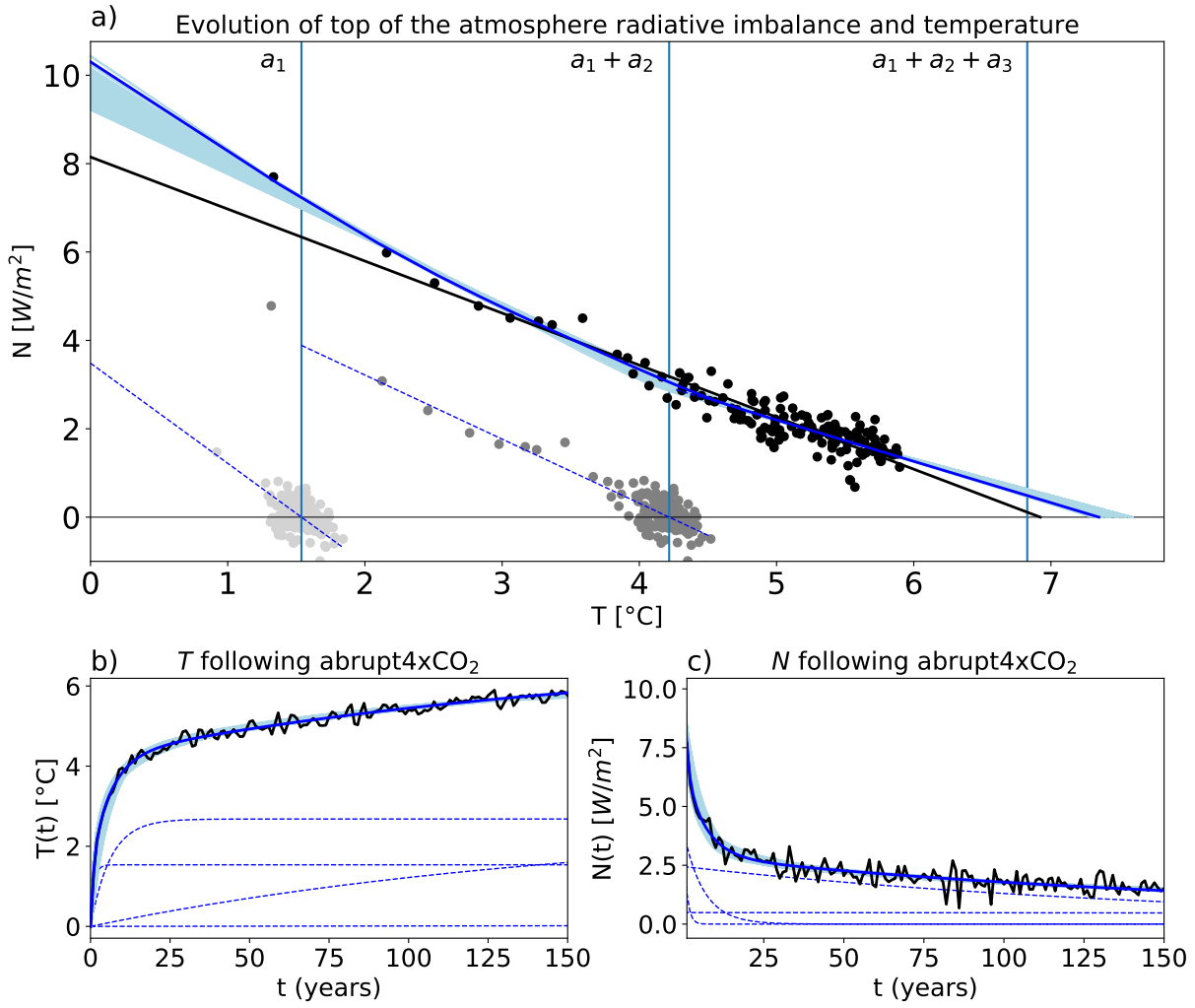
Figure S98. As Figure 1, but for the model MPI-ESM-MR.

a) 1% CO$_2$ effective forcing

b) 1% CO$_2$ temperature
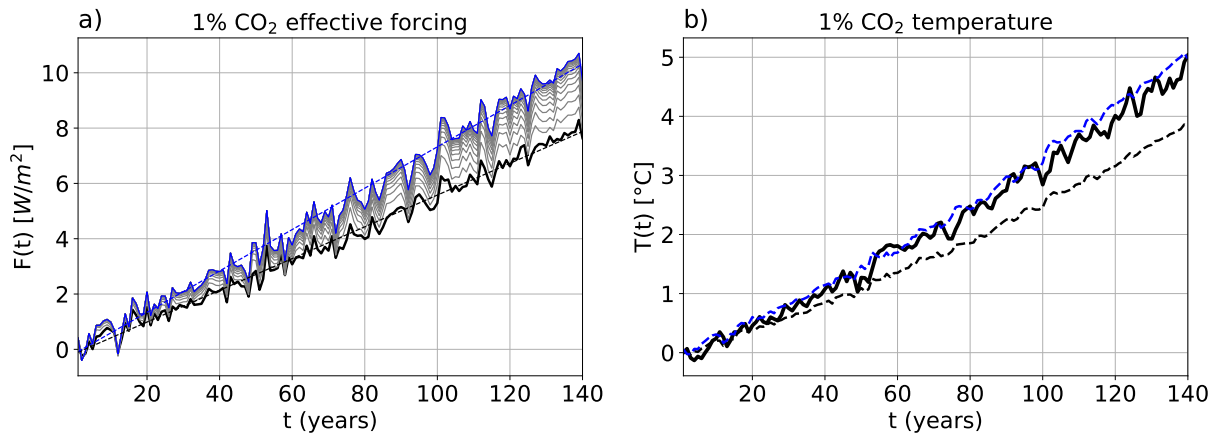
Figure S99. As Figure 3, but for the model MPI-ESM-MR.
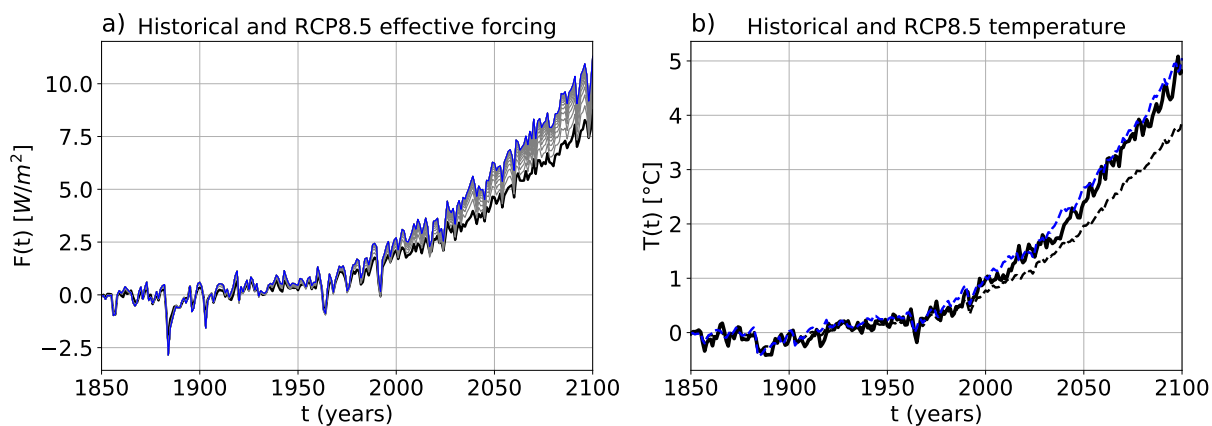
Figure S100. As Figure 4, but for the model MPI-ESM-MR.
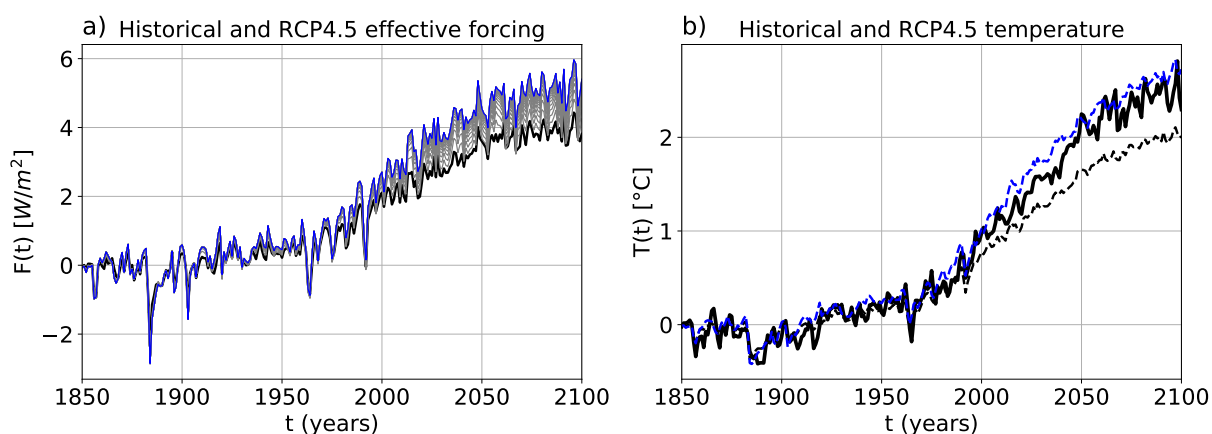
**Figure S101.** As Figure 4, but for the model MPI-ESM-MR and experiment RCP4.5.
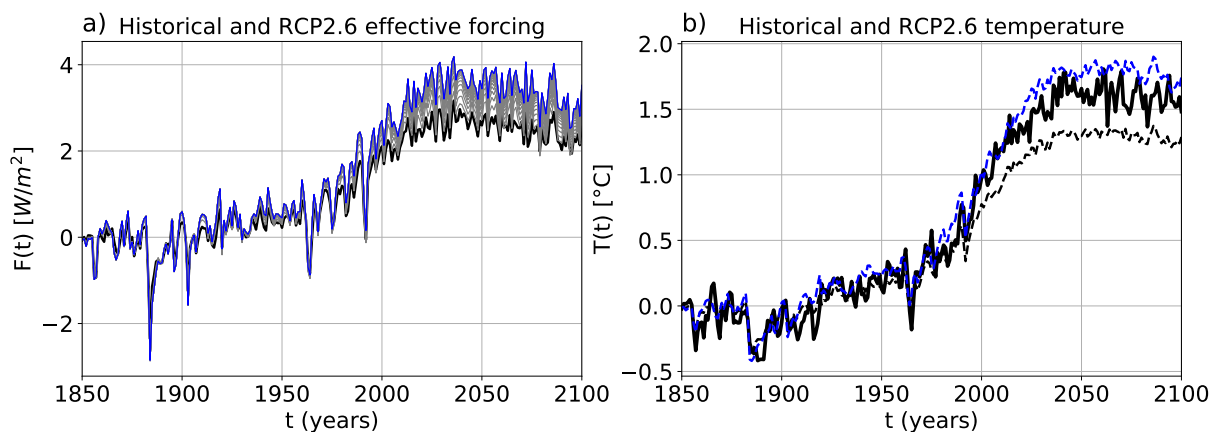
**Figure S102.** As Figure 4, but for the model MPI-ESM-MR and experiment RCP2.6.
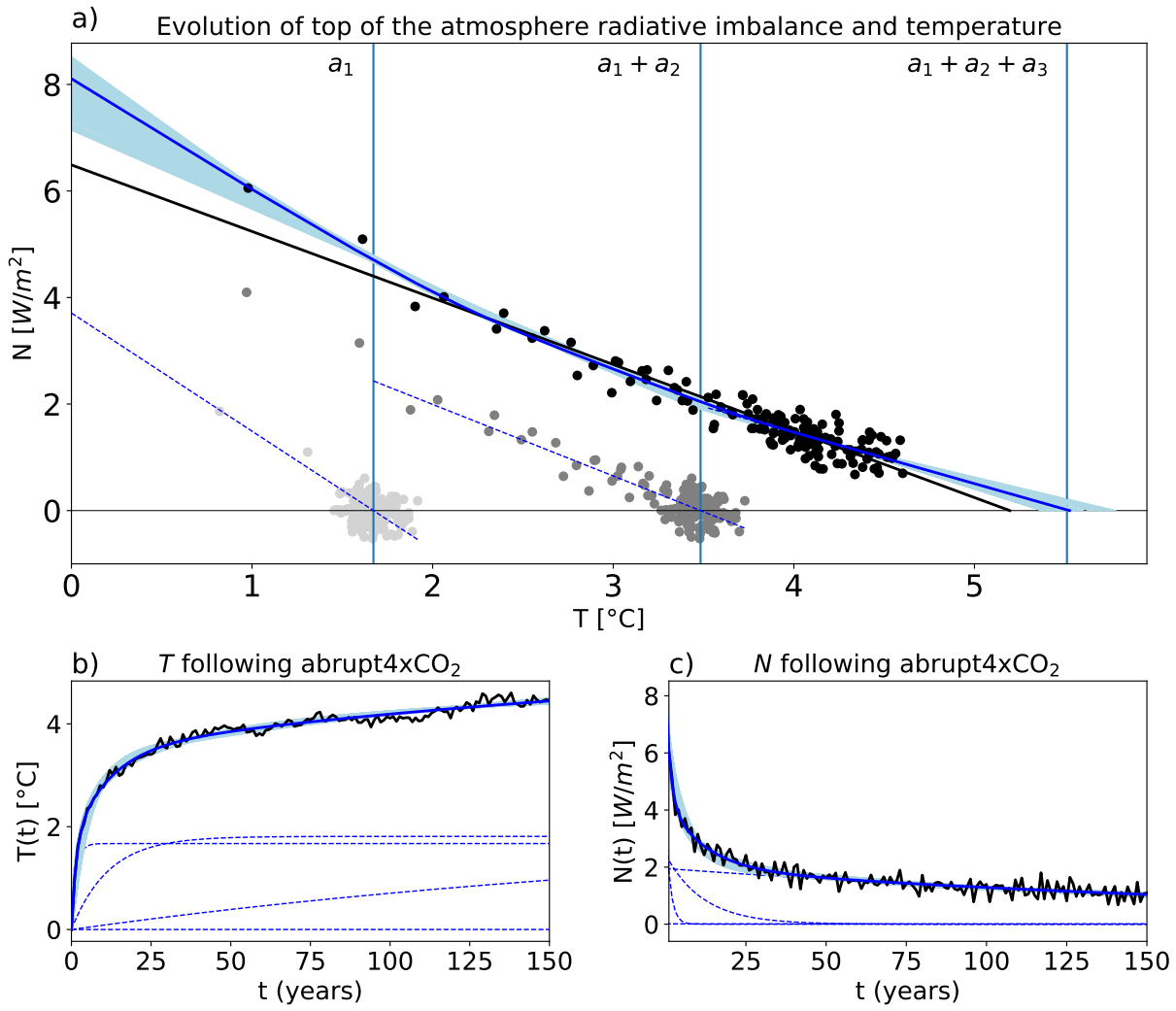
Figure S103.   As Figure 1, but for the model MRI-CGCM3.
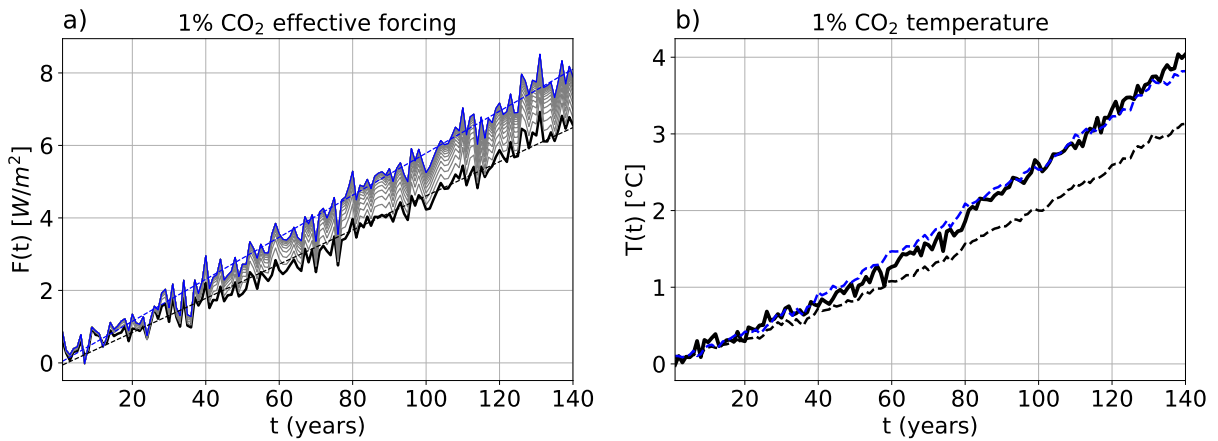
Figure S104.   As Figure 3, but for the model MRI-CGCM3.
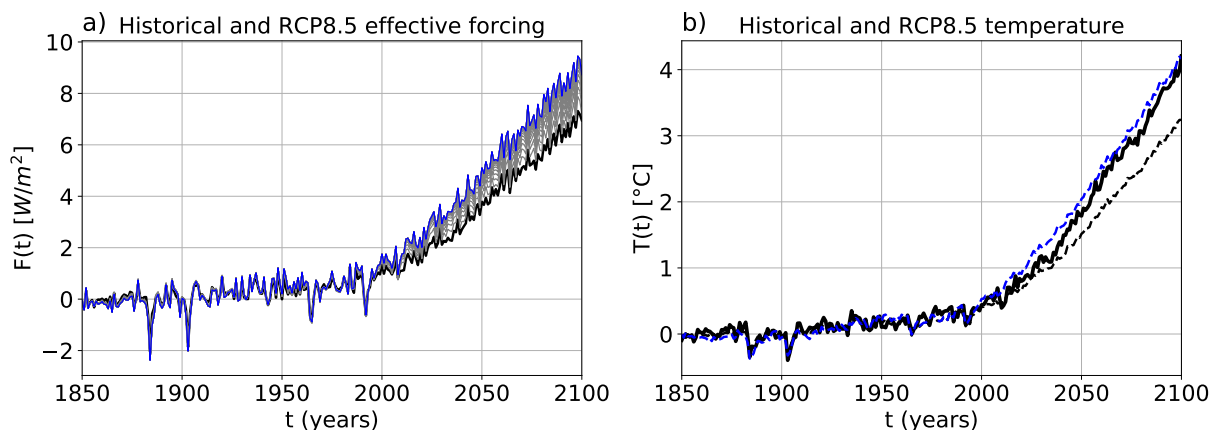
**Figure S105.**   As Figure 4, but for the model MRI-CGCM3.
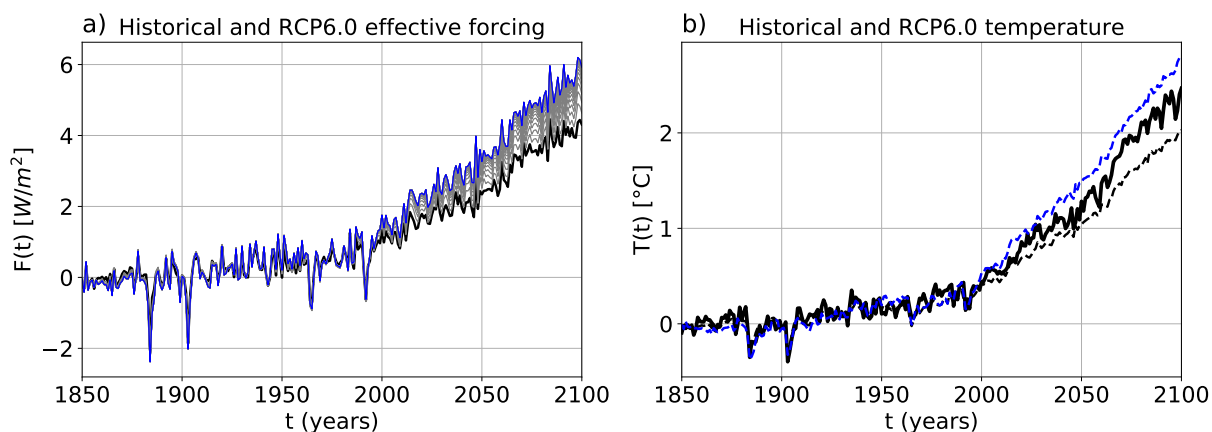
Figure S106.   As Figure 4, but for the model MRI-CGCM3 and experiment RCP6.0.
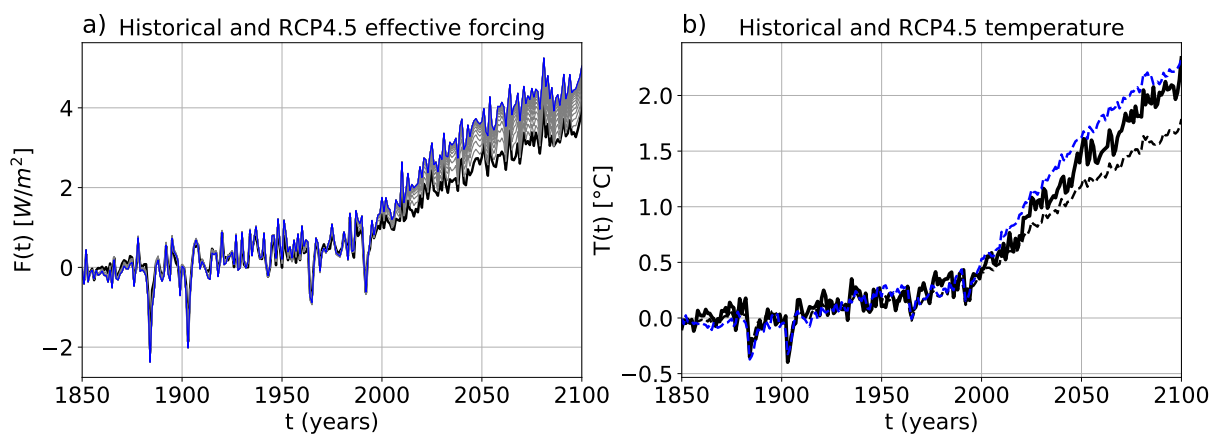
Figure S107.   As Figure 4, but for the model MRI-CGCM3 and experiment RCP4.5.
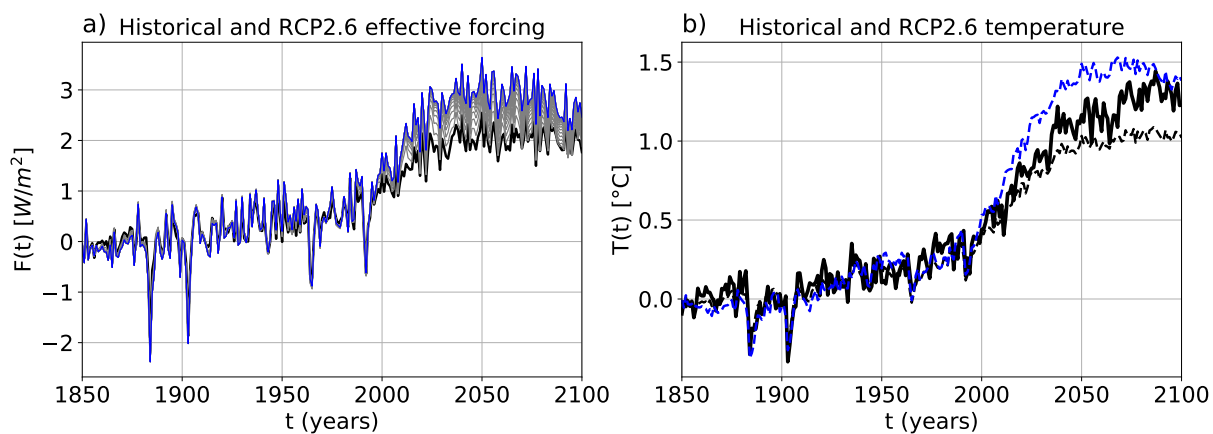
**Figure S108.**   As Figure 4, but for the model MRI-CGCM3 and experiment RCP2.6.
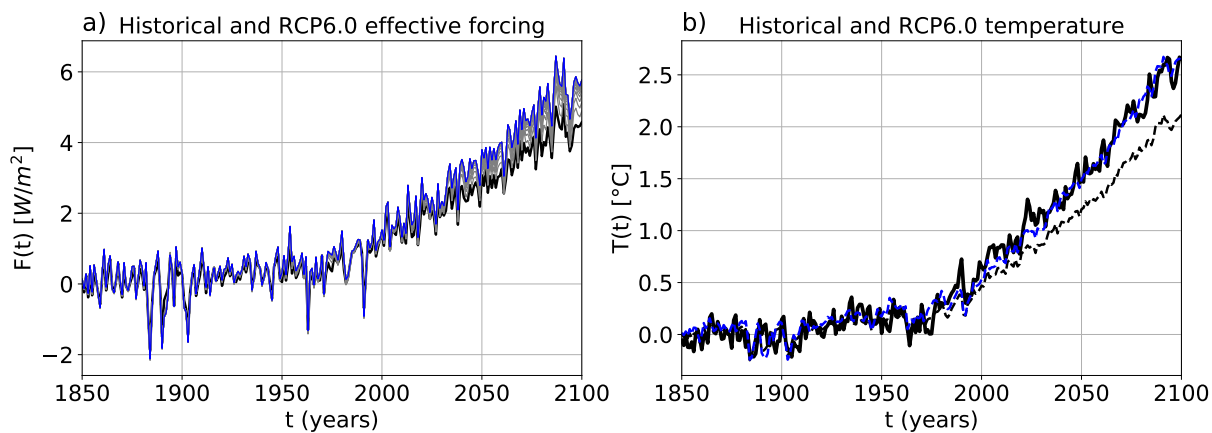
**Figure S109.** As Figure 4 with the model NorESM1-M, but for the experiment RCP6.0.
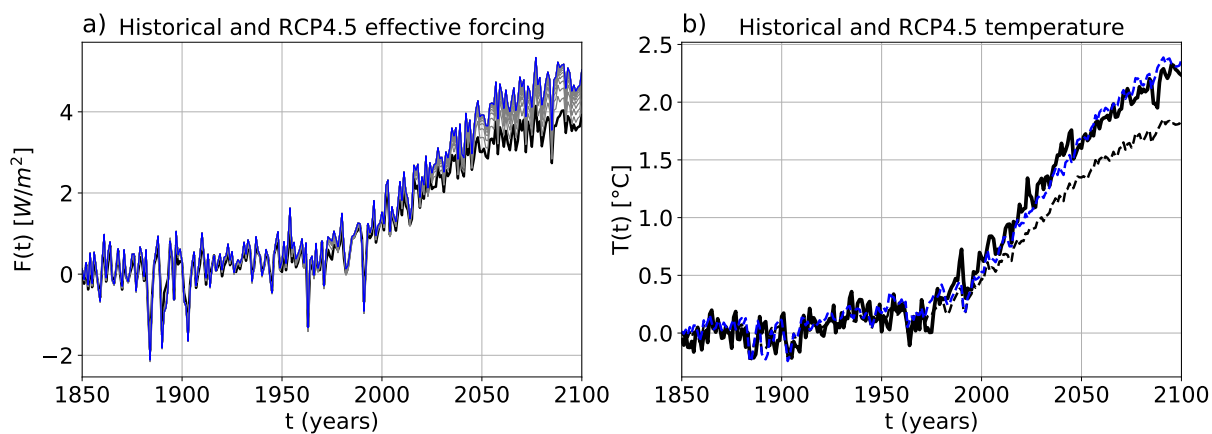
Figure S110. As Figure 4 with the model NorESM1-M, but for the experiment RCP4.5.
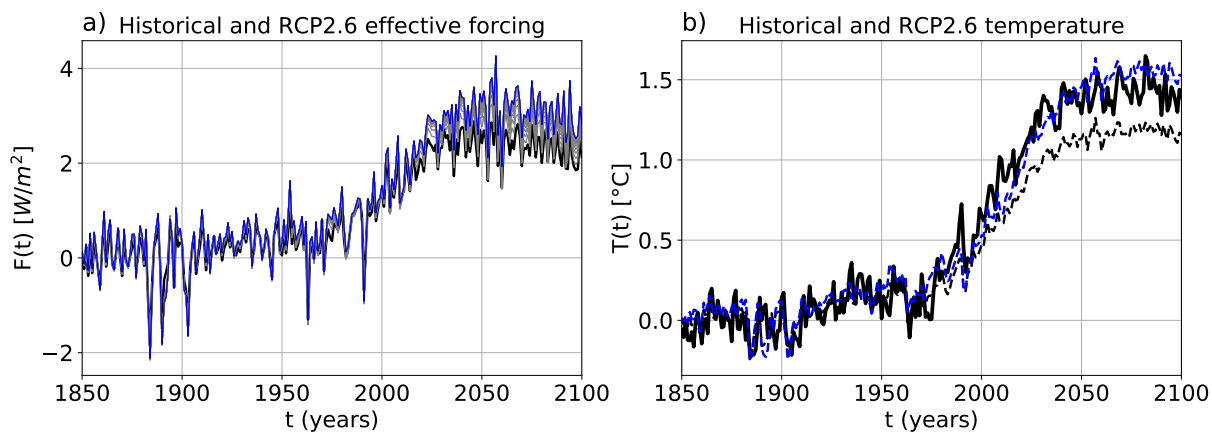

Figure S111. As Figure 4 with the model NorESM1-M, but for the experiment RCP2.6.

November 5, 2021, 9:27am

:

Table S1. The piControl trends computed over the 150 year period after branching of the abrupt4xCO$_2$ experiment. Temperature trends have units °C per year, and the top of atmosphere radiation components have units W/m^2 per year.

	ΔT/year	Δrlut/year	Δrsdt/year	Δrsut/year
ACCESS1-0	1.05e-03	1.52e-03	1.66e-06	-1.31e-03
ACCESS1-3	4.76e-04	1.14e-03	1.79e-07	-6.73e-04
CanESM2	1.80e-04	2.02e-04	9.70e-17	-2.18e-04
CCSM4	-5.03e-04	-4.86e-04	-1.28e-15	7.58e-04
CNRM-CM5	1.16e-03	1.61e-03	-1.09e-06	-9.32e-04
CSIRO-Mk3-6-0	6.71e-04	8.82e-04	-3.76e-09	-1.09e-03
GFDL-CM3	8.09e-04	1.51e-03	-1.29e-15	-9.08e-04
GFDL-ESM2G	-1.04e-03	-1.86e-03	0.00e+00	1.93e-03
GFDL-ESM2M	-1.11e-04	-3.93e-04	0.00e+00	-3.21e-04
GISS-E2-H	8.76e-04	9.77e-04	-1.02e-15	-6.38e-04
GISS-E2-R	5.33e-04	7.95e-04	-3.75e-16	-6.00e-04
HadGEM2-ES	-2.84e-04	1.06e-04	0.00e+00	1.67e-04
inmcm4	-7.63e-04	-1.18e-03	1.48e-06	1.03e-03
IPSL-CM5A-LR	-3.86e-04	-3.81e-04	1.02e-10	1.01e-03
IPSL-CM5B-LR	1.36e-03	2.84e-03	-2.39e-10	-1.62e-03
MIROC-ESM	6.67e-04	7.70e-04	-2.85e-06	-9.82e-05
MIROC5	-3.60e-04	-2.79e-04	4.66e-10	6.02e-04
MPI-ESM-LR	-5.64e-05	2.76e-04	-8.26e-07	-1.28e-04
MPI-ESM-MR	2.89e-05	8.32e-05	-1.40e-07	-1.91e-05
MRI-CGCM3	2.93e-04	1.07e-03	2.75e-06	-4.39e-04
NorESM1-M	-4.72e-04	-9.77e-04	1.14e-10	3.36e-04
min	-1.04e-03	-1.86e-03	-2.85e-06	-1.62e-03
max	1.36e-03	2.84e-03	2.75e-06	1.93e-03